



Reverberation Modelling using a Parabolic Equation Method

*Mr. Craig A. Hamm
Dr. Gary H. Brooke
Dr. David J. Thomson
Mr. Martin L. Taillefer
Maritime Way Scientific Ltd*

*Prepared by:
Maritime Way Scientific Ltd
2110 Blue Willow Crescent
Ottawa, ON Canada K1W 1K3*

Contract Project Manager: *Mr. Martin Taillefer, 613-824-6300*

Contract number: W7707-125517/001/HAL

Scientific Authority: Dr. Dale D. Ellis

The scientific or technical validity of this Contract Report is entirely the responsibility of the contractor and the contents do not necessarily have the approval or endorsement of Defence R&D Canada.

Defence R&D Canada – Atlantic

Contract Report
DRDC Atlantic CR 2012-077
October 2012

This page intentionally left blank.

Reverberation Modelling using a Parabolic Equation Method

Mr. Craig A. Hamm
Dr. Gary H. Brooke
Dr. David J. Thomson
Mr. Martin L. Taillefer
Maritime Way Scientific Ltd

Prepared by:
Maritime Way Scientific Ltd
2110 Blue Willow Crescent
Ottawa, ON Canada K1W 1K3

Contract Project Manager: Mr. Martin Taillefer, 613-824-6300

PWGSC Contract number: W7707-125517/001/HAL

Contract Scientific Authority: Dr. Dale D. Ellis

The scientific or technical validity of this Contract Report is entirely the responsibility of the contractor and the contents do not necessarily have the approval or endorsement of Defence R&D Canada.

Defence R&D Canada – Atlantic

Contract Report
DRDC Atlantic CR 2012-077
October 2012

Principal Author

Originally signed by Craig Hamm

Mr. Craig Hamm
Maritime Way Scientific Ltd

Approved by

Original signed by Dan Hutt

Dan Hutt
Head / Underwater Sensing

Approved for release by

Original signed by Calvin Hyatt

Calvin Hyatt
Chair / Document Review Panel

- © Her Majesty the Queen in Right of Canada, as represented by the Minister of National Defence, 2012.
- © Sa Majesté la Reine (en droit du Canada), telle que représentée par le ministre de la Défense nationale, 2012.

Abstract

DRDC Atlantic has developed a Clutter Model for range-dependent environments based on adiabatic normal modes. However, this approach is expected to fail for strongly range-dependent environments. Alternatively, parabolic equation (PE) models are robust in strongly range-dependent environments. In this study the DRDC PE model 'PECan' is used to determine the feasibility of computing reverberation and target echo fields in various ocean waveguides. Calculations are compared to problems from the US Reverberation Modeling Workshops. The PE Method reverberation estimates compare favourably to previously published results obtained by other authors and methods.

Résumé

RDDC Atlantique a élaboré un modèle de fouillis d'échos acoustiques fondé sur les modes normaux adiabatiques pour les environnements dont les caractéristiques varient en fonction de la distance. Toutefois, on s'attend à ce que cette approche échoue pour les environnements dont les caractéristiques varient fortement en fonction de la distance. D'un autre côté, les modèles à équation parabolique sont robustes pour ce genre d'environnement. Dans la présente étude, on utilise le modèle à équation parabolique de RDDC, le « PECan » (*PE* pour *parabolic equation*), pour déterminer la faisabilité du calcul du champ acoustique et de la réverbération des échos de cibles dans différents guides d'ondes océaniques. On compare ces calculs à ceux de problèmes tirés des ateliers américains sur la modélisation de la réverbération. Les estimations de la réverbération effectuées par la méthode de l'équation parabolique sont comparables aux résultats déjà publiés par d'autres auteurs ayant appliqué des méthodes différentes.

This page intentionally left blank.

Executive summary

Reverberation Modelling using a Parabolic Equation Method

Craig Hamm, Gary Brooke, Dave Thomson, Martin Taillefer; DRDC Atlantic CR 2012-077; Defence R&D Canada – Atlantic; October 2012.

Introduction or background: DRDC Atlantic has developed a Clutter Model for range-dependent environments based on adiabatic normal modes; however, this approach is expected to fail for strongly range-dependent environments where mode coupling can occur. Alternatively, parabolic equation (PE) models are robust in strongly range-dependent environments. Preliminary studies suggest there may be simpler techniques that can be employed directly within a PE model that yield sufficiently accurate estimates of reverberation and possibly target echo.

The objective of this contract is to investigate the use of the PE model (in particular PECan [1]) for computing approximations to the reverberation and target echo fields in realistic ocean waveguides. Attention is focused on shallow water and low frequencies to obtain efficient and sufficiently accurate values for these two quantities in range-dependent waveguides. In this regime adiabatic mode methods exceed the limits of their applicability.

Results: Transmission loss estimates produced by the PECan parabolic equation acoustic model were used in concert with MatlabTM scripts to estimate surface, volume and bottom reverberation between frequencies 25 to 3500 Hz. This was done in a various shallow water scenarios. The reverberation estimates compare favourably to results obtained previously using more traditional methods (e.g. ray modelling, normal mode modelling). Also, the method developed was used to determine target echo. In some cases the compliance to accepted independent reference test case results is good for ranges that are very close-to-source (tens of metres) and at great distance (60 km). In other cases, there is room for improvement, particularly surface reverberation echo levels which behave similarly but are largely offset to the independent reference data. For the sea-surface reverberation the results are highly sensitive to the variations in transmission loss in near proximity to the sea surface. The target echo level also requires some improvement in level estimation, although the reference data may also be suspect in some cases. The vertical structure of the acoustic field could not be adequately determined by FFT analysis.

Significance: Clutter is one of the most important effects affecting sonar performance in shallow water. Reverberation and target echo models are giving consistent results for flat bottom cases. However, very few results are available for range-dependent environments. The parabolic equation method is quite reliable for predicting transmission loss in range-dependent environments. The results here demonstrate the parabolic equation transmission loss model, normally reserved for passive modelling, is able to provide the basis for estimating the reverberation and target echo for active sonar scenarios. This was shown for both range independent and range dependent ocean environments. Methods described in this report show promise that efficient active sonar modelling in shallow range dependent environments is possible when used in concert with a parabolic equation passive acoustic model.

Future plans: The authors of this report recommend further study be undertaken to: solve the surface reverberation sensitivity when using the free surface boundary condition, implement more

physics-based boundary scattering functions, and undertake a more complex set of range-dependent scenarios. Use of the technique using other types of acoustic models should be undertaken. Furthermore, as the current method when applied as-is results in estimates that reflect the coherent interference structure of the coherent transmission loss. It is desirable to determine a more smooth reverberation estimate similar to that which can be obtained using incoherent summation of rays or modes. The calculation of echo excess for performance prediction from estimated reverberation and target echo is also desired.

Sommaire

Reverberation Modelling using a Parabolic Equation Method

Craig Hamm, Gary Brooke, Dave Thomson, Martin Taillefer; DRDC Atlantic CR 2012-077; R & D pour la défense Canada – Atlantique; octobre 2012.

Introduction ou contexte : RDDC Atlantique a élaboré un modèle de fouillis d'échos acoustiques fondé sur les modes normaux adiabatiques pour les environnements dont les caractéristiques varient en fonction de la distance. Toutefois, on s'attend à ce que cette approche échoue pour les environnements dont les caractéristiques varient fortement en fonction de la distance en raison de la possibilité de couplage de modes. D'un autre côté, les modèles à équation parabolique sont robustes pour ce genre d'environnement. Des études préliminaires portent à croire que des techniques plus simples pourraient être employées directement dans un modèle à équation parabolique qui produit une estimation suffisamment exacte de la réverbération et possiblement des échos de cibles.

L'objet du présent contrat est une étude du recours à un modèle à équation parabolique, en particulier le PECan (*PE* pour *parabolic equation*) [1], pour le calcul d'approximations du champ acoustique de la réverbération et des échos de cibles dans des guides d'ondes océaniques réalistes. On a concentré l'étude sur les eaux peu profondes et les basses fréquences dans le but d'obtenir des valeurs suffisamment exactes et utiles pour ces deux grandeurs pour les guides d'ondes dont les caractéristiques varient en fonction de la distance. De telles conditions excèdent les limites d'applicabilité des méthodes reposant sur le mode adiabatique.

Résultats : On a utilisé les estimations de perte de transmission produites par le modèle acoustique à équation parabolique PECan avec des scripts Matlab^{MC} pour estimer la réverbération de surface, de volume et de fond pour les fréquences allant de 25 à 3 500 Hz et pour divers scénarios en eau peu profonde. Les estimations de la réverbération sont comparables aux résultats déjà obtenus par l'application de méthodes plus classiques (p. ex. les modèles fondés sur la théorie des rayons et ceux fondés sur la théorie du mode normal). De plus, on a appliqué la méthode mise au point au calcul des échos de cibles. Dans certains cas, la conformité aux résultats obtenus dans le cas d'un scénario d'essai de référence indépendant reconnu est bonne lorsque les distances sont très courtes (dizaines de mètres de la source) ou très longues (60 km) par rapport à la source. Dans d'autres cas, on pourrait obtenir de meilleurs résultats, en particulier pour ce qui est du niveau des échos en réverbération de surface, dont les valeurs varient de façon similaire aux données de référence indépendantes, mais présentent un important décalage par rapport à celles-ci. Pour ce qui est de la réverbération de surface, les résultats sont fortement liés aux variations de la perte de transmission à proximité de la surface de la mer. L'estimation du niveau des échos de cibles doit également être améliorée, bien que la validité des données de référence puisse être douteuse dans certains cas. On n'a pas réussi à déterminer de façon adéquate la structure verticale du champ acoustique à l'aide d'une analyse fondée sur la transformée de Fourier rapide.

Importance : Le fouillis d'échos est l'un des effets nuisant le plus à la performance des sonars en eau peu profonde. Les modèles de réverbération et d'échos de cibles donnent des résultats cohérents pour les scénarios où le fond est plat. Par contre, on dispose de très peu de résultats

pour les environnements dont les caractéristiques varient en fonction de la distance. La méthode de l'équation parabolique est relativement fiable pour la prédiction de la perte de transmission dans les environnements dont les caractéristiques varient en fonction de la distance. Les résultats obtenus montrent que le modèle à équation parabolique de perte de transmission, qui est normalement réservé à la modélisation de scénarios de détection passive, est en mesure de fournir une estimation de base de la réverbération et des échos de cibles pour les scénarios de détection par sonar actif. La démonstration en a été faite tant pour les environnements dont les caractéristiques varient en fonction de la distance que pour les environnements homogènes. Les méthodes décrites dans le présent rapport portent à croire en la possibilité d'une modélisation efficace de la détection sonar active pour les environnements en eau peu profonde dont les caractéristiques varient en fonction de la distance lorsque l'on applique conjointement un modèle acoustique à équation parabolique pour le sonar passif.

Recherches futures : Les auteurs du présent rapport recommandent la tenue d'autres études afin de résoudre le problème de la susceptibilité à la réverbération de surface lorsque l'on a recours à la condition de surface-limite libre, de mettre en application des fonctions de diffusion aux limites qui soient davantage fondées sur la physique et, finalement, de préparer un ensemble plus complexe de scénarios dont les caractéristiques varient en fonction de la distance. On devrait appliquer la technique avec d'autres types de modèles acoustiques. De plus, la méthode actuelle appliquée telle quelle produit des estimations reflétant la structure d'interférence cohérente de la perte de transmission cohérente. Il est souhaitable de pouvoir obtenir une estimation plus lisse de la réverbération, comme celle obtenue par la sommation incohérente des rayons ou des modes. Il est également souhaitable de pouvoir calculer l'excès d'échos en se fondant sur l'estimation de la réverbération et des échos de cibles pour la prédiction de la performance.

Table of contents

Abstract	i
Résumé	i
Executive summary	iii
Sommaire	v
Table of contents	vii
List of figures	x
List of tables	xiv
Acknowledgements	xv
1 Overview.....	1
2 Background and Objectives.....	2
2.1 Background.....	2
2.2 PECO - The Model.....	2
2.3 PECO – Theory	3
2.4 PECO – Reverberation and Target Echo	5
3 Summary of Project Results	10
3.1 Tasking	10
3.2 Chronology of Effort.....	10
3.3 Deliverables.....	12
3.3.1 Teleconference Meetings	12
3.3.2 Software, Databases and Documentation.....	12
3.3.3 Report.....	15
3.4 Methodology.....	15
3.4.1 Reverberation	17
3.4.1.1 Surface Reverberation	19
3.4.1.2 Volume Reverberation.....	21
3.4.1.3 Bottom Reverberation.....	21
3.4.2 Target Echo	22
3.4.3 Vertical Field.....	23
3.4.4 Reducing θ_{\max} as a Function of Range	25
3.5 Reverberation and Target Echo Results	25
3.5.1 Reverberation Workshop Problem 11 (RI, Isovel.).....	26
3.5.2 Reverberation Workshop Problem 12 (RI, Summer).....	27
3.5.3 Reverberation Workshop Problem 13 (RI, Winter)	28
3.5.4 Reverberation Workshop Problem 17 – Wedge (RD, Isovel.).....	28
3.5.5 Surface Reverberation – Boundary Effects.....	29
3.6 Vertical Field Results	31

3.6.1	Reducing θ_{\max} as a Function of Range	32
3.7	What constitutes a ‘good fit’ to the reference data?	32
3.8	Recommendations for Changes to PECan	34
4	Conclusions and Proposed Future Work	36
4.1	Conclusions	36
4.2	Proposed Future Work	36
	References	39
Annex A ..	Results – Reverberation and Targe Echo	41
A.1	Reverberation Workshop Problem 11 (RI, Isovel.)	41
A.1.1	Reverberation Components	41
A.1.2	Target Echo	43
A.2	Reverberation Workshop Problem 12 (RI, Summer)	44
A.2.1	Reverberation Components	44
A.2.2	Target Echo	46
A.3	Reverberation Workshop Problem 13 (RI, Winter)	47
A.3.1	Reverberation Components	47
A.3.2	Target Echo	49
A.4	Reverberation Workshop Problem 17 (RD, Isovel.)	50
A.4.1	Reverberation Components	51
A.4.2	Target Echo	52
A.5	Surface Reverberation – Boundary Effects	54
Annex B...	Vertical Field	63
B.1	Fourier Transform Analysis	63
B.2	Reducing θ_{\max} as a Function of Range	66
Annex C...	‘Goodness of Fit’ Results	67
Annex D ..	Software: PECan modifications and Matlab TM Scripts	69
D.1	PECan modifications	69
D.1.1	Output File: Petlr.out	69
D.1.2	Output File: Pervb.out	69
D.2	Matlab TM Environment Setup	70
D.3	Matlab TM Script Listings	71
D.3.1	Reverb_pervb4.m	71
D.3.2	Header Reads for pervb.out and petlr.out	82
Annex E...	PECan Input and Output Files	85
E.1	PECan Input Files	85
E.1.1	Naming Convention for this study	85
E.1.2	PECan Input File description	85
E.1.3	PECan Input File examples	88
E.2	Output Files	90

List of symbols/abbreviations/acronyms/initialisms	92
Distribution list.....	93

List of figures

Figure 1. A multi-path propagation environment.....	5
Figure 2. Reverberation time series illustration.....	6
Figure 3. Defining the target echo in time and aligning with the reverberation.....	7
Figure 4. A preliminary comparison of reverberation computations between PE and a ray code methods.....	9
Figure 5. Geometry for true bi-static calculation of reverberation and target echo.....	18
Figure 6. Cross-section (from rotation of 2π) of geometry used to calculate volume and boundary reverberation components. Transmission loss for the reverberation components are available in the PECan pervb.out output file.....	18
Figure 7. Chapman-Harris sea-surface scattering function at the three frequencies in this study.	20
Figure 8. Equation (14) plotted between θ_{Max} 10 and 30 degrees for Chapman-Harris surface scattering.	20
Figure 9. Equation (12) Mackenzie-Lambert bottom scattering function with $\mu_{\text{dB}} = -27$ dB.....	21
Figure 10. Equation (14) plotted between θ_{Max} 0 and 30 degrees for MacKenzie-Lambert bottom scattering.	22
Figure 11. Setup for FFT of the vertical acoustic field.	24
Figure 12. Linear reduction of θ_{max} with increasing range.	25
Figure 13. Geometry for Reverberation Workshop Problem 11. The annotated parameters are universal for RW problems 12, 13 and 17, below.....	27
Figure 14. Geometry for Reverberation Workshop Problem 12 ('summer').	27
Figure 15. Geometry for Reverberation Workshop Problem 13 ('winter').	28
Figure 16. Geometry for Reverberation Workshop Problem 17. Note: By agreement with DRDC, the environment was modelled assuming a rotation of the image plane about $R=0$, modelling a bowl environment, and not the 3D planar wedge.....	29
Figure 17. Reverberation Workshop Problem 11: PE method reverberation results for surface (top), volume (middle), and bottom reverberation at 250 Hz. Note the biases applied to the surface and bottom reverberation levels as noted on the graphs.	41
Figure 18. Reverberation Workshop Problem 11: PE method reverberation results for surface (top), volume (middle), and bottom reverberation at 1000 Hz. Note the biases applied to the surface and bottom reverberation levels as noted on the graphs.	42
Figure 19. Reverberation Workshop Problem 11: PE method reverberation results for surface (top), volume (middle), and bottom reverberation at 3500 Hz. Note the biases applied to the surface and bottom reverberation levels as noted on the graphs.	42
Figure 20. Reverberation Workshop Problem 11: PE method target echo results at 250 Hz.....	43

Figure 21. Reverberation Workshop Problem 11: PE method target echo results at 1000 Hz.....	43
Figure 22. Reverberation Workshop Problem 11: PE method target echo results at 3500 Hz.....	44
Figure 23. Reverberation Workshop Problem 12: PE method reverberation results for surface (top), volume (middle), and bottom reverberation at 250 Hz.	44
Figure 24. Reverberation Workshop Problem 12: PE method reverberation results for surface (top), volume (middle), and bottom reverberation at 1000 Hz.....	45
Figure 25. Reverberation Workshop Problem 12: PE method reverberation results for surface (top), volume (middle), and bottom reverberation at 3500 Hz.....	45
Figure 26. Reverberation Workshop Problem 12: PE method target echo results at 250 Hz.....	46
Figure 27. Reverberation Workshop Problem 12: PE method target echo results at 1000 Hz.....	46
Figure 28. Reverberation Workshop Problem 12: PE method target echo results at 3500 Hz.....	47
Figure 29. Reverberation Workshop Problem 13: PE method reverberation results for surface (top), volume (middle), and bottom reverberation at 250 Hz.	47
Figure 30. Reverberation Workshop Problem 13: PE method reverberation results for surface (top), volume (middle), and bottom reverberation at 1000 Hz.....	48
Figure 31. Reverberation Workshop Problem 13: PE method reverberation results for surface (top), volume (middle), and bottom reverberation at 3500 Hz.....	48
Figure 32. Reverberation Workshop Problem 13: PE method target echo results at 250 Hz.....	49
Figure 33. Reverberation Workshop Problem 11: PE method target echo results at 1000 Hz.....	49
Figure 34. Reverberation Workshop Problem 13: PE method target echo results at 3500 Hz.....	50
Figure 35. Problem 17 environment represented in terms of reverberation (and target echo) time. The source depth, target depth and receiver depth are shown on the plot. Intersections with the bathymetry are shown for the target and receiver depths.	50
Figure 36. Reverberation Workshop Range Dependent Problem 17: PE method reverberation results for surface (top), volume (middle), and bottom reverberation at 250 Hz.....	51
Figure 37. Reverberation Workshop Range Dependent Problem 17: PE method reverberation results for surface (top), volume (middle), and bottom reverberation at 1000 Hz.....	51
Figure 38. Reverberation Workshop Range Dependent Problem 17: PE method reverberation results for surface (top), volume (middle), and bottom reverberation at 3500 Hz.....	52
Figure 39. Reverberation Workshop Range Dependent Problem 17: PE method target echo results at 250 Hz using PE method, normal mode method, and ray method.....	52
Figure 40. Reverberation Workshop Range Dependent Problem 17: PE method target echo results at 1000 Hz.....	53
Figure 41. Reverberation Workshop Range Dependent Problem 17: PE method target echo results at 3500 Hz.....	53
Figure 42. Comparison of sea surface reverberation for three different boundary conditions, showing the full range. The solid heavy line is derived from the ray model.	54

Figure 43. Comparison of sea surface reverberation for the free surface and the rigid surface boundary conditions at short range. The solid heavy line is derived from the ray model.....	54
Figure 44. Scatterplots comparing the rigid surface to the free surface reverberation (top), and the air layer to the free surface reverberation (bottom) which are identical save for a constant bias.	55
Figure 45. RW Problem 11 at 250 Hz (isovelocity). Reverberation time series based on near surface transmission loss. Top plot shows full time series for using TL result at depth 0.6λ ; middle plot shows near range reverberation time series detail for all near surface depths; bottom plot shows long range reverberation time series detail for all near surface depths.	55
Figure 46. Correlation of transmission loss at depths of $0.4 - 1\lambda$ to the transmission loss computed at a depth of 0.2λ . Frequency = 250 Hz, $\lambda = 6\text{m}$	56
Figure 47. RW Problem 11 at 1000 Hz (isovelocity). Reverberation time series based on near surface transmission loss. Top plot shows full time series for using TL result at depth 0.6λ ; middle plot shows near range reverberation time series detail for all near surface depths; bottom plot shows long range reverberation time series detail for all near surface depths.	57
Figure 48. Correlation of transmission loss at depths of $0.4 - 1\lambda$ to the transmission loss computed at a depth of 0.2λ . Frequency = 1000 Hz, $\lambda = 1.5\text{m}$	58
Figure 49. RW Problem 11 at 3500 Hz (isovelocity). Reverberation time series based on near surface transmission loss. Top plot shows full time series for using TL result at depth 0.6λ ; middle plot shows near range reverberation time series detail for all near surface depths; bottom plot shows long range reverberation time series detail for all near surface depths.	59
Figure 50. Correlation of transmission loss at depths of $0.4 - 1\lambda$ to the transmission loss computed at a depth of 0.2λ . Frequency = 3500 Hz, $\lambda = 0.4286\text{m}$	60
Figure 51. RW Problem 12 at 250 Hz (summer profile). Reverberation time series based on near surface transmission loss. Top plot shows full time series for using TL result at depth 0.6λ ; middle plot shows near range reverberation time series detail for all near surface depths; bottom plot shows long range reverberation time series detail for all near surface depths.	61
Figure 52. RW Problem 12 at 1000 Hz (summer profile). Reverberation time series based on near surface transmission loss. Top plot shows full time series for using TL result at depth 0.6λ ; middle plot shows near range reverberation time series detail for all near surface depths; bottom plot shows long range reverberation time series detail for all near surface depths.	61
Figure 53. RW Problem 12 at 3500 Hz (summer profile). Reverberation time series based on near surface transmission loss. Top plot shows full time series for using TL result at depth 0.6λ ; middle plot shows near range reverberation time series detail for all near surface depths; bottom plot shows long range reverberation time series detail for all near surface depths.	62

Figure 54. ASA Wedge (25 Hz) showing real and imaginary vertical field components at 4 ranges (10, 20, 30 and 40 km). File peAllModes.tlz. Script: vert_field.m.	63
Figure 55. Spectra for the ASA Wedge (25 Hz) case containing three modes, and simulated data. Components simulated are at $k_z = 0.014, 0.027, 0.041 \text{ m}^{-1}$. File peAllModes.tlz; Scripts: vert_field.m and determine_spectrum_params.m.	63
Figure 56. Synthetic time series with frequency components at 15, 50 and 100 Hz. From top to bottom the time series contain 1/2, 3/4, 1, and 3 wave cycles of the lowest frequency component (15Hz).	64
Figure 57. Spectra of the time series shown in Figure 12. Vertical red lines indicate the frequency component locations. Only when there is one full cycle of the lowest frequency to resolve does the spectrum reflect the true frequency content. Frequency components at 15, 50 and 100 Hz.	64
Figure 58. Vertical pressure field for the first four output ranges in the P11_f3500_S30R50_pe.tlz file.	65
Figure 59. Vertical field spectra for the first eight ranges output in the P11_f3500_S30R50_pe.tlz file. Source depth = 30m.	65
Figure 60. Comparison between two wavenumber spectra at 2.5 km range when the source depth is changed from 30m to 15m. Files: RW_P11_f3500_S15R50_pe.tlz and RW_P11_f3500_S30R50_pe.tlz.	66
Figure 61. Bottom reverberation plotted as a function of time, computed for a reduction of θ_{Max} with range, shown for the maximum ranges where the effect is greatest. The solid red line is the reference data of Fromm [19].	66
Figure 62. Output from modelled_histogram.m, simulated signal. Three different levels are shown, the mean, the RMS, and the threshold (85% of total energy) based on the histogram. Note: the histogram is computed in linear space, but has been shown in log-log for visual purposes only.	67
Figure 63. Mean, RMS, and histogram method applied to reverberation data and compared to Fromm (250 Hz, Problem 11). Black lines: Fromm; Red lines: RMS, Magenta: Mean; Green: Histogram-sum with threshold at 60%.	67
Figure 64. Directory structure and orchestration via Matlab TM scripts.	71

List of tables

Table 1. Chronology of effort and corresponding contract task.....	10
Table 2. Communications and Meetings.	12
Table 3. Catalog and description of developed Matlab TM scripts.....	13
Table 4. Table of Environmental properties See Ref [19].....	16
Table 5. Table of signal parameters.....	17
Table 6. Summary of frequencies, wavenumber, vertical sample period and Nyquist frequency for vertical spectra.....	25

Acknowledgements

Maritime Way Scientific (MWS) and Brooke Numerical Solutions (BNS) would like to thank Dr. Dale Ellis for his prompt cooperation with data and advice when required during the course of the investigation.

This page intentionally left blank.

1 Overview

This document represents the final Maritime Way Scientific (MWS) Contractor's report for the Reverberation Modelling contract: W7707-12517/001/HAL.

The specific tasks completed during the contract are discussed in detail below. Essentially, these tasks fall in one of five main categories as follows: (i) definition of test cases; (ii) development of MatlabTM scripts to produce estimates of reverberation and target echo; (iii) comparison of these estimates to results obtained independently by other means or authors; (iv) investigation of the acoustic field in an effort to improve the estimates, and; (v) to provide recommendations to DRDC with regards to using the parabolic equation for reverberation prediction. The definition of test cases comprises Task 1. Development of MatlabTM scripts to produce estimates of reverberation and target echo comprises Task 2 and Task 3. Task 4 involved an investigation of the acoustic field in the vertical in an anticipatory effort to improve the estimates, and Task 5 provides recommendation to DRDC with respect to PECAN model [1] code changes (if desired) and an alternate way forward if this method of predicting reverberation is to be developed further. Per instruction of the Scientific Authority (SA), importance was given to the reverberation estimates.

In what follows, Section 2 describes the project background and objectives. Section 3 provides a summary of the tasking, the work performed and the deliverables created. Section 4 presents a summary of conclusions and proposals for future work.

2 Background and Objectives

2.1 Background

DRDC Atlantic has developed a Clutter Model for range-dependent environments based on adiabatic normal modes [2-4] and has used it to compare with results from some reverberation and sonar test cases [5, 6]. Unfortunately, the adiabatic mode method is limited to small slopes and, thus, is not suitable for predicting reverberation in strongly range-dependent environments. Alternatively, the parabolic equation method is well-suited to propagation in these strongly range-dependent environments. Adaptations, such as the two-way PE [7-9], which have the potential to yield an accurate accounting of the reverberation, are simply too inefficient and unwieldy for realistic ocean environments. However, there is reason to believe that there may be simpler techniques that can be employed directly within a PE model like PECan and that yield sufficiently accurate reverberation data.

The detailed technical approach will be to use (and possibly modify) PECan to compute reverberation and target echo according to the adaptations described below. Initially, PE-based results will be compared to the Reverberation Workshop results for a suite of benchmark problems. Comparisons of reverberation and target echo will be made to the DRDC Clutter Model for a problem set defined by the Scientific Authority.

The subsections that follow describe the PECan model as it is, and then describes the scientific basis for algorithms, or direct modifications to PECan, that would allow the investigation into reverberation and target echo to proceed.

2.2 PECan - The Model

PECan, the Canadian Parabolic Equation (PE) model, is a fully modern underwater acoustic propagation modelling tool capable of computing efficient acoustic predictions in realistic oceanic environments [1]. Numerical propagation models based on the parabolic approximation [10] are now considered ‘mature’ after extensive improvements in the 1980-2000 time frame. In recent years, the focus of naval applications has shifted from deep to littoral waters, where the effects of bottom-interacting sound become more significant. As a consequence, not surprisingly, as the focus of the underwater acoustics community has shifted to littoral waters, finite-difference methods have assumed a more prominent role. Currently, most finite-difference algorithms are not only accurate for solving the PE, but energy-conserving [11], and efficient. Moreover, some PE models are also capable of treating complicated waveguide effects such as elasticity [12-13], backscatter [7-9], porosity [14], and surface roughness [15-16].

PECan is a versatile propagation model that generates coherent acoustic predictions in 3D range-dependent environments, including those with elastic properties in the sediments. It features an energy-conserving, split-step Padé algorithm that marches the acoustic field in range, depth, and azimuth i.e., performs traditionally what is known as $N \times 2D$ propagation modelling. Pecan also allows the User to optionally apply a correction to the $N \times 2D$ field using an azimuthal-coupling operator. This correction provides an approximation to full 3D acoustic modelling.

PECan has been exercised against several benchmark-type test cases that include range-dependent oceanographic parameters and bathymetry, 3D effects, and shear in the ocean bottom. These test cases were presented at the SWAM'99 Acoustics Modelling conference and are reported in [17].

2.3 PECan – Theory

Consider a range-independent acoustic medium in cylindrical coordinates (r, z, ϕ) bounded above by a free surface at $z = 0$, with a sound speed profile that supports long range propagation (as $r \rightarrow \infty$) in the upper part of the waveguide. For a harmonic point source located at $(0, z_s, 0)$, the spatial part of the pressure $p(r, z, \phi)e^{i\omega t}$ in $r \geq 0$ satisfies the scalar Helmholtz equation

$$r^{-1} \frac{\partial}{\partial r} \left(r \frac{\partial p}{\partial r} \right) + \rho \frac{\partial}{\partial z} \left(\rho^{-1} \frac{\partial p}{\partial z} \right) + r^{-2} \frac{\partial^2 p}{\partial \phi^2} + k_0^2 N^2 p = 0 \quad (1)$$

Here, $k_0 = \omega / c_0$ is a reference wavenumber, $\rho(z)$ is the density, $N(z) = n(z)[1 + i\alpha(z)]$ where $n(z) = c_0 / c(z)$ is the refractive index, $c(z)$ is the sound speed, and $\alpha(z)$ is the absorption loss. For numerical work, it is convenient to introduce the reduced 3D-field Ψ via

$$p(r, z, \phi) = \frac{e^{ik_0 r}}{\sqrt{r}} \Psi(r, z, \phi) . \quad (2)$$

Substituting (2) into (1), and factoring the result into outgoing and incoming fields, yields the one-way, far-field $k_0 r \gg 1$) wave equation for the forward-propagating component in the form

$$\frac{\partial \Psi}{\partial r} = ik_0 \left(-1 + \sqrt{1 + X_3} \right) \Psi . \quad (3)$$

In (3), X_3 denotes the 3D differential operator

$$X_3 = X_2 + X_\phi , \quad (4)$$

Where X_2 is the 2D depth operator in the rz -plane

$$X_2 = N^2 - 1 + k_0^2 \rho \frac{\partial}{\partial z} \left(\rho^{-1} \frac{\partial}{\partial z} \right) \quad (5)$$

and X_ϕ is the azimuthal operator

$$X_\varphi = (k_0 r)^{-2} \frac{\partial^2}{\partial \varphi^2} . \quad (6)$$

Using the Taylor expansion

$$\Psi(r + \Delta r, z, \varphi) = e^{\Delta r \partial_r} \Psi(r, z, \varphi) , \quad (7)$$

in conjunction with (3), yields a marching algorithm that forms the basis for all PE methods,

$$\Psi(r + \Delta r, z, \varphi) = e^{i\delta(-1+\sqrt{1+X_2+X_\varphi})} \Psi(r, z, \varphi) \quad (8)$$

where we have set $\delta = k_0 \Delta r$. In its present form, (8) is unsuitable for numerical work.

However, if the azimuthal coupling effects are sufficiently small, then we can approximate the full 3D propagator to $\mathcal{O}(\delta)$ by writing

$$\Psi(r + \Delta r, z, \varphi) \approx e^{i\delta(-1+\sqrt{1+X_\varphi})} e^{i\delta(-1+\sqrt{1+X_2})} \Psi(r, z, \varphi) \quad (9)$$

where we have used a wide-angle splitting approximation to separate the azimuthal operator X_φ from the depth operator X_2 . From (9), it is seen that 3D PE solutions involve first propagating the known PE field out from r to $r + \Delta r$ for each azimuth using the Nx2D propagator, and then correcting this field as a function of azimuth using the azimuthal propagator. It is important to realise that for 3D calculations, azimuthal coupling must be accounted for at each range step. Even though the azimuthal operator is applied independently at each depth, the propagation from one range step to the next couples all depths together. There are many numerical PE approaches currently available for solving (9) that differ only in the treatment used to approximate the square-root operators. Most PE solution techniques involve discretizing the environment onto a regular grid in range, depth, and bearing. The PE fields are then solved on a computational grid that can either coincide with or be offset from the environmental grid.

Typically, however, we usually restrict ourselves to cases where azimuthal dependence is absent or minimal allowing neglect of the azimuthal term i.e., $X_\varphi \rightarrow 0$, in which case (9) reduces to

$$\Psi(r + \Delta r, z) \approx e^{i\delta(-1+\sqrt{1+X_2})} \Psi(r, z) = \left[1 + \sum_{m=1}^{M_p} \frac{a_m X_2}{1 + b_m X_2} \right] \Psi(r, z) \quad (10)$$

Where M_p denotes the number of Padè coefficients $\{a_m, b_m\}$ are used to represent the exponential operator. Eq. (10) forms the basis for the PEECan algorithm. The numerical implementation of (10) ultimately involves solving a tridiagonal system of equations for each of the terms in the Padè summation. Since the PE is a ‘marching solution’, we start it off at $r = 0$ using a suitably selected ‘starting field’. PEECan supports a number of different starting fields including the capability to inject a single ‘mode’ into the waveguide; this latter feature may be of some use in this contract study.

2.4 PEECan – Reverberation and Target Echo

PEECan is a full-wave model. That is, at each range step, the finite-difference algorithm provides a solution for the ‘total field’ as a function of depth (i.e., on the depth grid) in the waveguide. In contrast, modal solutions or ray solutions allow one to get at individual ‘components’ of the total field (modes or eigenrays) and ultimately time delay information. The active sonar problem which utilises pulses to isolate targets in time has not traditionally been an application for the PE.

It is instructive to view how a ray-code (for example) might construct an approximation to the reverberation and the target echo. Consider the illustrations in Figure 1 below.

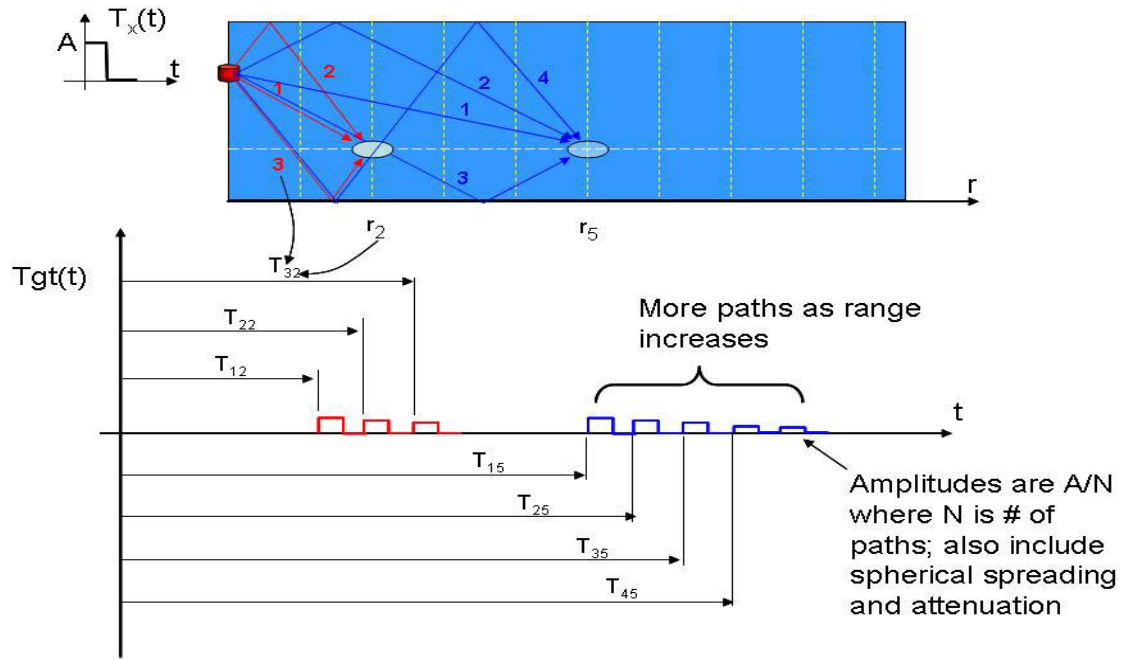


Figure 1. A multi-path propagation environment.

In Figure 1 we show how a pulse injected into the water at $r = 0$ is spread out in time by the different time delays associated with the eigenrays that connect the source with the target. Target echo can be computed by assigning a ‘scattering level’ to each of the pulses and then propagating them back to the receiver. A similar picture can be obtained for reverberation by effectively

moving the target or ‘scatterer’ onto the boundaries of the waveguide. Computation of reverberation involves collecting the energy from all of the multipath returns as illustrated in Figure 2. Acoustic returns from a particular range are first summed together and then folded into the ‘total’ reverberation summation yielding a ‘reverberation’ time series that decays away with time.

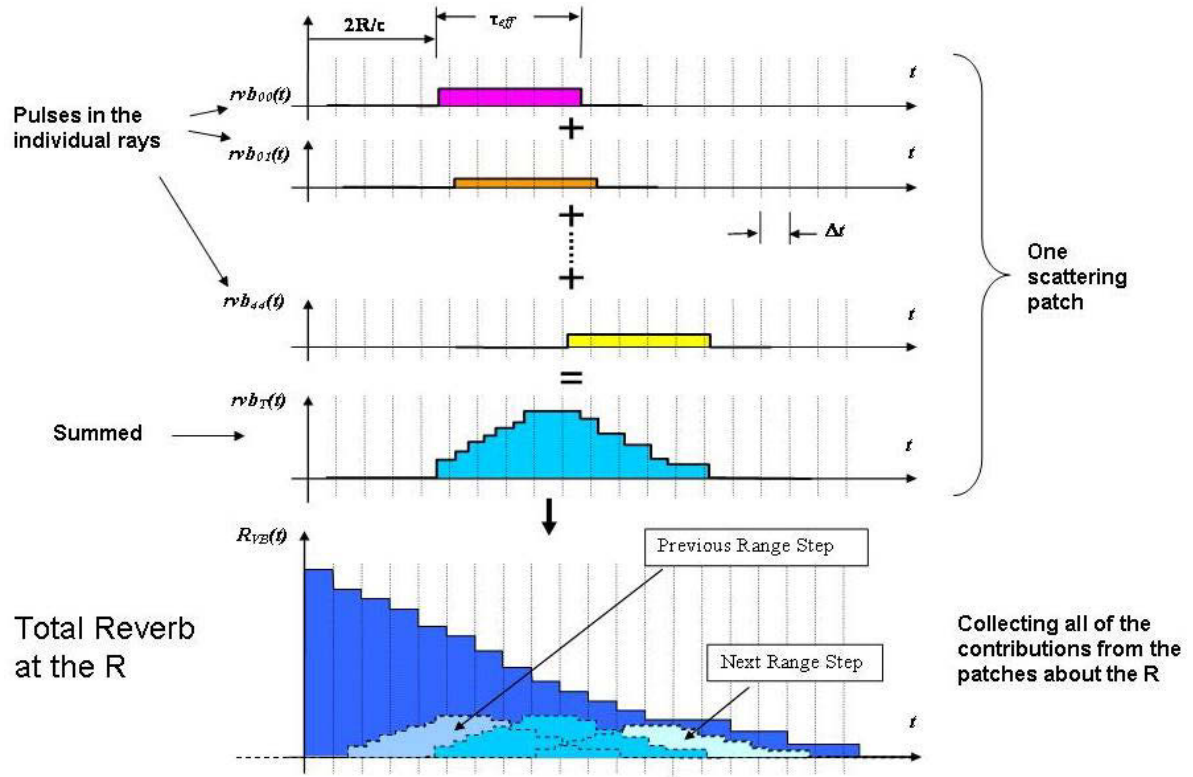


Figure 2. Reverberation time series illustration.

The calculation for target echo is illustrated below in Figure 3. The calculation is similar to that of the reverberation. However, since the target echo is the ‘signal’ in this problem some care must be taken to capture only those portions that are scattered from the target – hence, the ‘integration’ window. Once the target echo portion has been calculated it is a relatively simple matter to align it in time with the reverberation. The result is an approximation to the signal to noise ratio and ultimately, the probability of detection by treating the problem as one of signal detection in noise.

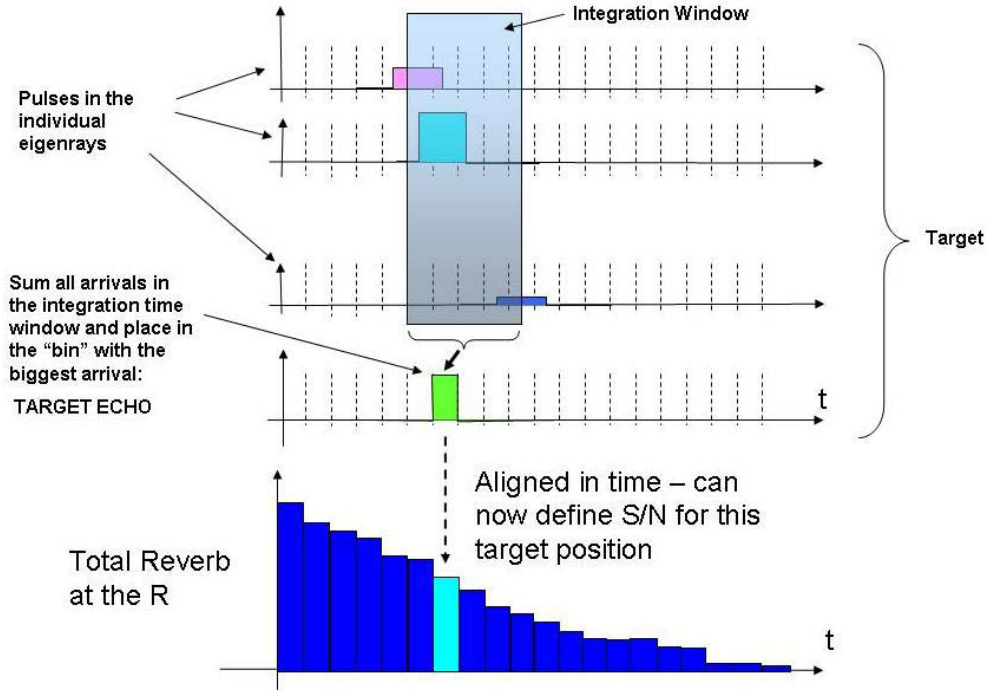


Figure 3. Defining the target echo in time and aligning with the reverberation.

Clearly, the PE cannot replicate exactly these steps, as illustrated in Figures 2 and 3 because it does not allow us to isolate the individual multipaths. The question is, can the PE yield any kind of information that can be related to time of arrival – the answer is: yes, it can but only in an average sense. Consider making the transformation $r = c_0 \cdot t$ in (3) above. The result can be written as

$$\frac{1}{c_0} \frac{\partial \Psi(c_0 t, z, \varphi)}{\partial t} = i\omega \left(-1 + \sqrt{1 + X_3} \right) \frac{\Psi(c_0 t, z, \varphi)}{c_0} \quad (11)$$

which is essentially a ‘scaled’ time-domain PE. Rather than solve (11) directly, we recognise that the same information can be obtained from the solutions of (3) in the spatial domain and then by associating r with $c_0 t$.

From the point of view of the reverberation and target echo, we would essentially propagate the PE out to the range-of-interest as we would normally do. At each range interval and at a particular depth (target) or at the boundaries these calculations define a value of transmission loss (TL) for the total field at a particular time, $t = r/c_0$. If we adjust the field at this range by some scattering coefficient, S , then back at the receiver (assume for the moment it is monostatic), the received level at time $2 \cdot t$ will be $S \cdot TL \cdot TL$. If we have a pulse of length, τ , we need to spread the pulse evenly over N bins starting at time $2 \cdot t$. We do this at each range step and once we get out to range we then add up the levels in each bin to get the total backscattered signal. The

number of bins N is determined by $\tau/(r/c_0)$ assuming we use $\Delta r/c_0$ as our binning time interval where Δr is the range step employed in the PE. Note, if the problem is not monostatic then we need to do a PE run for each sensor in order to define the appropriate TL values.

Finally, it should be noted that the scattering at range is angle dependent. The PE does not give us access to angle information directly. It is possible to take an FFT (over depth) of the PE field at any range and extract information about the vertical angle content. Of course, extensive use of the FFT will compromise the efficiency of the PE and therefore should be minimized – this is also a subject that can be investigated in this contract. In the absence of these results, it is possible to ‘normalize’ the angle dependency of the scattering as follows. Consider the cases for boundary scattering. For ocean bottom scattering we employ the Mackenzie-Lambert scattering equation in which the scattering coefficient, $S_B(\theta)$, behaves according to

$$S_B(\theta) = \mu \sin^2 \theta \quad (12)$$

For sea surface scattering we employ the Chapman-Harris scattering equation

$$S_S = 3.3\beta \log_{10}\left(\frac{\theta}{30}\right) - 42.4 \log_{10} \beta + 2.6 + 0.77 \quad [dB/m^2] \quad (13)$$

where

$$\beta = 158 \left(W f_{kHz}^{1/3} \right)^{-0.58}.$$

Equations (12) and (13) are clearly angle-dependent as it depends on the grazing angle, θ . In order to apply this formula to the PE field we apply (as a first approximation) a ‘cookie cutter’ approach in which we find an ‘average’ value of the scattering coefficient, S_{av} , by computing

$$S_{av} = \frac{1}{\theta_{max}} \int_0^{\theta_{max}} S(\theta) d\theta \quad (14)$$

where θ_{max} is determined by the ‘maximum’ vertical angle content of the propagating energy. It follows that we apply the value S_{av} in the calculation of the boundary reverberation using the PE adaptation discussed above. This procedure is applied to the boundary scattering laws in this contract.

As an example, consider Problem 11 from the Reverberation Workshop I [19] held in Austin, TX in 2006. The waveguide is 100 m deep, the water column is isovelocity at 1500 m/s, the frequency is 250 Hz, and there is Lambert scattering at the ocean bottom with $\mu = -27$ dB. The waveguide is ‘pulsed’ at a depth of 30 m by rectangular pulse of duration 0.08 sec and source level equal to -6.29 dB. A preliminary comparison of results obtained using the simple PE

technique outlined above is compared with a 'ray solution' in Figure 4 below. Note, the receiver used in the PE calculations is also at 30 m depth whereas for the ray result, the receiver has been placed at a depth equal to 50 m. However, other investigations have shown that the reverberation field is quite insensitive to the depth of the receiver. Overall there is very promising agreement between the two results shown in Figure 4. The over-prediction of reverberation at the longer times may well be a result of the 'average' scattering law (for this reverberation workshop problem, θ_{\max} is approximately 27°).

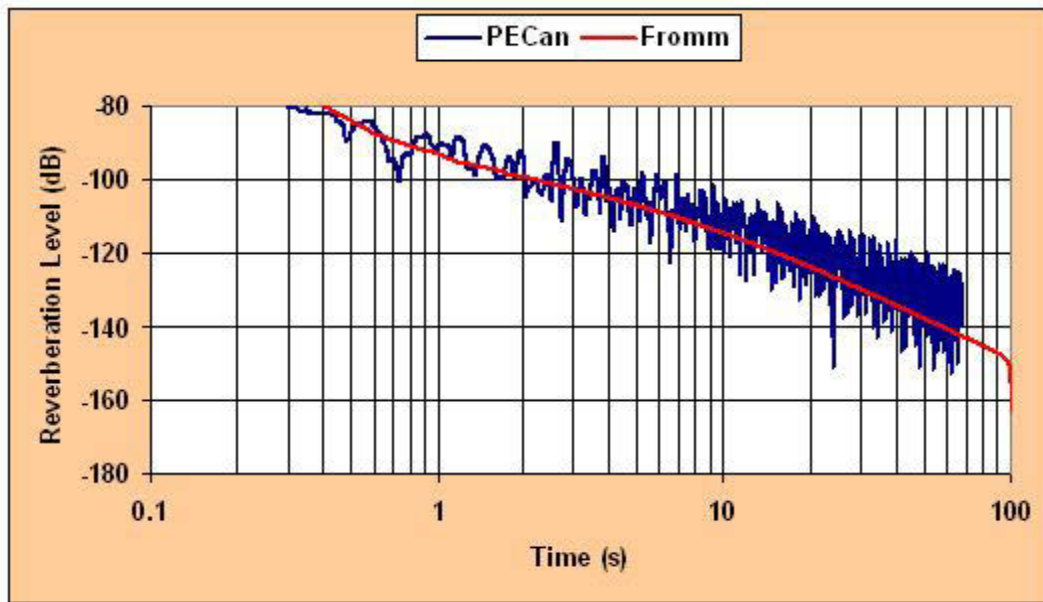


Figure 4. A preliminary comparison of reverberation computations between PE and a ray code methods.

3 Summary of Project Results

This section contains a summary review of the progress that BNS made during the project.

3.1 Tasking

The tasks completed by the project team are as follows:

Kickoff Meeting;

Task 1: Definition of model test cases, input data preparation;

Task 2: Compare PE reverberation to independent data;

Task 3: Compare PE target echo to independent data;

Task 4: Examine vertical PE field with range; and

Task 5: Recommendations for modifications to PECan – Go/No-Go decision for Task 6; and

Task 6: Make modifications to PECan (Please see paragraph below); and

Task 7: Final Reporting (mislabelled in the proposal as Task 6).

It was agreed during the Kickoff Meeting on 13 February that the project team would take the approach to make short, preliminary, attempts at Tasks 2, 3 and 4, in order to gain a rapid appreciation for any difficulties. This approach was found to be very useful to the project team. It became apparent early on that the vertical PE field study (Task 4) was more difficult than expected, and that the surface reverberation (in Task 2) was problematic. It became apparent in mid-March that there was insufficient time to continue the investigation and make substantive algorithmic changes in PECan without seriously affecting the core objectives of the study. Task 6 was therefore determined 'No-Go'.

3.2 Chronology of Effort

A chronology of effort in 2012 is set out in Table 1 below, cross-referenced to task number.

Table 1. Chronology of effort and corresponding contract task.

Period	Activities	Task(s)
Feb 13 - 15	Install Matlab™, get PECan to run, learn use of PECan, prepare modelling infrastructure on laptop. Preliminary definition of test cases. Prepare for kick-off meeting.	1
Feb 13	Kickoff Meeting (teleconference). Begin definition of test cases.	1

Feb 14-21	<p>Cataloging of available Reverberation Workshop data (and plotting in Matlab™)</p> <p>Initial work on writing Matlab™ scripts to recreate the bottom reverberation results presented previously in Dr. Gary Brooke's PowerPoint slides.</p> <p>Programming scattering functions.</p>	1, 2
Feb 22-26	<p>Initial work on examining the vertical field. FFT analysis via Matlab™ scripts.</p>	4
Feb 27-29	<p>Return to scattering functions, incorporate average scattering strength, and incorporate change of scattering strength with range to demonstrate effect that vertical wavenumber might have.</p> <p>Attempt Fortran Gnu compiler installation. Unsuccessful.</p>	4
Mar 1-3	<p>Incorporate surface and volume reverberation. Initial look at Wedge problem (Case 17).</p> <p>Matlab™ script to calculate in-plane bistatic reverberation.</p>	2
Mar 4-12	<p>Surface reverberation, water-air boundary, rigid surface top boundary.</p> <p>Perform test runs at all three frequencies.</p> <p>Start target echo comparison to BNS ray model.</p> <p>Matlab™ script clean-up (this was ongoing as the scripts matured).</p> <p>Email exchange with DRDC-A re progress to-date, and assistance with target echo comparison to the DRDC normal mode results. (Mar 12).</p> <p>Learn PECan for range-dependent cases (RW Case 17).</p>	2, 3
Mar 13-20	<p>'Goodness of fit' between reference data and PE method.</p> <p>Look at surface reverberation estimate versus distance from surface boundary within the first wavelength. Histogram study.</p> <p>Matlab™ Script clean-up.</p>	2, 4

Mar 21-29	Complete report. Address review comments. Submit report.	5, 7
-----------	----------------------------------------------------------	------

3.3 Deliverables

3.3.1 Teleconference Meetings

One formal meeting was held to kick-off the project. Mr. Martin Taillefer was in attendance at DRDC-Atlantic with the Scientific Authority, Dr. Dale Ellis, and Dr. Sean Pecknold, with Dr. Gary Brooke and Mr. Craig Hamm joining by teleconference from Victoria and Ottawa, respectively. Two technical email exchanges took place, March 12 and March 27. These events are listed in Table 2.

Table 2. Communications and Meetings.

Date	Type	Comments
Feb 13	Kick-Off	Discussion of priorities.
Mar 8	Progress, by email	Description of all progress to this date, including issues with 6 dB bias on boundary reverberations and vertical field properties.
Mar 9	Email	Dr. Ellis agreed the use of Lambert's Law and Chapman-Harris scattering functions was OK. Also that the Wedge problem (Case 17) could be interpreted as a 'bowl' rather than the full 3D problem. Informed Dr. Ellis of No-Go on Task 6.
Mar 12	Progress, by email	Request of target echo data from DRDC. Discussion of general progress.
Mar 27	Email	Clarification on Problem 17 parameters.

3.3.2 Software, Databases and Documentation

During the project changes to the PECAN output files of transmission loss were made to facilitate the calculation of reverberation. These changes are documented in Annex D.1. MatlabTM programming language scripts were produced which enabled the calculation of reverberation, target echo, and related studies. All relevant MatlabTM script listings are provided on a DVD as part of the deliverables. Notes on the MatlabTM environment and listings of the scripts central to the reverberation investigation are included in hardcopy in Annexes D.2 and D.3, respectively.

The MatlabTM scripts in this contract are research oriented. Reasonable attempts have been made to make the scripts usable by those other than the developer through the use of extensive

comments, indentation, and usually descriptive parameter names. However, new users to the scripts will need some time to gain comfort in their use. As a general rule, if a script prefix ends in a number, use the highest number, as this typically represents a higher evolution of the script.

Table 3 provides a summary of the major scripts which DRDC-Atlantic may wish to execute at some time.

Table 3. Catalog and description of developed MatlabTM scripts.

MatlabTM script name	Purpose
plot_Fromm_P[11,12,13]_f[250,1000,3500]_botrvb.m	Plot Fromm's RW bottom reverberation reference data [19].
plot_ray_P[11,12,13,17]_f[250,1000,3500]_[volrvb,echo,sfcrvb,].m	Plot specific reference data from the BNS ray model. These are standalone scripts, but are also called by scripts which calculate reverberation.
plot_ellis_P17_[botrvb, echo].m	Plot reference data from DRDC-A Normal Mode clutter model. Standalone script, but also called by scripts which calculate reverberation.
read_RWreverbm plot_RWProb[11,12,13,15].m	User selects specific data from the RW. Standalone scripts.
read_PECan_petlr.m	Simply reads and plots petlr.out file contents.
reverb_pervb[1,2,3,4].m bistatic_pervb1.m reverb_petlr[1,2,2b,3,4].m reverb_airtop.m	The evolution of scripts which calculate reverberation from pervb.out and petlr.out files. Requires functions to read the PECan output file headers.
fn_read_pervb_header.m fn_read_petlr_header.m	Functions. Read the headers of pervb.out and petlr.out files. Called by: reverb_pervb[#].m bistatic_pervb1.m reverb_petlr[#].m reverb_airtop.m
fn_integrate_maclambert.m fn_integrate_chapmanharris.m	Functions. Provide the result of integrating the surface scattering functions to θ_{\max} per Eq. (14). Called by: reverb_pervb[#].m bistatic_pervb1.m reverb_petlr[#].m reverb_airtop.m

	reverb_histogram.m
PEcan_run.m (single input file run) PEcan_batch_run.m (multiple input files)	Used to run PECan.exe via the Matlab™ shell. Enables managing input and output filenames beyond the fixed filename structure of PECan.
psd.m psdchk.m specplot.m fftfilt.m check_order.m spectrum.m hanning.m boxcar.m	MATLAB™ Signal Processing toolbox functions used for the vertical field study.
reverb_surface_study.m symbols.m (Greek symbols)	Scripts required to examine the results of computing surface reverberation from transmission loss within one wavelength of the sea surface boundary.
vert_field.m	For studying the vertical spectrum from the pe.tlz output file.
plot_integrated_scattering_fns.m	Plot Eq. (14) versus θ_{Max} for both boundary scattering functions.
shortening_timeseries.m wavenumber_angle.m weighting_fn.m	Explore effect of shortened data length on spectrum output. Determining angle from vertical wavenumber, k_z . Explore behaviour of some empirical wavenumber/scattering weighting functions.
determine_spectrum_params.m	Assists in setting spectrum/FFT parameters for use in the vertical wavenumber study.
reverb_histogram.m modelled_histogram.m	Scripts for exploring ideas re ‘goodness of fit’ to reference data.
compare_surface.m	Script to compute and compare surface reverberation for Problem 11, 250 Hz, using free surface, air layer and a rigid

The PECan source code was also altered during the course of the project to enable the investigation. The main changes to PECan source code enabled:

- Larger array sizes for greater horizontal range;
- Larger array sizes for greater depth (3500 Hz cases)
- Simplified output of the pe.tlr file, written to a new output file petlr.out
- A new output file pervb.out which contains transmission loss along the top and bottom boundaries as well as in the water column at the source depth.
- Refer to Annex D for a detailed description of these two new output files.

3.3.3 Report

This report constitutes the Contractor's Report in the DRDC format, due on March 30, 2012, the termination date of the contract. Due to the short timeframe in which the contract was awarded and executed there are no other formal technical reports.

3.4 Methodology

This section describes the methodology used to calculate estimates of reverberation and target echo. Methodologies for estimating reverberation, target echo and the vertical field properties are provided in sections 3.4.1, 3.4.2 and 3.4.3, respectively. Section 3.4.4 describes a simple method for seeing the effects of changing the average scattering function angle from Eq. (14), θ_{\max} , with range.

The high level methodology is described. The problem set was drawn from the Reverberation Workshop [19]. Specifically Problems 11, 12, 13, and 17 were used to assess the suitability of the methods proposed in section 2. Problems vary in complexity from range independent (Problems 11 through 13) to range dependent (Problem 17). Surface, volume, and bottom reverberation time history estimates were calculated, as well as the target echo time history. This was done for frequencies 250 Hz, 1000 Hz and 3500 Hz, covering almost four octaves. For surface, volume, and target echo, results obtained by the 'PE method' were primarily compared to results obtained from a proprietary ray-based model provided by Brooke Numerical Services (BNS). For bottom reverberation estimates, the PE method results were compared to the results provided by Fromm, whose data are included in the Reverberation Workshop data set [19]. The Fromm data was calculated using the BiRASP ray-based model [20].

For each Reverberation Workshop (RW) Problems the transmitter and receiver are in the same vertical plane, but not co-located. Therefore the PECan model was run for two PECan source depths allowing the bistatic estimate of reverberation and target echo to occur in post-processing. The algorithms for estimating reverberation and target echo were carried out by post-processing the PECan output. The post-processing was carried out using a set of scripts developed in the

MatlabTM scripting environment. The primary scripts used to calculate the reverberation and target echo estimates are provided in Annex D.3.

Tables 4 and 5 provide the environmental parameters and the signal parameters used to form the reverberation and target echo estimates.

Table 4. Table of Environmental properties See Ref [19].

Parameter	Value (units)	Notes
Sound speed in Water	a) 1500 m/s b) $c(z) = 1530 - 0.3 z$ c) $c(z) = 1490 + 0.1 z$	a) RW Problems 11 & 17 b) RW Problem 12 (summer) c) RW Problem 13 (winter) <i>Sea surface at $z = 0$.</i>
Water Depth	RW Problem 11, 12, 13: 100 m RW Problem 17: 200 m to 5 m over 7.4 km.	
Absorption Losses in Water	$f = 250$ Hz: 0.00006276 dB/ λ $f = 1000$ Hz: 0.000104 dB/ λ $f = 3500$ Hz: 0.00010275 dB/ λ	As defined by the Thorp equation [21] and sourced directly from [22].
Absorption Losses in Sediment	0.5 dB/ λ	The bottom material is modelled as a fluid.
Density of the medium	Water: $\rho = 1.0$ g/cm ³ Sediment: $\rho = 2.0$ g/cm ³	Below the sediment layer a Perfectly Matched Layer boundary condition is employed, therefore Block 7 of the PECan input file (second last line in pe.dat) is ignored.
Sound speed in Sediment	1700 m/s	Compressional only.
Sediment Thickness	20 m	Perfectly Matched Layer is used.
Bottom Scattering	Mackenzie-Lambert formula $\mu_{dB} = -27$ dB	See Section 2.4 Eq. (12); and [23].
Sea Surface Scattering	Chapman-Harris formula Wind = 19.44 kts (10 m/s)	See Section 2.4, Eq. (13); and [24]
Volume Scattering	$S_V = -73$ dB/m ³	See Section 3.4.1
Calculation Grid		
Dr	$f = 250$ Hz: 5 m $f = 1000$ Hz: 2.5 m $f = 3500$ Hz: 2.5 m	$\sim \lambda$ $\sim 2 \lambda$ $\sim 6 \lambda$
Dz	$f = 250$ Hz: 0.25 m $f = 1000$ Hz: 0.05 m $f = 3500$ Hz: 0.02 m	$\lambda / 24$ $\lambda / 30$ $\lambda / 21$

Table 5. Table of signal parameters.

Parameter	Value (units)	Notes
Source Level	SL = - 6.29 (dB)	See Ref [25]. Based on Gaussian shaded waveform.
Pulse duration	$\tau = 0.02$ sec (250 Hz) $\tau = 0.08$ sec (1000 Hz) $\tau = 0.005714$ sec (3500 Hz)	Based on Gaussian shaded 3-dB bandwidth of $f/20$.
Target Strength	TS = 0 dB (default) TS = 8 dB (See Notes)	For Problem 17 only.

3.4.1 Reverberation

The methodology for reverberation follows the description given in section 2.4. Under this contract the method is implemented in the MatlabTM software language. The implementation details are provided in this section. The MatlabTM scripts are provided in Annex D.3.

While many MatlabTM scripts were produced, the MatlabTM scripts employed to calculate reverberation based on the output from PECan transmission loss output are few. There are three main scripts to consider, all of which contain the same core algorithm as described in section 2.4. The main differentiator between the scripts is what output files they read in order to support the reverberation algorithm. Any mention of bi-static in this report refers only to the source and receiver being within the same vertical plane.

The series of scripts named `reverb_petlr[n].m` read the `petlr.out` file from PECan. This is a new file (described in detail in Annex D.1.1) which is based on the `pe.tlr` output file, which has been modified to output the transmission loss in decibel format. This file provides transmission loss versus range, at the receiver depth(s) as defined and contained in the file `pe.dat` (PECan input file). When the bathymetry is not flat, the `petlr.out` file is not useful for obtaining bottom transmission loss as it does not track the bathymetry as does the `pervb.out` file. When using the `reverb_petlr.m` scripts, the user is responsible to match the desired reverberation component with the appropriate receiver depth.

The series of scripts named `reverb_pervb[n].m` read the `pervb.out` file from PECan for reverberation, and `petlr.out` files for target echo. The `pervb.out` file is an entirely new file (described in detail in Annex D.1.2). This file provides transmission loss versus range, at the following depths: the sea-surface boundary (for surface reverberation), the source depth (which is used for volume reverberation), and the bottom depth (for bottom reverberation). Note that `pervb.out` is necessary when using a case with range-dependent bathymetry as the bottom transmission loss tracks the bathymetry when extracting the transmission loss from the internal PE field.

The MatlabTM script `bistatic_pervb1.m` calculates reverberation in the bi-static case. This script requires more attention on behalf of the user. Manual editing is required to setup the correct inputs and reference data. In order to calculate bi-static reverberation, we must perform two PECan runs because we cannot place a source on a boundary in the PE model. The geometry is illustrated in Figure 5. If we were able to place a source on the boundary we could invoke

reciprocity and perform a single PECan run. The two required PECan runs are: one run with the source at the transmitter depth, and one run with a source at the receiver depth. This will provide both outgoing and return path transmission losses. The input files, using our naming convention, required for this kind of calculation would be, for example: RW_P11_S(Tx depth)R(target depth) for outgoing path, and S(Rx depth)R(target depth) for the return path. Note: Using the target depth as a receiver depth in the PECan input file will provide the two transmission loss paths required for the target echo in the petlr.out file.

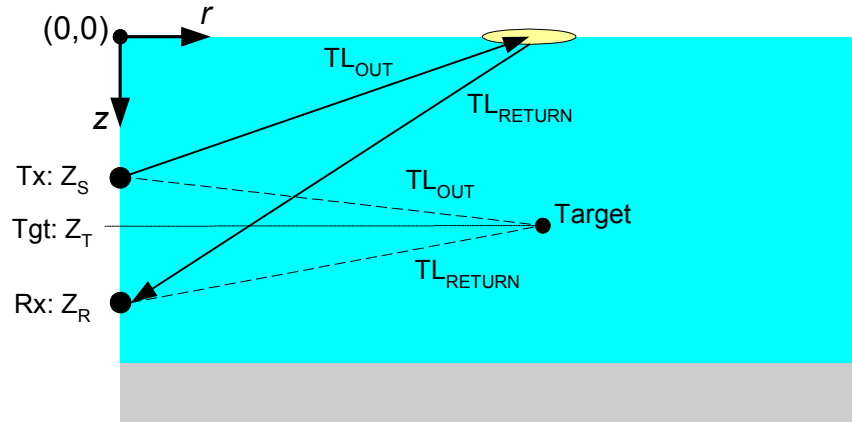


Figure 5. Geometry for true bi-static calculation of reverberation and target echo.

Figure 6 shows the geometry used to calculate the reverberation components and echo level. The propagation paths for TL_S , TL_V and TL_B represent the outgoing paths. As described above, the pervb.out file returns the transmission loss from these paths.

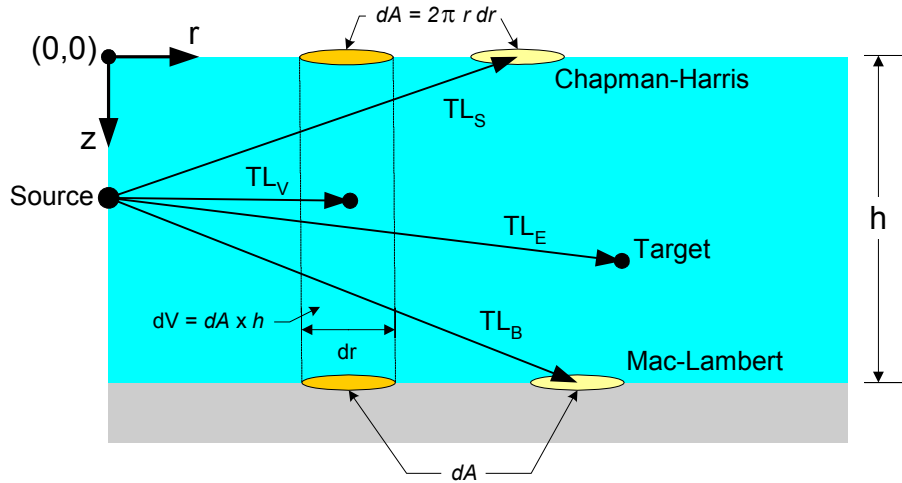


Figure 6. Cross-section (from rotation of 2π) of geometry used to calculate volume and boundary reverberation components. Transmission loss for the reverberation components are available in the PECan pervb.out output file.

3.4.1.1 Surface Reverberation

The calculation of surface reverberation provided the largest source of difficulty during the study. These difficulties are described in detail in section 3.5.5 and graphical results are provided in Annex A.5.

The PECan input file can toggle the sea-surface boundary condition between a free surface and a rigid surface. Normally the sea surface is toggled to a free surface. In an effort to understand the surface reverberation difficulties, three approaches for treating the boundary conditions at the sea-surface were explored. These included: a free surface, a rigid surface, and a 5m air layer over top of the sea-surface interface.

For all surface reverberation calculations the Chapman-Harris equation, Eq. (13), was used, as was the ‘cookie-cutter’ approach of Eq. (14). The Chapman-Harris scattering function for the three frequencies in this study are shown in Figure 7, while the integration of this function, Eq. (14), is given in Figure 8.

To determine the energy scattered from a surface scattering patch, the averaged surface scattering strength S_{av} (m^{-2}) is multiplied by the scattering patch area, dA . This patch has a radial dimension determined by the distance between each range sample in the transmission loss. This is shown in Figure 2, where $\Delta t = \Delta r/c_0$ is the time between range samples. The integration over the pulse length occurs in Figure 2 where the time bins are summed over a time interval representing the pulse length, τ_{eff} .

It is very important to note that throughout this report, 6 dB have been subtracted from both the displayed surface reverberation and the bottom reverberation.

The rationale for this is explained here. There were two independent sources of bottom reverberation, the RW cases (multiple problems, three frequencies) and the proprietary ray model operated by BNS. In one case there were three estimates when including the results of the DRDC normal mode model. For bottom reverberation it was observed in all cases that the reverberation estimates from the PE method (this work) were consistently about 6 dB high. At near ranges, when using a rigid surface boundary condition, the surface reverberation estimates also appeared 6 dB high. That is, both boundary reverberations appeared 6 dB high. But the volume reverberation suffered no such effect.

The volume reverberation exception provides a clue. The PE accounts for all of the propagating energy in the waveguide (up-going and down-going) and combines that energy together. In the volume reverb case where an effective scatterer is placed at a distinct point in the water column (by integrating the volume scattering strength through depth) the agreement straight out of the PE is excellent. This is likely because there is actually up and down going energy interacting with the effective volume scatterer. When ray theory is used, effectively only the down-going rays that hit the ocean bottom are used in the reverberation calculation. Just above the bottom there are two types of rays. These ray types merge when the field point moves onto the surface (similarly for the ocean surface, except we speak of up-going rays). In the ray model the liberty exists to choose these rays, but not so with the PE. The PE automatically includes both ‘ray types.’ Therefore in this comparison to the ray approach it is possible that the one-way TL should be divided by a factor of 2 (2-way TL by a factor of 4) yielding the factor of 6 dB.

Now we compare to the normal mode approach for surface and bottom transmission loss. Consider an isovelocity water column. The modal depth function for the receiver is $\sin(kz \cdot z)$ which vanishes at $z = 0$ to satisfy the pressure-release boundary condition there. But $\sin(kz \cdot z) = [\exp(i \cdot kz \cdot z) - \exp(-i \cdot kz \cdot z)]/2i$, which can be interpreted as the sum of an up-going and a down-going 'ray' – here kz is one of the eigenvalues of the normal modes. At the surface, $z = 0$, the down going contribution is dropped, leaving $1/2i$ at the surface. Similarly, at the bottom, the $\exp(i \cdot kz \cdot z)$ term is discarded and $\exp(-i \cdot kz \cdot z)$ term is retained. The result is a factor of $1/2i$ in pressure, which is equivalent to 6 dB in TL.

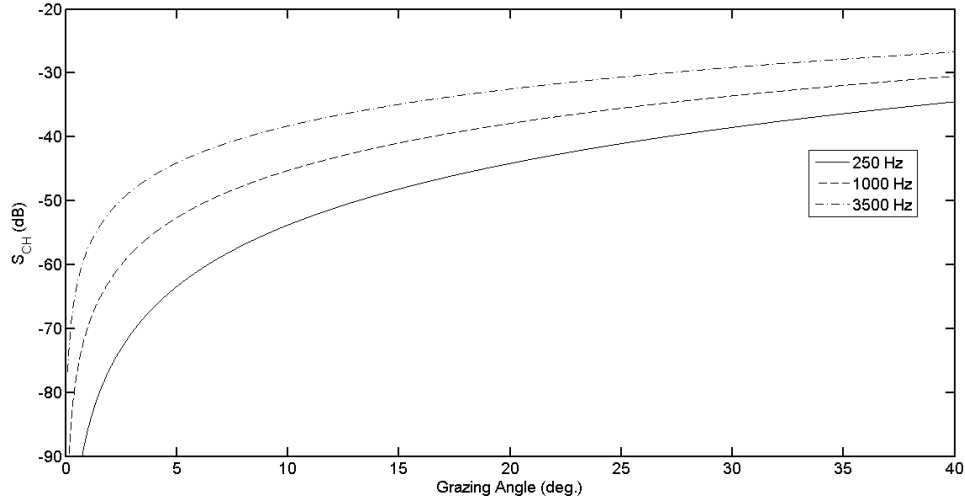


Figure 7. Chapman-Harris sea-surface scattering function at the three frequencies in this study.

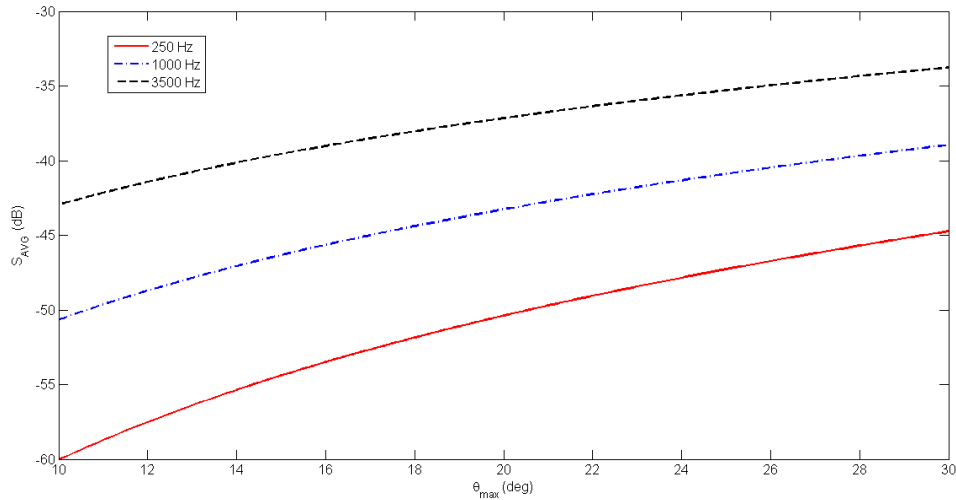


Figure 8. Equation (14) plotted between θ_{Max} 10 and 30 degrees for Chapman-Harris surface scattering.

3.4.1.2 Volume Reverberation

The volume reverberation is calculated using a single volume scattering strength, S_V [m^{-3}], integrated over the scattering volume, dV . The scattering volume is calculated by multiplying the same scattering area, dA , as determined for the surface and bottom reverberation and then multiplied by the water column, h . In terms of transmission loss, the volume element is assumed to be at the same depth as the transmitter, as is shown in Figure 6.

Unlike the surface and bottom reverberation (sections 3.4.1.1 and 3.4.1.3) no corrections to the result provided by PECAN and the MatlabTM scripts are necessary for volume reverberation.

3.4.1.3 Bottom Reverberation

For all bottom reverberation calculations the MacKenzie-Lambert Eq. (12) was used, as was the ‘cookie-cutter’ approach of Eq. (14). The MacKenzie-Lambert scattering function is independent of frequency, and is shown in Figure 9, while the integration of this function, Eq. (14), is given in Figure 10.

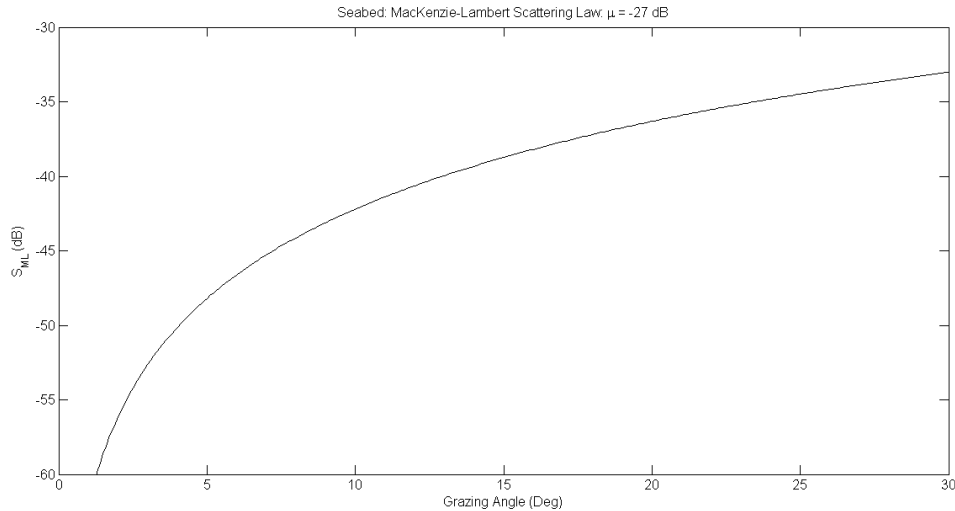


Figure 9. Equation (12) Mackenzie-Lambert bottom scattering function with $\mu_{dB} = -27$ dB.

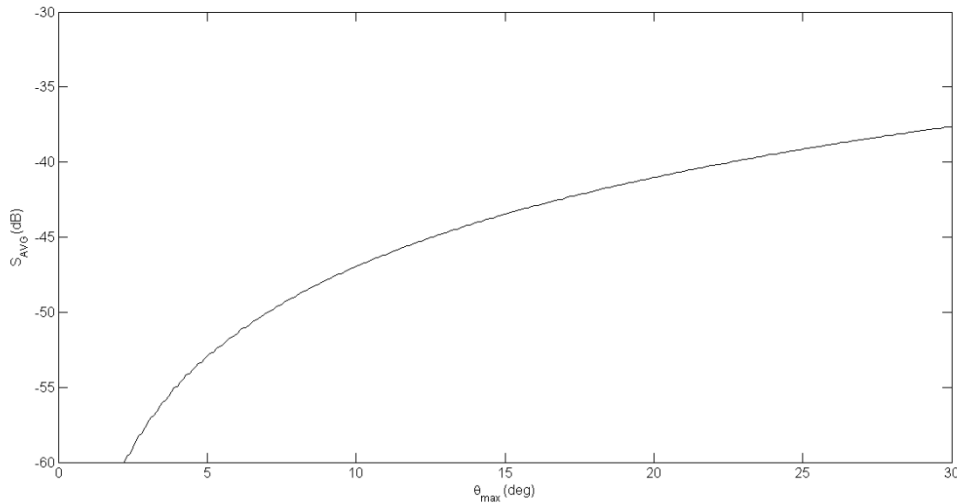


Figure 10. Equation (14) plotted between θ_{Max} 0 and 30 degrees for MacKenzie-Lambert bottom scattering.

The methodology to determine the energy scattered from a surface scattering patch is the same as described for surface scattering.

It is very important to note that throughout this report, 6 dB have been subtracted from both the displayed surface reverberation and the bottom reverberation. The rationale for this is discussed in section 3.4.1.1.

3.4.2 Target Echo

The target echo is calculated using a single point scatterer. In terms of the MatlabTM scripts it is calculated the same as the volume reverberation with the exception that the scattering strength is replaced by the Target Strength, TS. As for the reverberation calculation the target echo energy is summed at each range step of the PE model output. However, when this occurs the target strength is applied as though it applies to the entire pulse length, which over counts the contribution. Therefore to obtain the final estimate for target echo the target echo sum is divided by the number of time bins contained within the pulse duration ($\tau / \Delta r / c_0$, *nbins* in the MatlabTM scripts) to account for the overestimate.

The series of scripts named `reverb_petlr[n].m` read the `petlr.out` file from PECAN. This is a new file (described in detail in Annex D.1.1) which is based on the `pe.tlr` output file, which has been modified to output the transmission loss in decibel format. This file provides transmission loss versus range, at the receiver depth(s) as defined and contained in the file `pe.dat` (PECAN input file). This file, therefore, is used in every instance when the target echo transmission is required. In the special case that the target depth is the same as the source depth, then the volume transmission loss obtained from the `pervb.out` file can be used. If the bathymetry is not flat, `petlr.out` is not useful for obtaining bottom transmission loss as it does not track the bathymetry.

Referring to Figure 5, in a bi-static scenario, when only the target echo is required reciprocity can be used to reduce the problem to one model run. In order to obtain the two transmission paths the input file source is placed at the target depth, and two receivers are placed at the sonar Tx depth (outgoing) and the sonar Rx depth (return).

3.4.3 Vertical Field

In this section we describe the methodology for examining the vertical pressure field produced by the PECan model. We define the vertical field as the variation of acoustic pressure with depth in the calculated PE field. This vertical field may be observed at any range from the source location. In PECan this information is captured in the `pe.tlz` file. The motivation of this exercise was to see if information from the vertical field could be used to more accurately model the boundary reverberation. For example, if the reverberation estimates were too high, we could limit the influence of the energy propagating at all angles by restricting the scattering functions to account for energy up to maximum grazing angles.

In the PE model methodology there is no direct control over the angular content of the propagating energy, such as exists in a ray model where ray angles can be individually tracked. For boundary reverberation we are, at this time, restricted to the ‘cookie cutter’ approach using Equation (14), repeated here for convenience,

$$S_{av} = \frac{1}{\theta_{max}} \int_0^{\theta_{max}} S(\theta) d\theta \quad (14)$$

Where S_{av} is the average scattering strength, and θ_{max} defines the cutoff (the ‘cookie cutter’) grazing angle for the maximum vertical angle content of the propagating energy. Once calculated, the single value S_{av} is applied equally to all propagating angles. This occurs implicitly since energy at all propagating angles is included in the transmission loss and this is all we have at our disposal. Decreasing the angular content could be partially achieved by limiting the launch angles of the source-function; however this would also restrict the near-range performance at high grazing angles.

Nominally the value for θ_{max} can be set at the critical angle, θ_{crit} , defined as,

$$\cos \theta_{crit} = \frac{c_w}{c_{sed}} \quad (15)$$

where c_w is the sound speed in water, and c_{sed} is the compressional sound speed in the sediment. Using values $c_w = 1500$ m/s and $c_s = 1700$ m/s, the critical angle is approximately 27° . Which is the angle used in this study.

In spatial analysis positions (x , y and z) and their corresponding wavenumbers (k_x , k_y and k_z) each form a Fourier Transform pair. This relation is exploited to obtain the k -space spectrum of the

vertical field. The k -space spectrum in turn provides the desired angular information via the relation,

$$k_z = |\vec{k}| \sin \theta_g \quad (16)$$

where θ_g is the grazing angle.

PECan was set, arbitrarily, to output the .pe.tlz file once every 1000 range steps to provide a manageable number of vertical fields with range. As illustrated in Figure 11, at each of the output ranges a Fast Fourier Transform (FFT) was applied to the in-water portion of the vertical field (e.g. sediment contributions ignored). The FFT length was chosen such that the smallest power-of-two FFT length would encompass the in-water portion of the vertical field. The FFT length invariably exceeds the data length so the difference is made up with zero padding. The FFT was shaded with a Hanning window and there was no overlap. Many combinations were attempted and this approach yielded output which was free of sidelobes introduced by a boxcar window and also provided enough spectral resolution to differentiate between any close modes. For example, if at 3500 Hz the vertical sampling ‘period’ is 0.02 m, and a 512 point FFT is calculated the spectrum resolution will be $1 / (0.02 \cdot 512) \cong 0.1 \text{ m}^{-1}$. For a 1024 point FFT, this value is halved.

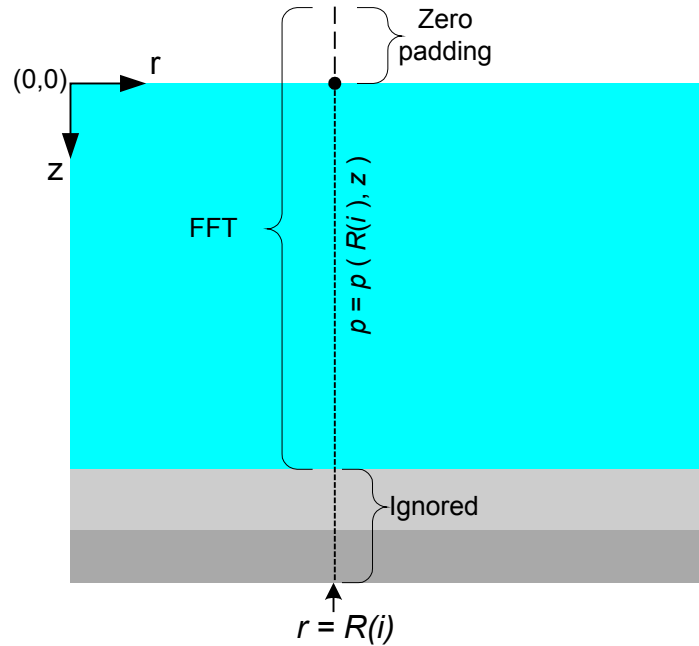


Figure 11. Setup for FFT of the vertical acoustic field.

Table 6. Summary of frequencies, wavenumber, vertical sample period and Nyquist frequency for vertical spectra.

Frequency (Hz)	Wavenumber \underline{k} (m ⁻¹)	Vertical Sample (m)	Nyquist Frequency (m ⁻¹)
25	0.105	0.125	4
250	1.05	0.25	2
1000	4.19	0.05	10
3500	14.66	0.02	25

3.4.4 Reducing θ_{\max} as a Function of Range

It is expected that as the propagation continues down-range that the higher grazing angle components are attenuated through bottom and spreading losses. This can be modelled by forcing a reduction in θ_{\max} with increasing range. Simply to observe the effect of this reduction with range, θ_{\max} was reduced linearly with range as shown in Eq (17) and indicated in Figure 12. Reverberation Workshop Problem 11 at 250 Hz was used to compute the bottom reverberation using this method. In the results presented in Section 3.6 the value of θ_{\max} at zero range was 30°. At maximum range the value of θ_{\max} was reduced to: 30° (e.g. no effect), 20° and 10°. At each range step θ_{\max} was calculated using,

$$\theta_{Max}(r_i) = \frac{\theta_{Max}(R_{max}) - \theta_{Max}(R = 0)}{R_{max}} r_i + \theta_{Max}(R = 0). \quad (17)$$

The results of this demonstration are described in Section 3.6.1 and graphical results are provided in Annex B.

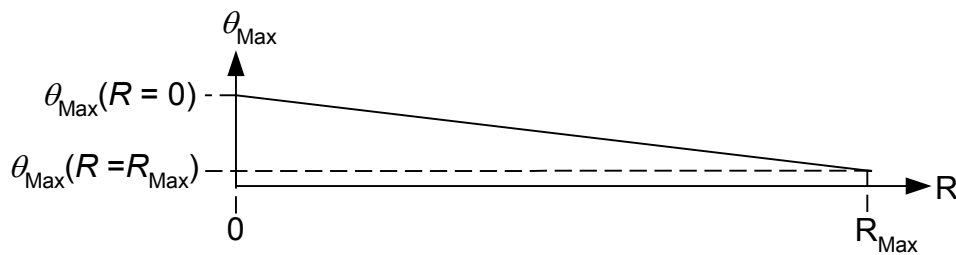


Figure 12. Linear reduction of θ_{\max} with increasing range.

3.5 Reverberation and Target Echo Results

In this section an overview of the results of the contract work is given. Graphical results for this section are supplied in Annex A and organised by Reverberation Workshop problem number. Annexes A.1 through A.4, inclusive, contain the results for RW Problems 11, 12, 13, and 17, respectively. Each of these sections contains estimates of the reverberation for surface, volume, and bottom reverberation and estimates of the target echo. In most cases estimates are provided at

250 Hz, 1000 Hz and 3500 Hz, spanning approximately 4 octaves. An additional subsection, A.5, contains the results of the study on how the sea surface boundary condition affects estimate of the surface reverberation.

For bottom reverberation the reference data is taken from the Reverberation Workshop data set [19] which was computed using the BiRASP ray-based performance model of Fromm *et al.* [20]. For surface and volume reverberation the estimates are compared to a proprietary ray model provided by Brooke Numerical Services. Target echo estimates are also compared to the BNS ray model result. In all cases but one the reference data is plotted as a solid red line on each plot. The PE method estimates are plotted in solid black lines. In all RW Problems the source is at 30 m depth and the receiver is at 50 m depth. The target is at 50 m depth in all cases except in Problem 17 where it is 10 m. In the case of Problem 17 a comparison to results from the DRDC Clutter Model is also available. The DRDC model is based on adiabatic normal modes [3].

The BNS ray model has compared very favourably to many benchmark cases on reverberation. Similarly, the results for target echo appear to compare favourably to the reference data. However, with respect to the Target echo it is less certain because the ray model may have limited the number of rays involved in the estimate i.e., windowing. The ray model, for reverberation, simply integrates all of the available energy, but this is not so with target echo. With this caveat in mind we suggest that it may be prudent for DRDC to check some of the PE target echo results with a standard model such as CASS-GRAB, for example. MWS would welcome this comparison.

The surface reverberation results presented in this section all utilised the free surface boundary condition. Due to the problems with the sea surface reverberation, described in section 3.5.5 all of the plotted results for surface reverberation have been biased by an additional 55 dB. This is to allow for better comparison to the shape of the reference ray based data. As described in section 3.1.4, both the surface and bottom reverberation also have 6 dB subtracted from the raw estimate of reverberation. The volume reverberation results have not been adjusted. The adjustments made to the surface and bottom reverberation estimates are clearly stated on each affected plot.

3.5.1 Reverberation Workshop Problem 11 (RI, Isovel.)

Figure 13 shows the geometry and environmental parameters for Reverberation Workshop Problem 11. The environment is comprised of a 100 m deep isovelocity water column over a lossy fluid bottom. The perfectly matched layer (PML) option of the PECan input file was used throughout the report analysis. Pictured in this diagram is an optional air layer of 5 m thickness. The air layer result is discussed separately in section 3.5.5, and that result is shown in Annex A.5, Figure 37.

The results of the reverberation calculations are provided in Annex A.1.1, Figures 17 – 19 for 250 Hz, 1000 Hz and 3500 Hz, respectively. Overall the reverberation results appear to follow the reference data very well, with the exception of the surface reverberation at 1000 Hz which falls off with range (already taking into account the 55 dB bias).

The results of the target echo calculations are provided in Annex A.1.2, Figures 20 – 22 for 250 Hz, 1000 Hz and 3500 Hz, respectively. The PE Method target echo results compare favourably to the ray model reference data.

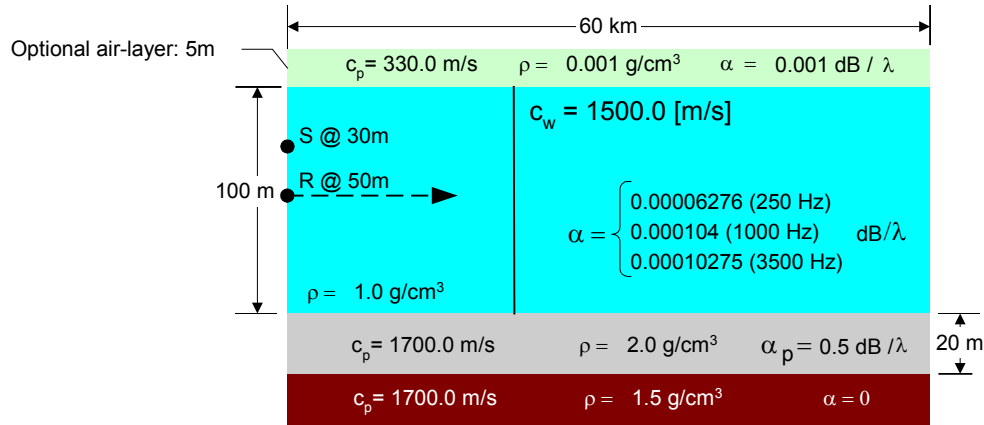


Figure 13. Geometry for Reverberation Workshop Problem 11. The annotated parameters are universal for RW problems 12, 13 and 17, below.

3.5.2 Reverberation Workshop Problem 12 (RI, Summer)

Figure 14 shows the geometry and environmental parameters for Reverberation Workshop Problem 12. The environment is comprised of a 100 m deep downward refracting water column over a lossy fluid bottom. Alternatively, this problem is referred to as containing the ‘summer’ sound speed profile. As for Problem 11 the perfectly matched layer (PML) option was used in the PECan input file.

The results of the reverberation calculations are provided in Annex A.2.1, Figures 23 – 25 for 250 Hz, 1000 Hz and 3500 Hz, respectively. The reverberation results appear to follow the reference data, with the exception, again, of the surface reverberation at 1000 Hz which falls off with range (already taking into account the 55 dB bias). The fall off appears more or less linear.

The results of the target echo calculations are provided in Annex A.2.2, Figures 26 – 28 for 250 Hz, 1000 Hz and 3500 Hz, respectively. The PE Method target echo results compare favourably to the ray model reference data.

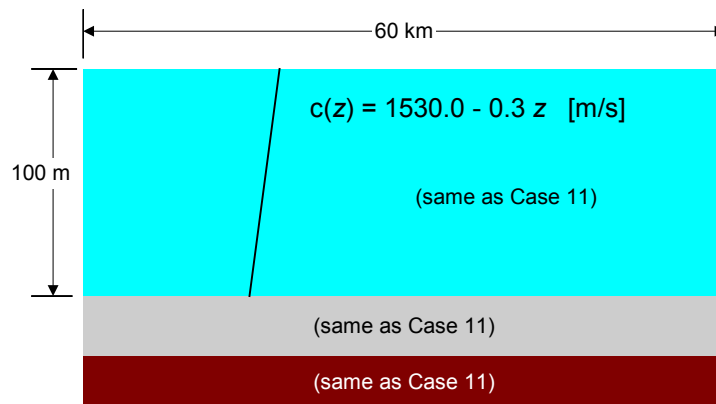


Figure 14. Geometry for Reverberation Workshop Problem 12 (‘summer’).

3.5.3 Reverberation Workshop Problem 13 (RI, Winter)

The geometry and environmental parameters for Reverberation Workshop Problem 13 is shown in Figure 15. The environment is comprised of a 100 m deep upward refracting water column over a lossy fluid bottom. Alternatively, this problem is referred to as containing the ‘winter’ sound speed profile. As for Problem 11 the perfectly matched layer (PML) option was used in the PECan input file.

The results of the reverberation calculations are provided in Annex A.3.1, Figures 29 – 31 for 250 Hz, 1000 Hz and 3500 Hz, respectively. Overall the reverberation results follow the reference data quite well, with some exceptions. The surface reverberation at 1000 Hz falls off with range (already taking into account the 55 dB bias) and the bottom reverberation appears to falter at the longer ranges (> 45 seconds). At 3500 Hz the bottom reverberation falters beyond about 55 seconds.

The results of the target echo calculations are provided in Annex A.3.2, Figures 32 – 34 for 250 Hz, 1000 Hz and 3500 Hz, respectively. The PE Method target echo results compare quite favourably to the ray model reference data.

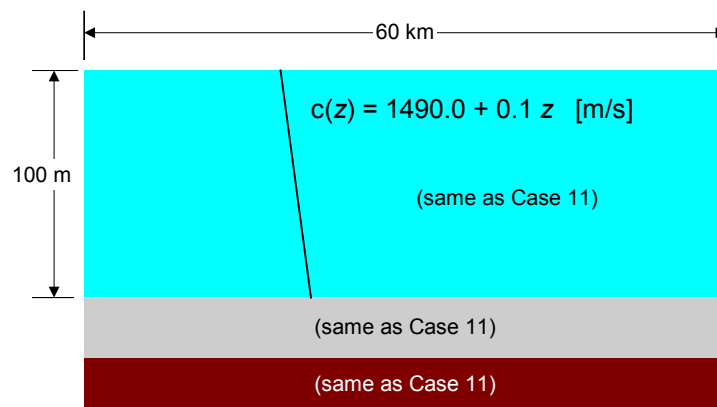


Figure 15. Geometry for Reverberation Workshop Problem 13 ('winter').

3.5.4 Reverberation Workshop Problem 17 – Wedge (RD, Isovel.)

The geometry and environmental parameters for Reverberation Workshop Problem 17 is shown in Figure 16. From the point of view of the source at zero range the RW bathymetry is comprised of a planar upslope wedge from 200 m depth to 0 m depth at 7.4 km. In this study we have, by agreement with the Scientific Authority, simplified the wedge to be a conical bowl. The geometry can therefore be imagined to be Figure 16 rotated about a vertical axis located at $R = 0$. We have extended the environment to 8 km range with the last 600 m comprised of a 5 m of water depth to avoid having zero water depth as a precaution. The sound speed profile is isovelocity placed over a lossy fluid bottom. Alternatively, this problem is referred to as the ‘wedge’. As for Problem 11 the perfectly matched layer (PML) option was used in the PECan input file.

Figure 35 of Annex A.4 shows a representation of the Problem 17 environment plotted as a function of time instead of the more usual down range distance. The PE model produces output

for all times in the plot. Eventually, in time, the computed transmission loss estimates interact with the bathymetry and yield transmission loss *within* the sediment beyond the bathymetry intersections. At times where this occurs, the target echo and reverberation results are unreliable.

The results of the reverberation calculations are provided in Annex A.4.1, Figures 36 – 38 for 250 Hz, 1000 Hz and 3500 Hz, respectively. Overall the reverberation results follow the reference data quite well. At 250 Hz, Figure 35, both the surface and volume reverberation compare well to the reference ray data. For the bottom reverberation the ray model and the normal mode agree well over the range, with the ray model and PE Method agreeing at short ranges (< 2 sec.). This is likely due to the normal mode lacking some of the high grazing angle energy at short range. The reverberation data by the PE method at 3500 Hz (Figure 37) appears to be slightly low as compared to other cases with the PE data just grazing the ray data.

The result of the target echo calculation is provided in Annex A.4.2, Figures 39 – 41 for 250 Hz, 1000 Hz and 3500 Hz, respectively. Due to the target depth intersecting the bathymetry we expect the estimates to reduce drastically at 9.86 sec. In this problem the reference target echo data was generated using a target strength of $TS = 8$ dB located at 10 m depth. The source is at 30 m depth and the receiver is at 50 m depth. The normal mode reference data sonar pulse characteristics were a “top hat” source of unit energy, $E_{NM} = 1$, with constant amplitude equal to the peak of a Gaussian pulse, and of duration τ_0 to provide equivalent energy – in essence the intensity is $1/\tau_0$ [26]. The pulse energy as employed in this study is $E_{PE} = -17.26$ dB. Therefore, for comparison the normal mode data were correspondingly reduced by E_{PE} at 250 Hz.

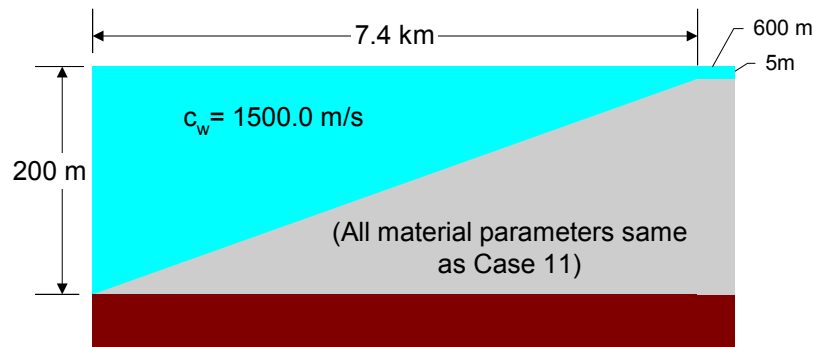


Figure 16. Geometry for Reverberation Workshop Problem 17. Note: By agreement with DRDC, the environment was modelled assuming a rotation of the image plane about $R=0$, modelling a bowl environment, and not the 3D planar wedge.

3.5.5 Surface Reverberation – Boundary Effects

In this section we show how the surface reverberation estimate is affected by the boundary condition and within a depth of the first wavelength.

The most problematic area during this research has been determining the surface reverberation. This is perhaps not too surprising since it is at a boundary where the acoustics pressure must go to zero. As seen in the results in Annex A, when the transmission loss nearest the surface is used and a large correction is applied, the fit to the ray data is quite good.

Alternate approaches to the free surface were to model the surface boundary as a rigid surface, and then to extend the water column with an overlying air layer. A selection of the results from these trials is provided in Annex A.5 in Figures 42 through 53, inclusive. Reverberation Workshop Problem 11 (RI, isovelocity) at all three frequencies (250 Hz, 1000 Hz and 3500 Hz) was employed for this demonstration.

Figure 42 shows the results of all three surface boundary conditions. The free surface and air layer results have large biases applied to them to illustrate their very low levels, and for presentation purposes. All results are compared to the BNS ray model. In terms of slope, one can see that the rigid surface result does not decay at the same rate as the other results. The rigid surface gives very good results at very short ranges (less than 3 seconds, Figure 43) when compared to the ray model reference, with no more than the 6 dB correction described in section 3.4.1. However, as the range increases the reverberation deviates much higher than the reference data. This occurs approximately linearly with range, with the estimate being high by about 15 to 20 dB at long range (~60 seconds). This was consistent across all cases when using the rigid boundary. Perhaps a deviation with range is no surprise, the rigid boundary changes the propagation as compared to the free surface (normal setting) condition, and it appears as though the difference accumulates with range. Furthermore, as the rigid surface boundary condition alters the propagation in the waveguide this negates usage of any other reverberation components (or echo). Therefore, two separate models runs must be done to get all reverberation components if using a rigid surface.

When a 5 m thickness layer of air was placed above the sea surface the slope was commensurate with the ray model output, and matching that of the free surface result. However, the air layer resultant reverberation level was more than 100 dB low (using the transmission loss on the boundary). From the scatter plot in Figure 44 observe that the rigid surface results and the free surface results are somewhat correlated (top plot). Observe the air layer and the free surface are identical except for a constant.

When using the rigid surface boundary condition the short range surface reverberation levels compare well with the reference data. Lacking in rigor, but potentially practical, it should be possible to compute very short range surface reverberation (less than 3 seconds, say) using a rigid surface boundary condition. This short range rigid surface result could then be used to calibrate a full range run using the free surface boundary condition. A more rigorous approach is clearly desirable, and some thoughts on this are forwarded in the Proposed Future Work (section 4.2).

We turn the discussion to demonstrate how the transmission loss changes with distance from the free surface top boundary, within the first wavelength of water depth. This was done by positioning five receiver depths at 0.2λ , 0.4λ , 0.6λ , 0.8λ and λ . Results were computed for Reverberation Workshop Problem 11 and Problem 12 (RI, summer profile) at all frequencies (250 Hz, 1000 Hz and 3500 Hz).

Graphical results are provided in the same Annex, Figures 45 to 53, inclusive. Due to the repetitive nature of these results only a subset of the model runs are presented in the Annex.

The following general conclusions are made from looking at these results:

1. Using the transmission loss within the first $\lambda/2$ of the surface will always yield an unacceptably low reverberation value (as compared to the employed reference data);
2. Using the transmission loss at $0.6-0.8 \lambda$ from the surface appears to yield a very good fit to the reverberation reference data;
3. Using the transmission loss from approximately 0.8λ to λ of the surface appears to yield a possibly high reverberation value (as compared to the employed reference data);
4. The reverberation (via the transmission loss) computed for each distance from the surface boundary is predominantly linearly correlated; and
5. Adding a bias of approximately 55 dB (after the -6 dB correction) appears to provide a reasonable estimate to the reverberation for all cases within the study (refer to surface reverberation in Figures contained in Annex A).

3.6 Vertical Field Results

In this section we describe the results of the analysis of the vertical pressure field. The graphical results are presented in Annex B.

Although the reverberation results appear quite favourable to the PE Method, we nonetheless expected to garner some detailed information about the angular content of the energy in the PE field. The hope was that this may lead to some refinement in the method, particularly if the predictions were unfavourable. The analysis did not bear fruit as was hoped. To illustrate, we show data from two scenarios: first, a case related to the 'ASA Wedge' at 25 Hz and second, Problem 11 from the Reverberation Workshop at 3500 Hz.

Figure 54 shows the complex vertical pressure field from the ASA Wedge (25 Hz) scenario at four ranges from the source (10, 20, 30 and 40 km). This data is extracted from the PECan output file `peAllModes.tlz`. One can see the pressure going to zero at the surface and generally non-zero as the field enters the sediment bottom. Looking at this data in terms of sines or cosines, from the surface to the depth of 200 m it is difficult to observe more than one full cycle. The spectrum of these data are shown in Figure 55 as the four lines without markers. The fifth line, with circular markers, indicates the spectrum of a simulated signal whose frequency components match those which are expected in the spectra of the real data. The simulated data spectrum was produced using the same FFT parameters as for the real data. This is to show that the FFT method parameters are capable of resolving the closely spaced spectral components when they exist. Therefore these data do not contain the expected spectral components.

In Figure 56 a synthesized time series with frequency components at 15, 50 and 100 Hz is shown. In this figure, from top to bottom the time series contain $\frac{1}{2}$, $\frac{3}{4}$, 1, and 3 wave cycles of the lowest frequency component (15 Hz), respectively. Figure 57 shows, one for one, the corresponding spectra of the time series shown in Figure 56. On the spectra the vertical red lines indicate the known frequency component locations. We are reminded in Figures 56 and 57 that when there is not at least one full cycle of a frequency component in a signal, even when that signal is highly sampled, that the signal is under sampled and will lead to aliasing.

We turn to a case using real data. Fig 58 shows the vertical pressure field for the first four vertical fields output in the P11_f3500_S30R50_pe.tlz file (source frequency 3500 Hz). The wavenumber at 3500 Hz is 14.7 m^{-1} . The source depth is 30 m. With a vertical sampling period of 0.02m, the sampling frequency is 50 m^{-1} , the Nyquist frequency is therefore 25 m^{-1} . Vertical field spectra corresponding to the data in Figure 58 (and four additional ranges) are shown in Figure 59. Above $k_z = 1$ there is no discernible signal in any of the spectra. Using Eq (16) relating the wavenumber to the vertical wavenumber and grazing angle, these spectra indicate θ_g of approximately 4° , which at close range seems intuitively much too small for the geometry.

Finally in Figure 60 we show a comparison between two wavenumber spectra at a range of 2.5 km. The spectra are observed to be different when the source depth is changed from 30 m to 15 m. There appears to be some modal behaviour in the spectra, but once more, the wavenumbers and corresponding grazing angles implied by these peaks are very low.

3.6.1 Reducing θ_{\max} as a Function of Range

Section 3.4.4 outlined the method for reducing the angle θ_{\max} as a function of range, according to Eq (17), thereby reducing the upper integration limit in Eq (14). The results of reducing θ_{\max} with increasing range are presented in Annex B.2.

Figure 61 presents the bottom reverberation plotted as a function of time for three different θ_{\max} (R_{\max}) values: 30° , 20° and 10° . In all cases the starting θ_{\max} ($R=0$) is 30° . The case where both angles (for $R = 0$ and $R = R_{\max}$) are 30° is the case where the method is not applied (no taper). The solid red line is the reference data of Fromm [19] at 250 Hz. From Figure 10 the average bottom scattering strength between 10° and 30° changes from approximately -47 dB to -37 dB, respectively. As expected this difference appears at the maximum range for the extreme case shown by the blue dash-dot line in Figure 61. The results demonstrate the effect of shading, or tapering, the scattering strength with range. They also demonstrate for this case (Problem 11 at 250 Hz) that the un-shaded scattering function provides a good estimate to the full range.

3.7 What constitutes a ‘good fit’ to the reference data?

In this study we have reference reverberation data as modelled independently by other investigators at our disposal. The reference data appear as smooth monotonically decreasing reverberation levels. Our calculations, for these environments and frequencies, present themselves with a lot of rapid variation, mimicking the interference character of the coherent propagation loss. The PE model provides the coherent transmission loss field which accounts for all the phase information, and this is the source of the rapid variation in the output. Preferably, we desire access to the incoherent field which should provide a smoother transmission loss result. Since reverberation is a convoluted sum of transmitted energy scattered from randomly arranged scatterers we cannot expect the phase to survive intact.

For the moment our PE transmission loss retains the coherent field. Our evaluation as to the suitability of the result, when the result is fair or better, is based on visual judgement. Two questions arise: First, what constitutes a ‘good fit’ of our data to the reference data. Second, in the absence of reference data, where would the smooth line be drawn through our results? If one was making a new prediction for which there is no precedent, and the reverberation output has a

variance of 10 dB or more, this would seriously affect the modelled sonar performance depending on where the line is drawn.

In order to get a better handle on this problem which is peripheral, but relevant, to the main intent of the study a short examination of how this might be handled in the future was undertaken. Due to time constraints the method described in this section was not retroactively applied to the output data in this study, save for one example.

Two MatlabTM scripts were written. First, to observe how the data might be handled in a general way, `modelled_histogram.m` was written. Second, to apply the idea to real data (RW_P11_f250_S30R50) the script `reverb_histogram.m` was written.

When time-series data are presented on a graph in decibels, since the decibel is logarithmic the values at the peaks of the signal have more value, or energy, than the values in the troughs. The reader is directed to the top plot of Figure 62 in Annex C. One cannot simply say that the mean value is the mid-value between the average of all the peaks and the average of all the troughs. This ignores the skewed, stronger, contributions from the peaks. The signal must first be converted to linear space, then perform all operations in linear units. The linear mean, and the linear RMS (root-mean-square) values can be determined, and then these linear values converted back to the decibel. If one wants to determine a level based on the total energy captured then an alternate approach may be to use histograms. A histogram effectively sorts the signal values from lowest to highest contributors over the data segment, as illustrated in the histogram of Figure 63 (middle plot). The histogram may then be summed until a suitable percentage of the total energy is captured, and the histogram abscissa value read and then converted back to decibels. This cumulative sum is shown in the third plot of Figure 62 where a threshold of 85% has been used, which in turn yielded a decibel value of 43.8 dB. One can see all three of these estimates plotted on the top plot of Figure 62, and also indicated on the histogram (shown by colour and line type).

We now turn to a case with reverberation data as determined by the PE-method, the Reverberation Workshop Problem XI at 250 Hz for bottom reverberation (RW_P11_f250_S30R50). In this report we have judged the PE-method of reverberation to be very good in agreement to the Fromm bottom reverberation.

The results are shown in Figure 63. The left column of plots show the reverberation time series which have been sectioned from the full data length, and are plotted along with the smooth data from Fromm's Reverberation Workshop data. The vertical axes on the time series all cover the same span of decibels. The data sections are from near the source, and the last plot is at long range. In the right column of plots the histogram for each data section is shown. All of the histogram axes are common. For each data section the histogram had 1000 levels available. The RMS (red), mean (magenta), and histogram method (green) are shown on the histograms. The vertical black line on the histograms indicate the mean value of the Fromm reference data (bottom reverberation). For this example the threshold for the histogram sum was set to 60% of the total signal energy for the data section.

One of the first things we notice in the histograms is how the median value decreases with range, coinciding with the propagation loss with range. Also, the topmost histogram shows the largest spread between the three methods. This is likely due to the quick fall-off in energy near the source, which is visually most evident in the corresponding time series. The near-to-source ranges

are likely skewing all the values as well. This illustrates the problem where the data does not have a slope near to zero. Notice that the RMS value is always too high in comparison with the Fromm data. And finally notice that in several plots the Fromm mean is close to the threshold method, but with only 60% of the energy being captured. That seems surprisingly low.

Lessons learned from this exercise include: shorter data sections may lessen the issue with data slope (at the cost of more coarse histograms), and the difference between the three methods can have a spread of between approximately 5 to 15 dB (based on the histograms) which has large implications for determining sonar performance. One advantage of the histogram-sum threshold method is that it allows the user to determine what percentage of energy should be captured in order to set the fit. One drawback is that setting the threshold may be subjective in itself, but it is possible a rule based on sonar performance could be determined.

3.8 Recommendations for Changes to PECan

During the brief contract period there was insufficient time to implement, and then test, the algorithms developed in MatlabTM. The changes made to PECan involved creating two new output files, described in detail in Annex D.

To further the development of a reverberation capability using PECan, DRDC could take either of two paths. The first is to leave PECan largely as it is, employing the changes that have already been made under this contract (e.g. new output files) and to use an external scripting language. MatlabTM appears to be a suitable scripting language with a wide user base. This has the advantage of not disturbing the core engine of the propagation loss calculation and allowing complex geometries to be handled by any number of specialised external scripts. One disadvantage with this option is that a separate software license and expertise may need to be maintained. The second option is to embed all of the processing into a new development stream of PECan. This would allow advanced development of PECan in a parallel code stream without the potential for adversely affecting the current version of PECan.

If the methodology described in this report is to be embedded directly into PECan we make the following general recommendations for changes to PECan source code:

1. Create a new development-stream of source code for the reverberation implementation. This may help compartmentalize the development without affecting the existing PECan;
2. Ideally, the PECan model should compute the incoherent transmission loss to avoid the highly oscillatory coherent interference patterns (requires investigation);
3. Boundary scattering functions need to be implemented;
4. Boundary reverberation estimates need to be corrected by 6 dB;
5. For surface reverberation: Ideally a robust physical based approach should be developed to deal with the free surface boundary condition. Alternately, follow a more empirical approach (e.g. compute and calibrate against the rigid surface estimate at short range);

6. For volume reverberation: A volume scattering strength needs to be available within the model parameters. For all environments the height of the scattering volume should be limited to the water depth.
7. For bottom reverberation: The transmission loss must be tracked along the bathymetry. This has been implemented in the modified PECAN code as described in Annex D.
8. For target echo: A target strength value needs to be available within the model, or in the most simple implementation, have the model assume a strength of 0 dB.
9. For all reverberation and target echo calculations: Signal parameters need to be available to the model, e.g. pulse bandwidth, and source level (or assume a source level of 0 dB).
10. PECAN array sizes were increased to accommodate estimates at 3500 Hz (12000 grid points in depth). The maximum desirable frequencies, depths, ranges and computational mesh sizes should define these array sizes based on DRDC's desired problem set.

4 Conclusions and Proposed Future Work

4.1 Conclusions

The purpose of this study was to explore the use of the parabolic equation model to provide estimates of reverberation and target echo as viable and efficient alternative to traditional active models. This study has shown the PE model to be a very viable alternative to more traditional reverberation and target echo techniques. This was shown using a range of realistic environmental characteristics over a frequency range of approximately four octaves. PE derived estimates of reverberation and target echo were compared to estimates of same from independent sources. Preliminary comparisons appear very favourable.

There were several challenges along the way. An adjustment of 6 dB was found to be required to align the bottom and surface reverberation estimates to reference benchmark data. The free surface boundary condition at the sea surface proved to be challenging when attempting to compute the surface reverberation. The area of surface reverberation requires further study. The idea of applying a simple FFT to the vertical field estimates in order to obtain an understanding of the angular content within the field did not bear fruit as was hoped. This is another area requiring further study. And the challenge in comparing the coherent transmission loss with its interference pattern characteristic to smooth reference data was explored.

While the intention of this work was to employ the PE model to investigate reverberation and target echo estimation, it is clear that *any* type of propagation model can be used in this manner. The advantage of one model type over another will lie in the advantages each model type has for certain types of environments. For example, ray methods, normal mode, fast field, or PE will all shine in certain circumstances. Using that vision, the method explored in this report could provide a modular post-processing extension to *any* existing passive model.

4.2 Proposed Future Work

The following list highlights the areas in which we believe future efforts could be directed towards:

1. This study examined one range dependent problem. A broader selection of range dependent problems should be examined and the results compared with results from other models.
2. This study used only empirical scattering models, integrated to an average strength. Strategies should be devised to handle true bistatic and physics-based scattering laws i.e., extend the cookie cutter approach, or other, to these cases.
3. Work should be carried out to produce an incoherent estimate of TL, thus removing the coherent interference patterns reflected in the reverberation and target echo results. Particular attention applied to the sea surface reverberation. The limits of this approach should also be determined.

4. The natural progression of this work is to enlist the PE model derived reverberation and target echo to compute performance predictions by the echo excess. This would make the PE stand on its own as a 'complete' active model.
5. DRDC may wish to see the algorithms in this report applied to a broader suite of passive models (DRDC Clutter, SAFARI, Bellhop, CASS GRAB, etc.). The outcome of these comparisons could be evaluated for their relative merits.

This page intentionally left blank.

References

- [1] G.H. Brooke, D.J. Thomson, and G.R. Ebbeson, "PECan: A Canadian parabolic equation model for underwater sound propagation," *J. Comp. Acoust.* 9, 69-100 (2001).
- [2] D. D. Ellis, J. R. Preston, P. C. Hines, and V.W. Young, "Bistatic signal excess calculations over variable bottom topography using adiabatic normal modes," in *International Symposium on Underwater Reverberation and Clutter*, P. L. Nielsen, C. H. Harrison and J.-C. Le Gac, eds., NATO Undersea Research Centre, La Spezia, Italy, 2008, pp. 97-104.
- [3] D. D. Ellis and J. R. Preston, "DRDC Clutter Model: Range-dependent predictions compared with towed array reverberation and clutter data from the Malta Plateau," in *Proceedings of Underwater Acoustics Measurements Conference*, Kos island, Greece, June 2011.
- [4] D. D. Ellis, "Solutions to range-dependent reverberation and sonar workshop problems using an adiabatic normal mode model," in *Proceedings of Underwater Acoustics Measurements Conference*, Kos Island, Greece, June 2011.
- [5] E. I. Thorsos and J. S. Perkins, "Overview of the reverberation modeling workshops," In Nielsen et al. [10], pp. 3-14, 2008.
- [6] M. Zampolli, M. A. Ainslie, and P. Schippers, "Scenarios for benchmarking range-dependent active sonar performance models," *Proc. Institute of Acoustics*, 32, Pt. 2, 2010. [in press].
- [7] M.D. Collins and R.B. Evans, A two-way parabolic equation for acoustic backscattering in the ocean, *J. Acoust. Soc. Am.* **91** (1992) 1357-1368.
- [8] G.H. Brooke and D.J. Thomson, A single-scatter formalism for improving PE calculations in range-dependent media, in *PE Workshop II: Proceedings of the Second Parabolic Equation Workshop*. S.A. Chin-Bing, D.B. King, J.A. Davis and R.B. Evans, eds. US Government Printing Office, Washington, DC, 1993, pp. 126-144.
- [9] M.D. Collins, A two-way parabolic equation for elastic media, *J. Acoust. Soc. Am.* **93** (1993) 1815-1825.
- [10] F.D. Tappert, The parabolic approximation method, in *Wave Propagation and Underwater Acoustics*. J.B. Keller and J.S. Papadakis, eds. Springer, New York, 1977, pp. 224-287.
- [11] M.D. Collins and E.K. Westwood, A higher-order energy-conserving parabolic equation for range-dependent ocean depth, sound speed, and density, *J. Acoust. Soc. Am.* 89 (1991) 1068-1075.
- [12] M.D. Collins, A higher-order parabolic equation for wave propagation in an ocean overlying an elastic bottom, *J. Acoust. Soc. Am.* 86 (1989) 1459-1464.
- [13] B.T.R. Wetton and G.H. Brooke, One-way wave equations for seismo-acoustic propagation in elastic waveguides, *J. Acoust. Soc. Am.* 87 (1990) 624-632.

- [14] M.D. Collins, W.A. Kuperman and W.L. Siegmann, A parabolic equation for poroelastic media, *J. Acoust. Soc. Am.* 98 (1995) 1645-1656.
- [15] D.J. Thomson, G.H. Brooke and E.S. Holmes, PE approximations for scattering from a rough surface, Tech. Memo. 95-21, Defence Research Establishment Pacific, Victoria, BC (1995).
- [16] G.H. Brooke and D.J. Thomson, Non-local boundary conditions for high-order PE models with application to scattering from a rough surface, Tech. Memo. DREA TM 1999-121, Defence Research Establishment Atlantic, Dartmouth, NS (1999).
- [17] K. Smith and A. Tolstoy, Summary of results for SWAM'99 test cases, SWAM'99: Proceedings of a Shallow Water Acoustic Modeling Workshop. Springer, New York, 2000.
- [18] Brooke, G.H., "An Update on the multi-static model, SPADES, and its application to the reverberation workshop test suite," 154th Meeting of the Acoustical Society of America, 27-31 November 2008, New Orleans, LS.
- [19] Reverberation Workshop II Problem Definition Website
http://aacs.nrl.navy.mil/ReverbWorkShop_II/index.html
- [20] D. M. Fromm, J. P. Crockett, L. B. Palmer, BiRASP – The Bistatic Range-dependent Active System Performance Model, Naval Research Laboratory, NRL/FR/7140-95-9723, September 30, 1996.
- [21] Computational Ocean Acoustics, by F. B. Jensen, W.A. Kuperman, M. B. Porter, and H. Schmidt, Springer-Verlag, New York, 2000. Eq. (1.34) on page 38.
- [22] Attenuation in water values sourced directly from:
ftp://ftp.ccs.nrl.navy.mil/pub/ram/RevModWkshp_II/Workshop_I_Problem_Definitions/Environmental_Information/Watercolumn_Properties/water_attenuation
- [23] Dale D. Ellis, "A Shallow Water Normal Modes Reverberation Model," in *J. Acoust. Soc. Am.*, 97, 2804-2814 (1995).
- [24] Underwater Acoustic Modelling, Principles, Techniques and Applications, Paul C. Etter, Elsevier Applied Science, 1991. See Pg 191, Eq. 8.2
- [25] Document Final_LePage_and_Thorsos_Gaussian_Waveform_Expression_103006.pdf available at
ftp://ftp.ccs.nrl.navy.mil/pub/ram/RevModWkshp_II/Workshop_I_Problem_Definitions/Source_Function/
- [26] Dale D. Ellis, Solutions to range-dependent reverberation and sonar Workshop problems using an adiabatic normal mode model, UAM 2011

Annex A Results – Reverberation and Targe Echo

A.1 Reverberation Workshop Problem 11 (RI, Isovel.)

A.1.1 Reverberation Components

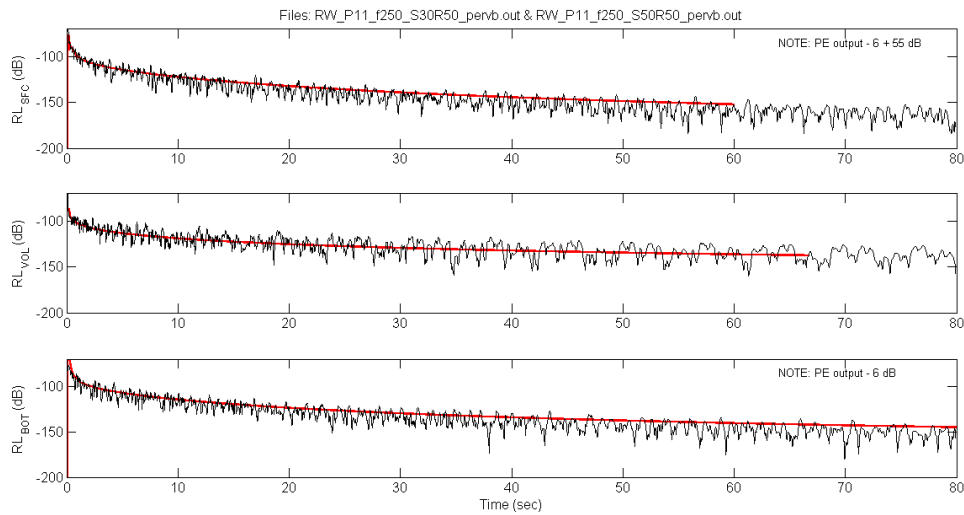


Figure 17. Reverberation Workshop Problem 11: PE method reverberation results for surface (top), volume (middle), and bottom reverberation at 250 Hz. Note the biases applied to the surface and bottom reverberation levels as noted on the graphs.

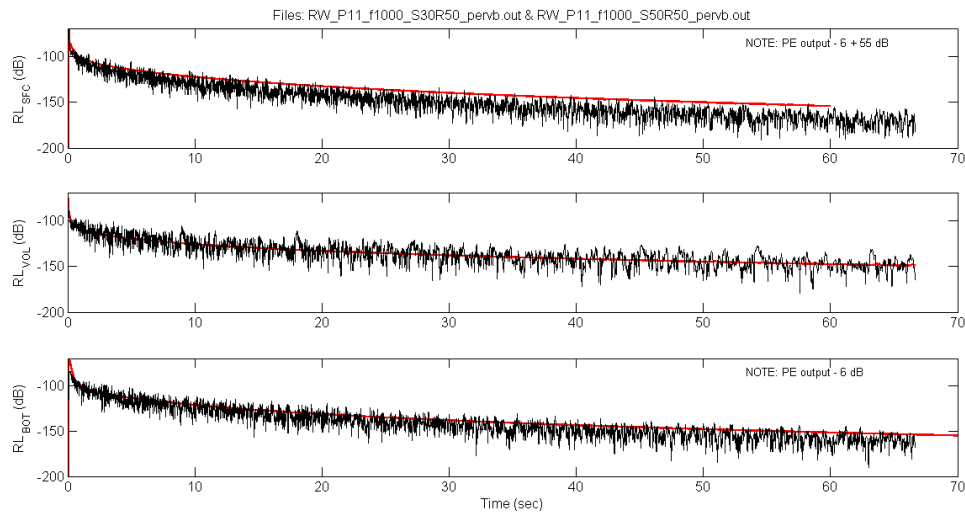


Figure 18. Reverberation Workshop Problem 11: PE method reverberation results for surface (top), volume (middle), and bottom reverberation at 1000 Hz. Note the biases applied to the surface and bottom reverberation levels as noted on the graphs.

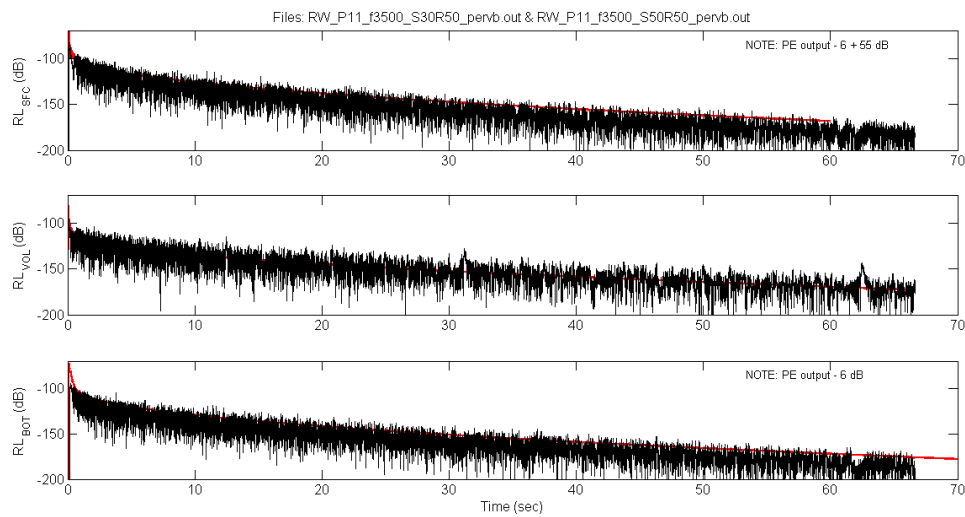


Figure 19. Reverberation Workshop Problem 11: PE method reverberation results for surface (top), volume (middle), and bottom reverberation at 3500 Hz. Note the biases applied to the surface and bottom reverberation levels as noted on the graphs.

A.1.2 Target Echo

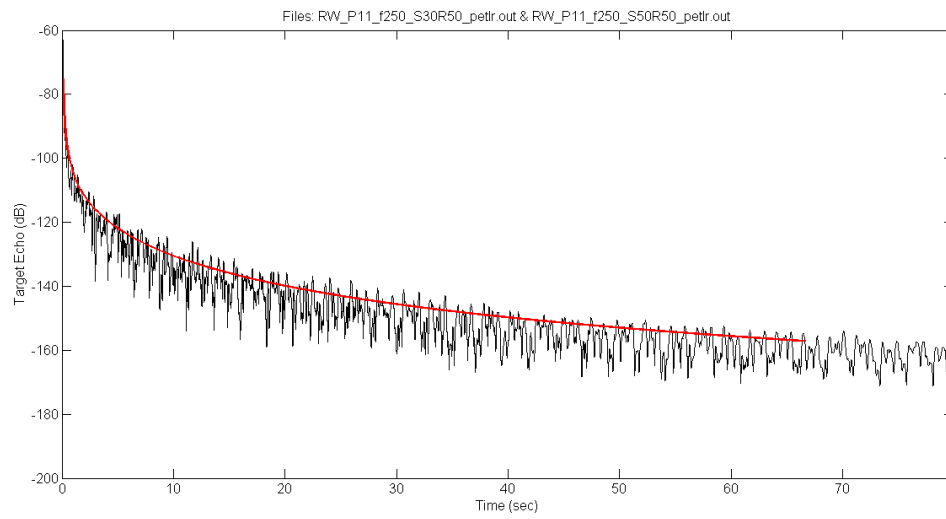


Figure 20. Reverberation Workshop Problem 11: PE method target echo results at 250 Hz.

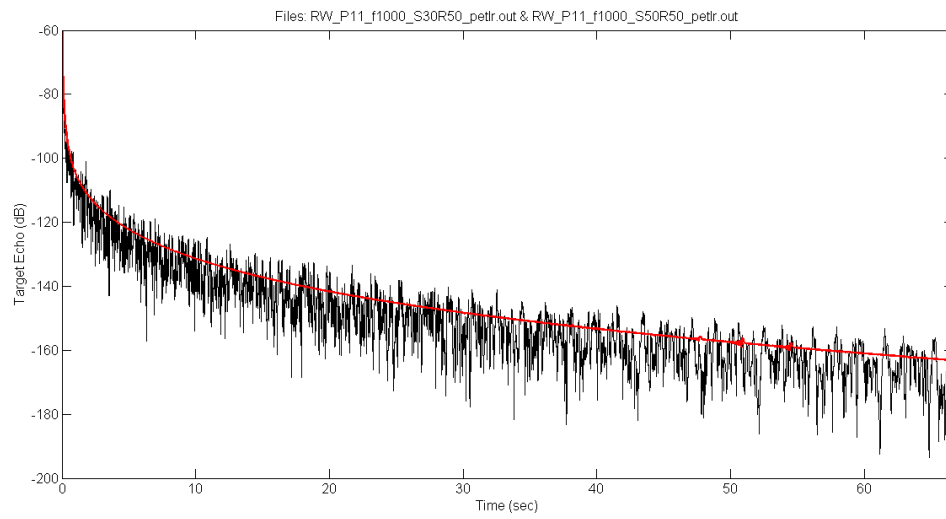


Figure 21. Reverberation Workshop Problem 11: PE method target echo results at 1000 Hz.

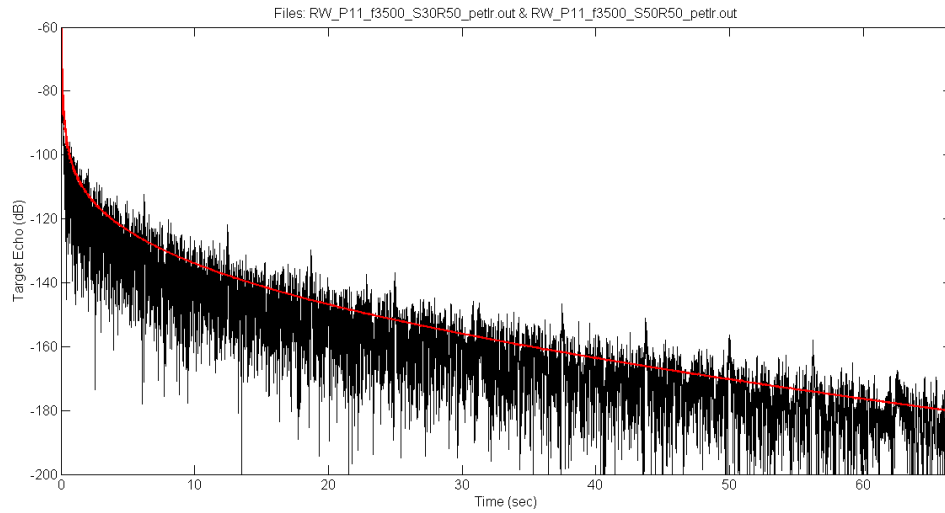


Figure 22. Reverberation Workshop Problem 11: PE method target echo results at 3500 Hz.

A.2 Reverberation Workshop Problem 12 (RI, Summer)

A.2.1 Reverberation Components

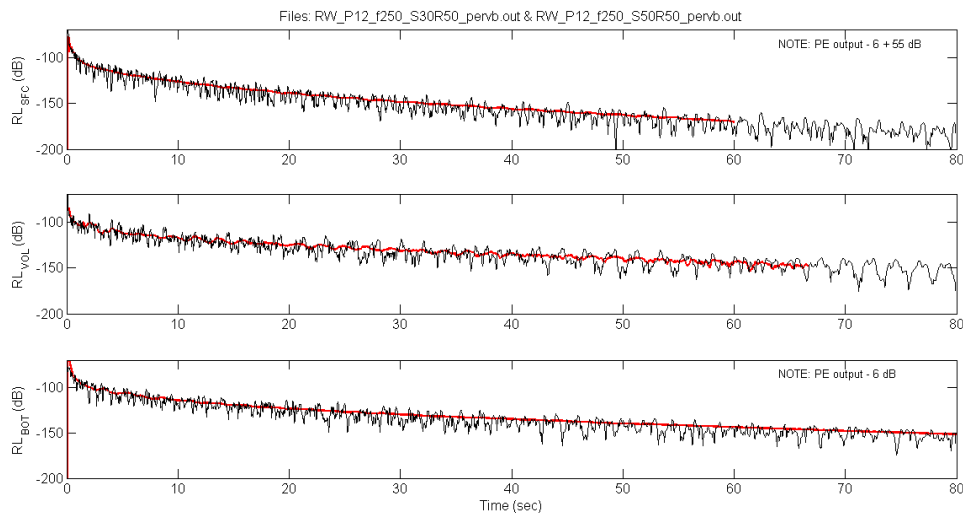


Figure 23. Reverberation Workshop Problem 12: PE method reverberation results for surface (top), volume (middle), and bottom reverberation at 250 Hz.

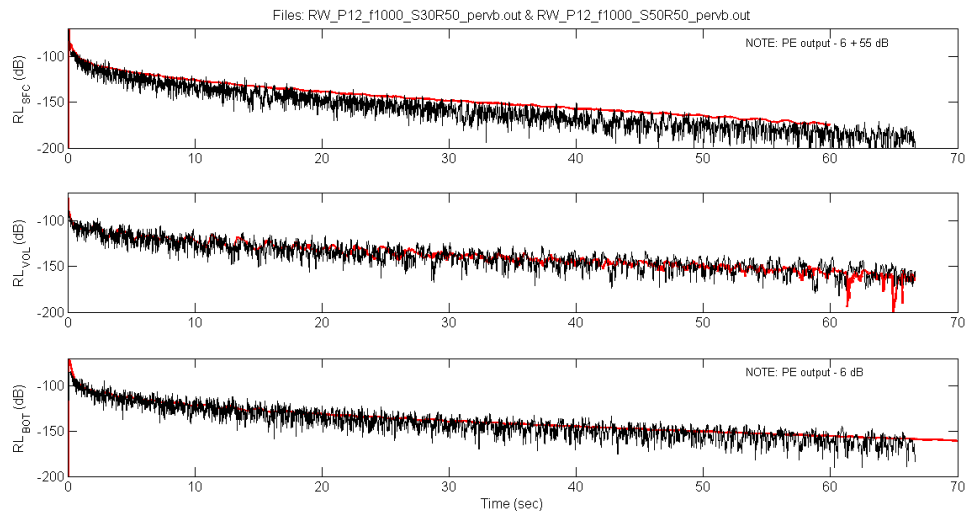


Figure 24. Reverberation Workshop Problem 12: PE method reverberation results for surface (top), volume (middle), and bottom reverberation at 1000 Hz.

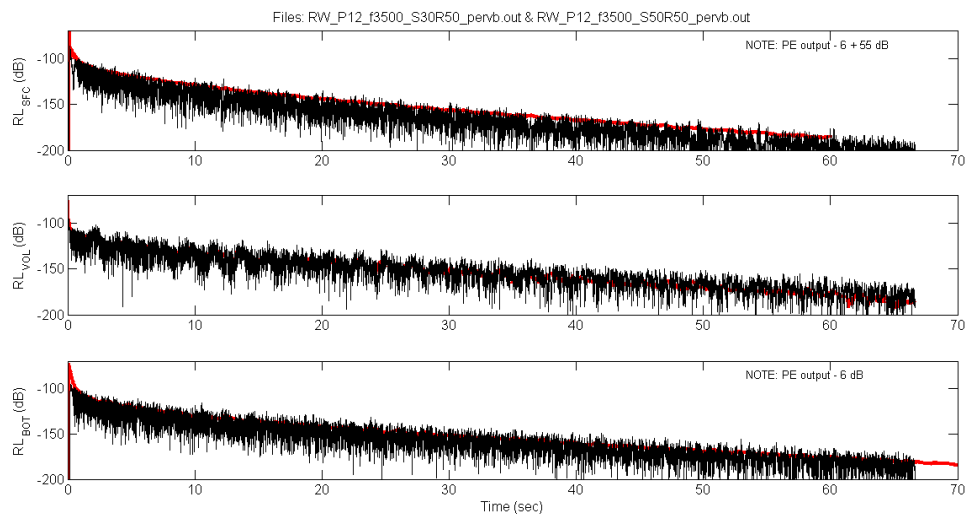


Figure 25. Reverberation Workshop Problem 12: PE method reverberation results for surface (top), volume (middle), and bottom reverberation at 3500 Hz.

A.2.2 Target Echo

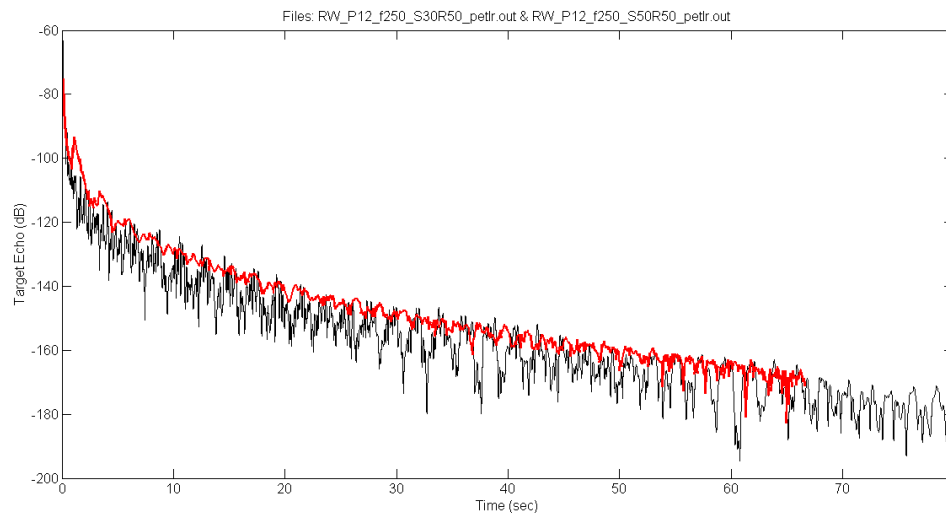


Figure 26. Reverberation Workshop Problem 12: PE method target echo results at 250 Hz.

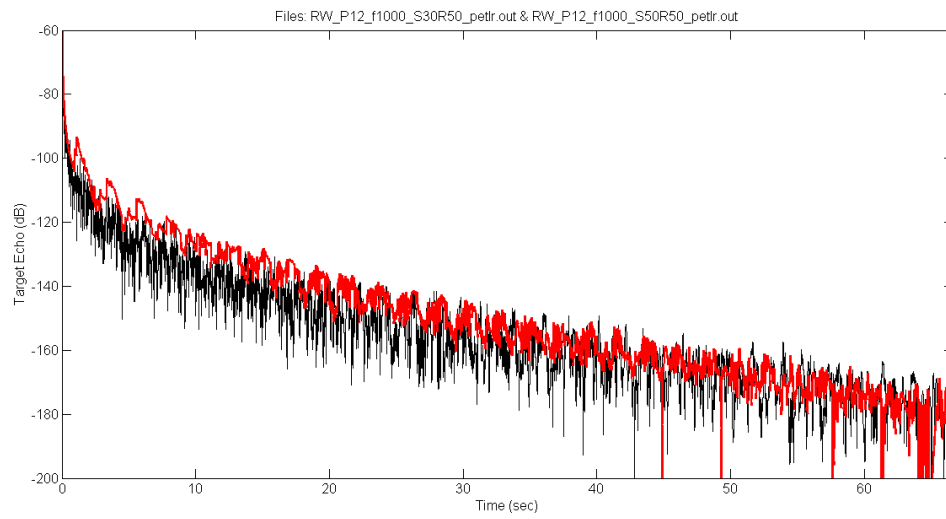


Figure 27. Reverberation Workshop Problem 12: PE method target echo results at 1000 Hz.

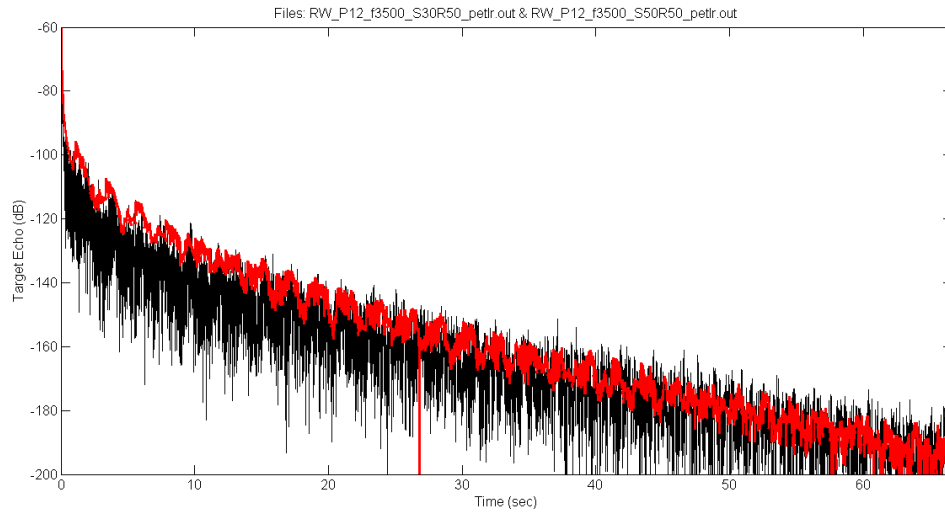


Figure 28. Reverberation Workshop Problem 12: PE method target echo results at 3500 Hz.

A.3 Reverberation Workshop Problem 13 (RI, Winter)

A.3.1 Reverberation Components

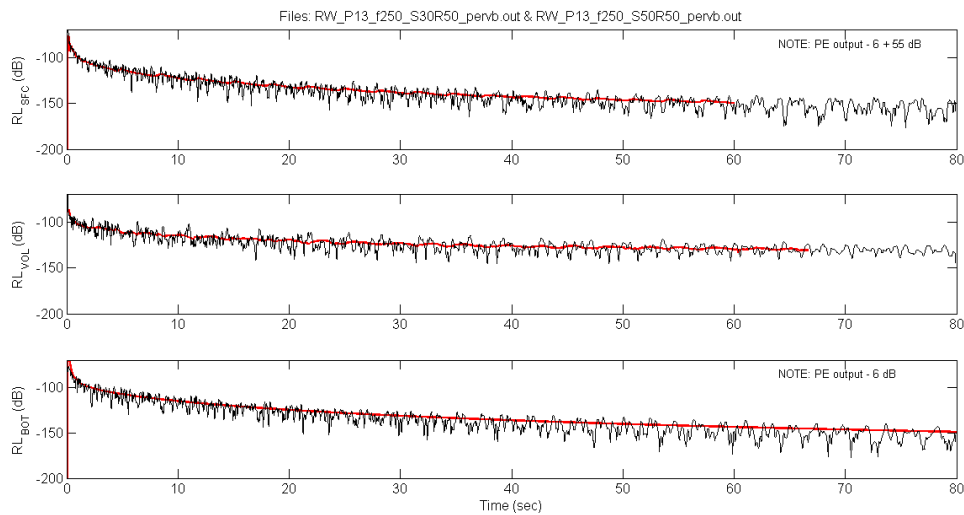


Figure 29. Reverberation Workshop Problem 13: PE method reverberation results for surface (top), volume (middle), and bottom reverberation at 250 Hz.

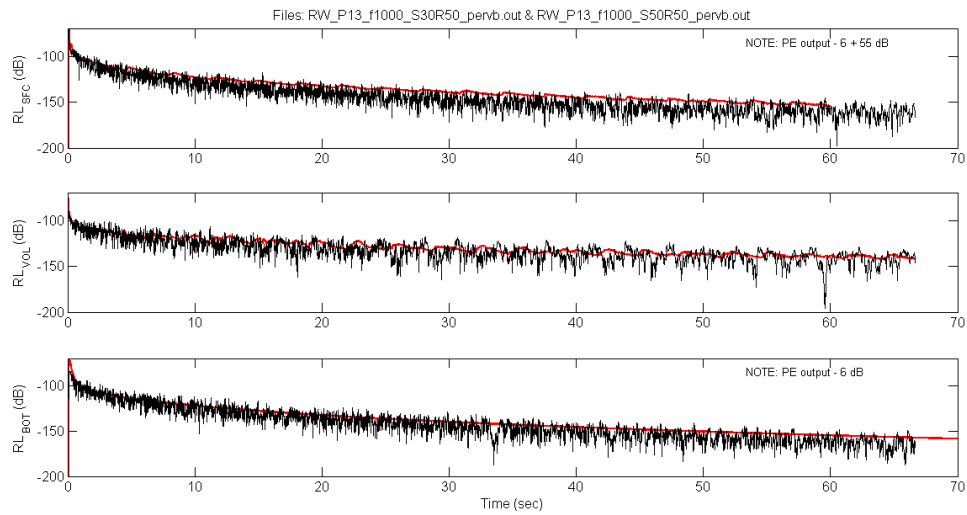


Figure 30. Reverberation Workshop Problem 13: PE method reverberation results for surface (top), volume (middle), and bottom reverberation at 1000 Hz.

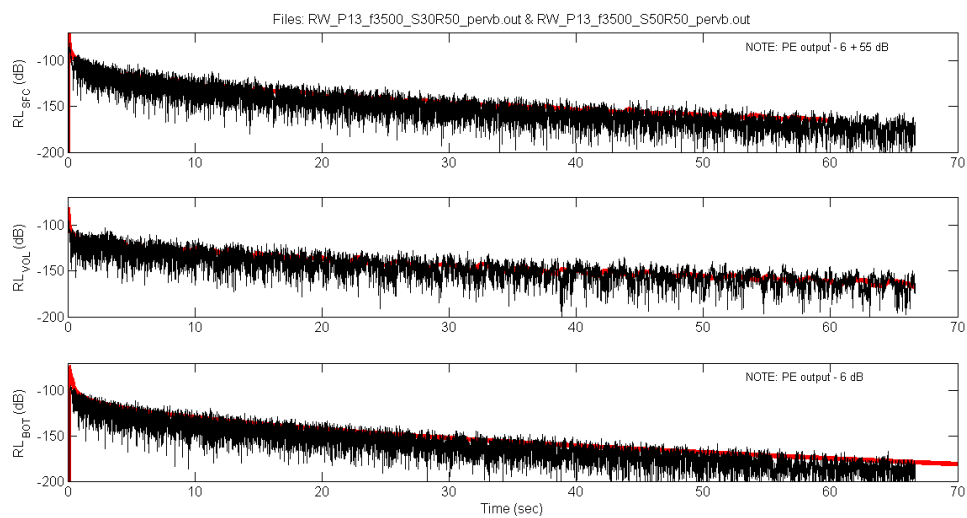


Figure 31. Reverberation Workshop Problem 13: PE method reverberation results for surface (top), volume (middle), and bottom reverberation at 3500 Hz.

A.3.2 Target Echo

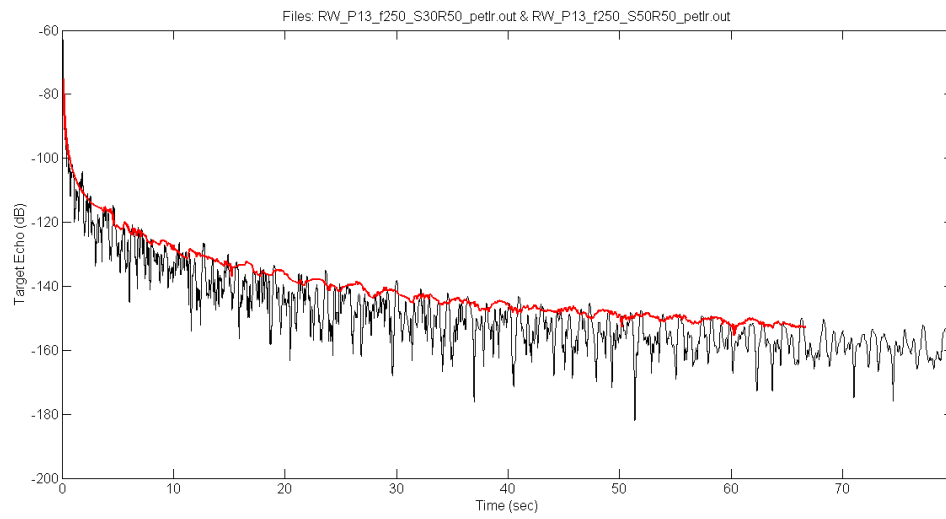


Figure 32. Reverberation Workshop Problem 13: PE method target echo results at 250 Hz.

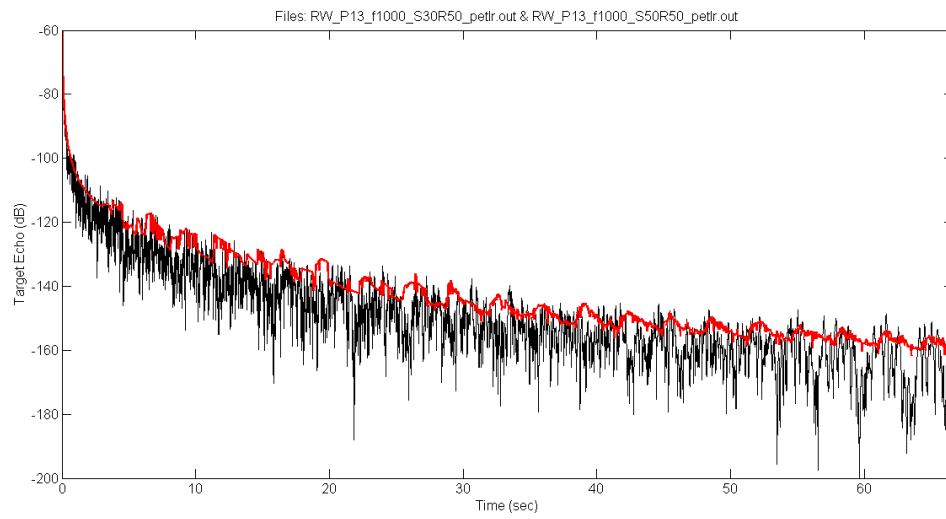


Figure 33. Reverberation Workshop Problem 11: PE method target echo results at 1000 Hz.

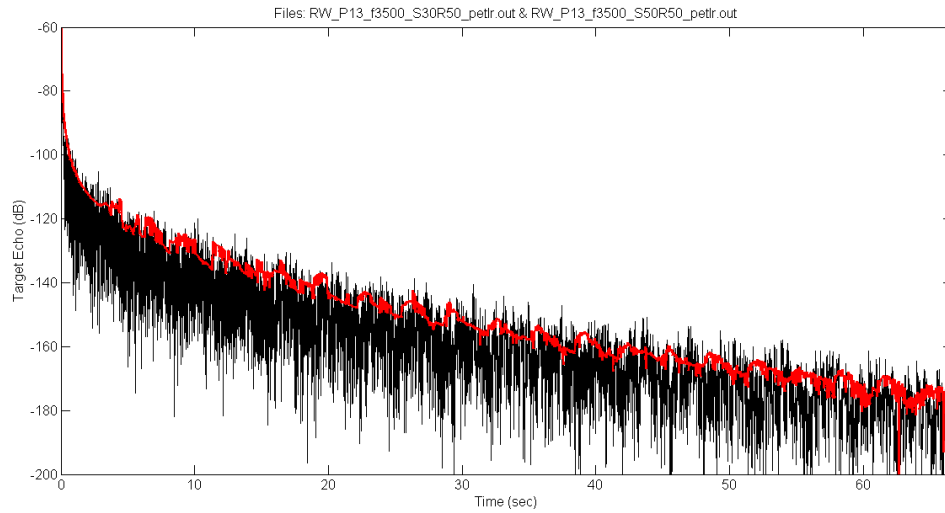


Figure 34. Reverberation Workshop Problem 13: PE method target echo results at 3500 Hz.

A.4 Reverberation Workshop Problem 17 (RD, Isovel.)

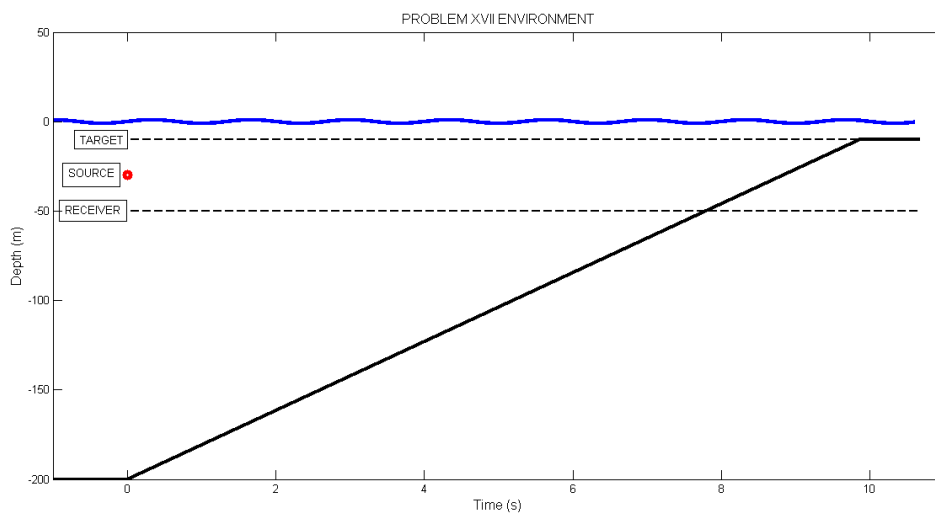


Figure 35. Problem 17 environment represented in terms of reverberation (and target echo) time. The source depth, target depth and receiver depth are shown on the plot. Intersections with the bathymetry are shown for the target and receiver depths.

A.4.1 Reverberation Components

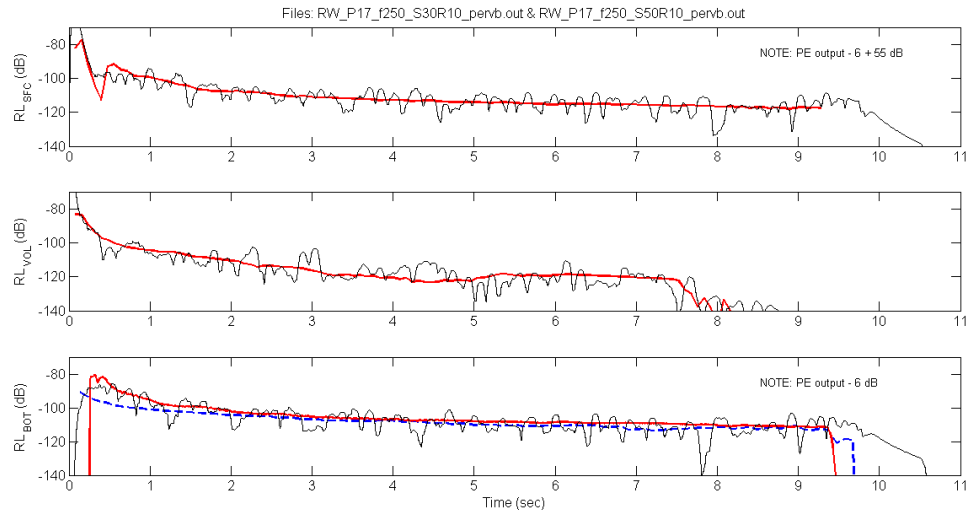


Figure 36. Reverberation Workshop Range Dependent Problem 17: PE method reverberation results for surface (top), volume (middle), and bottom reverberation at 250 Hz.

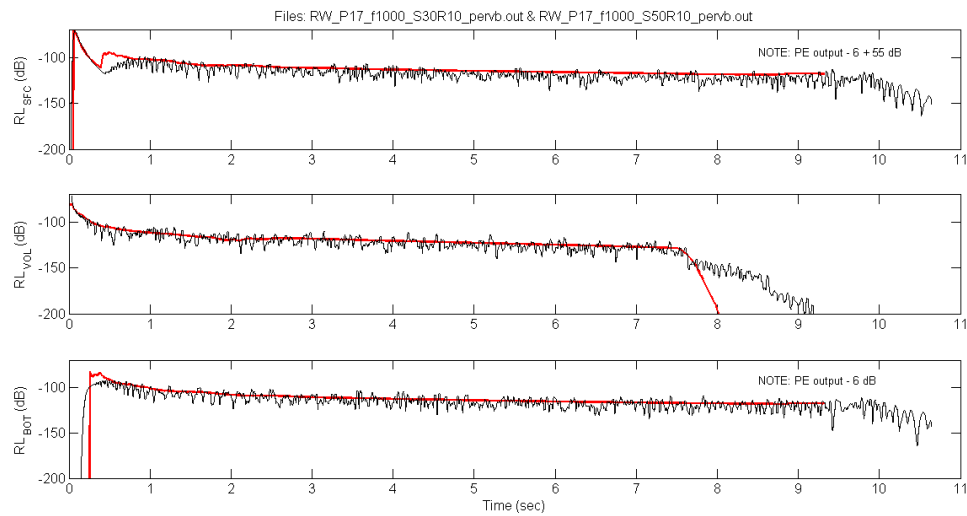


Figure 37. Reverberation Workshop Range Dependent Problem 17: PE method reverberation results for surface (top), volume (middle), and bottom reverberation at 1000 Hz.

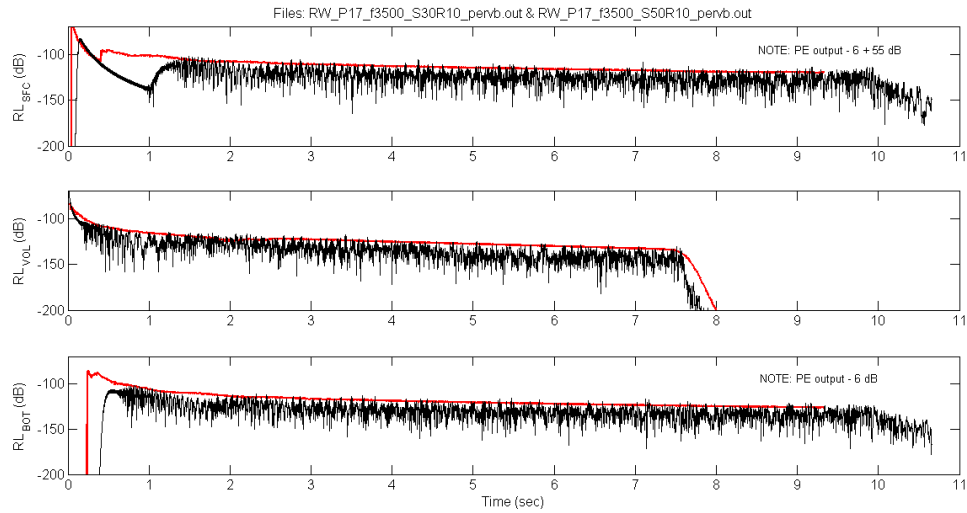


Figure 38. Reverberation Workshop Range Dependent Problem 17: PE method reverberation results for surface (top), volume (middle), and bottom reverberation at 3500 Hz.

A.4.2 Target Echo

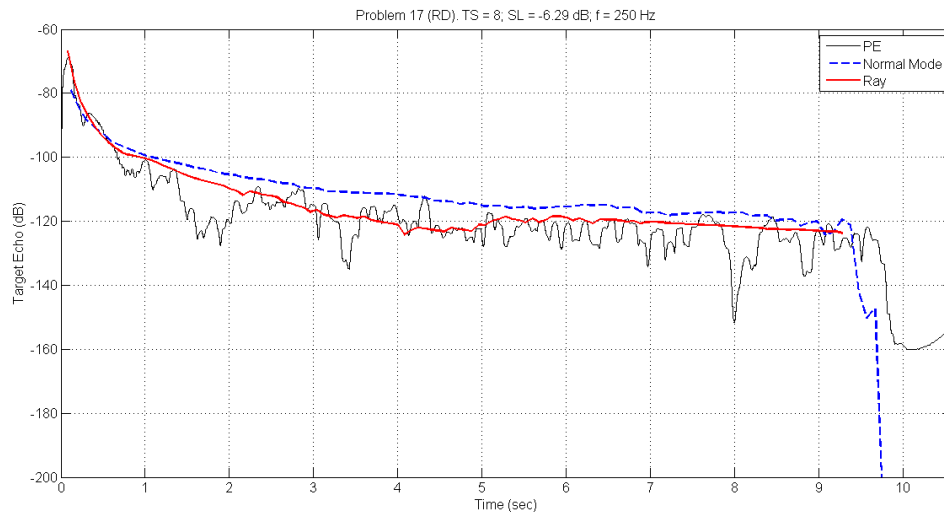


Figure 39. Reverberation Workshop Range Dependent Problem 17: PE method target echo results at 250 Hz using PE method, normal mode method, and ray method.

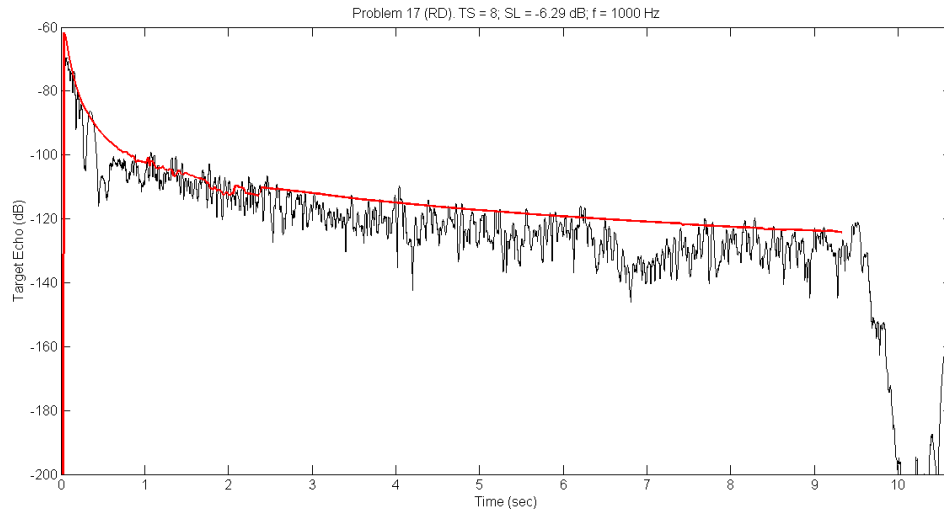


Figure 40. Reverberation Workshop Range Dependent Problem 17: PE method target echo results at 1000 Hz.

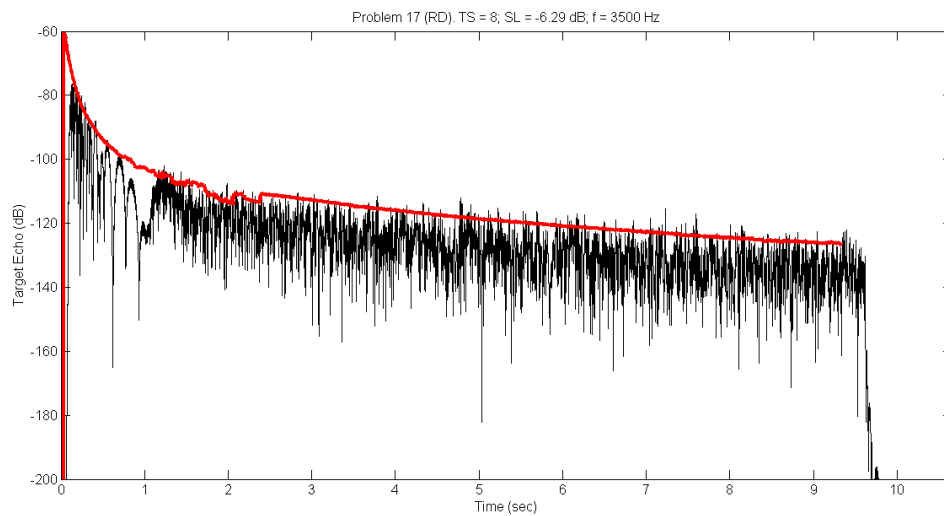


Figure 41. Reverberation Workshop Range Dependent Problem 17: PE method target echo results at 3500 Hz.

A.5 Surface Reverberation – Boundary Effects

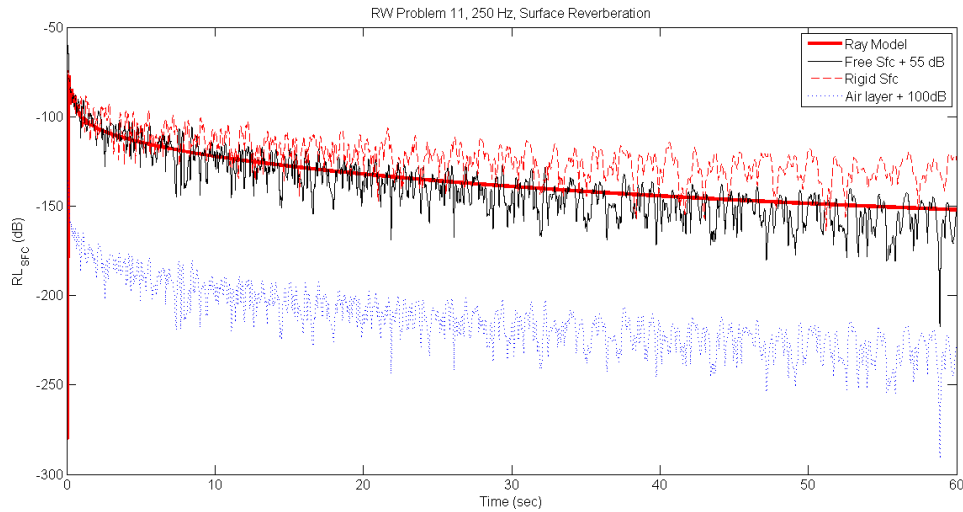


Figure 42. Comparison of sea surface reverberation for three different boundary conditions, showing the full range. The solid heavy line is derived from the ray model.

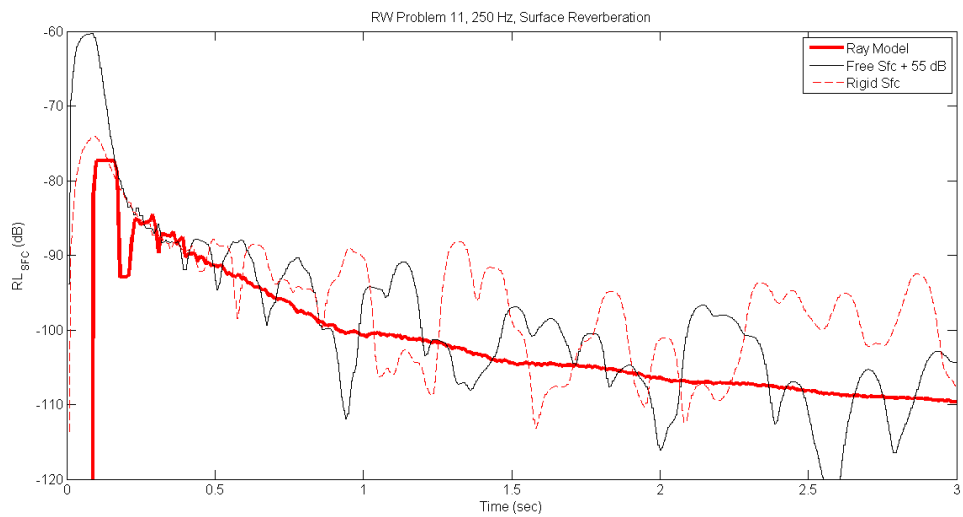


Figure 43. Comparison of sea surface reverberation for the free surface and the rigid surface boundary conditions at short range. The solid heavy line is derived from the ray model.

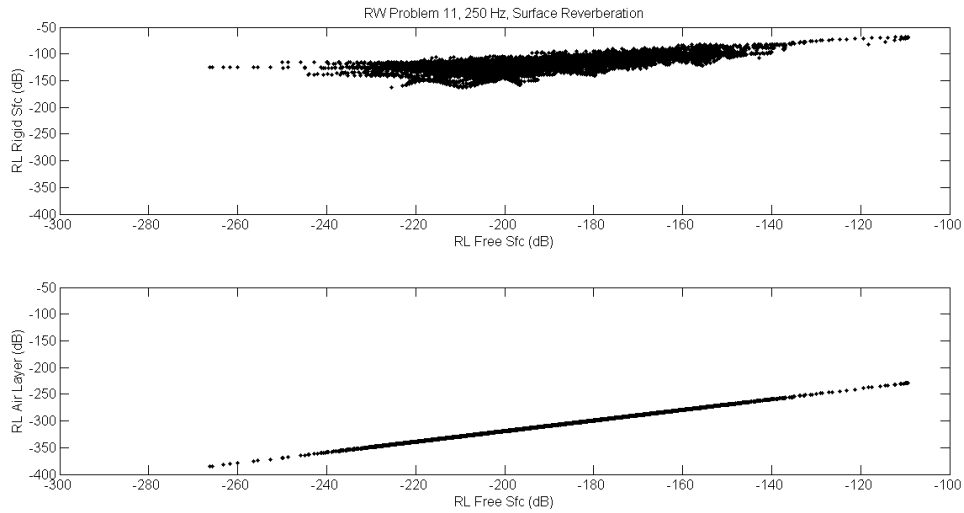


Figure 44. Scatterplots comparing the rigid surface to the free surface reverberation (top), and the air layer to the free surface reverberation (bottom) which are identical save for a constant bias.

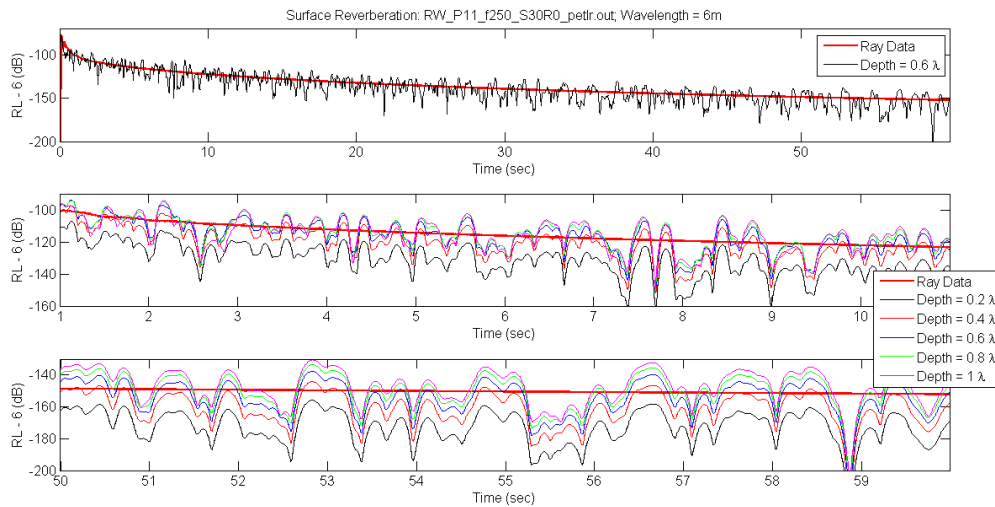


Figure 45. RW Problem 11 at 250 Hz (isovelocity). Reverberation time series based on near surface transmission loss. Top plot shows full time series for using TL result at depth 0.6λ ; middle plot shows near range reverberation time series detail for all near surface depths; bottom plot shows long range reverberation time series detail for all near surface depths.

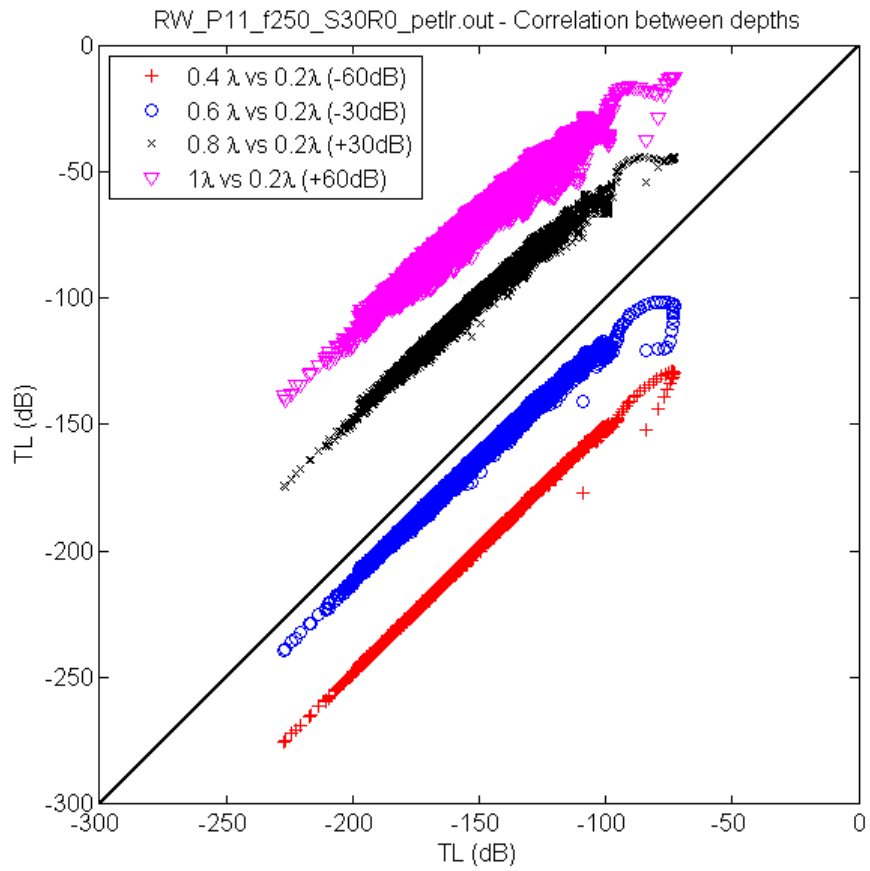


Figure 46. Correlation of transmission loss at depths of $0.4 - 1\lambda$ to the transmission loss computed at a depth of 0.2λ . Frequency = 250 Hz, $\lambda = 6m$.

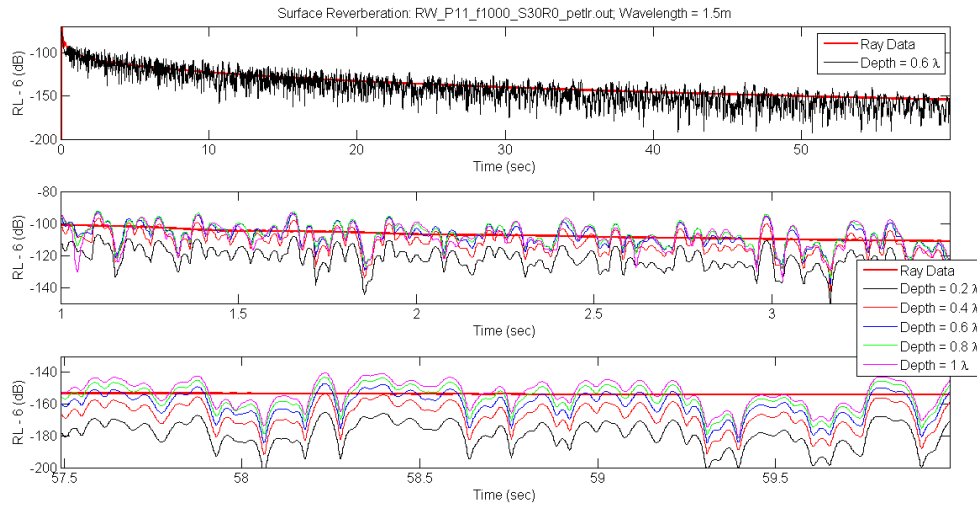


Figure 47. RW Problem 11 at 1000 Hz (isovelocity). Reverberation time series based on near surface transmission loss. Top plot shows full time series for using TL result at depth 0.6λ ; middle plot shows near range reverberation time series detail for all near surface depths; bottom plot shows long range reverberation time series detail for all near surface depths.

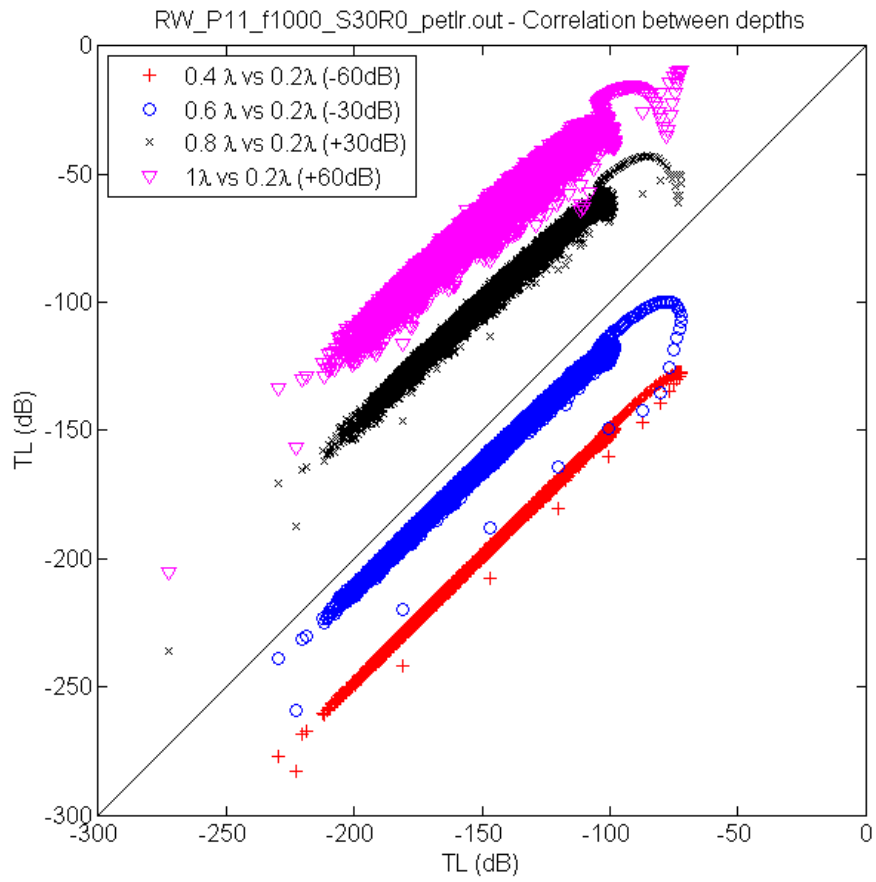


Figure 48. Correlation of transmission loss at depths of $0.4 - 1\lambda$ to the transmission loss computed at a depth of 0.2λ . Frequency = 1000 Hz, $\lambda = 1.5m$.

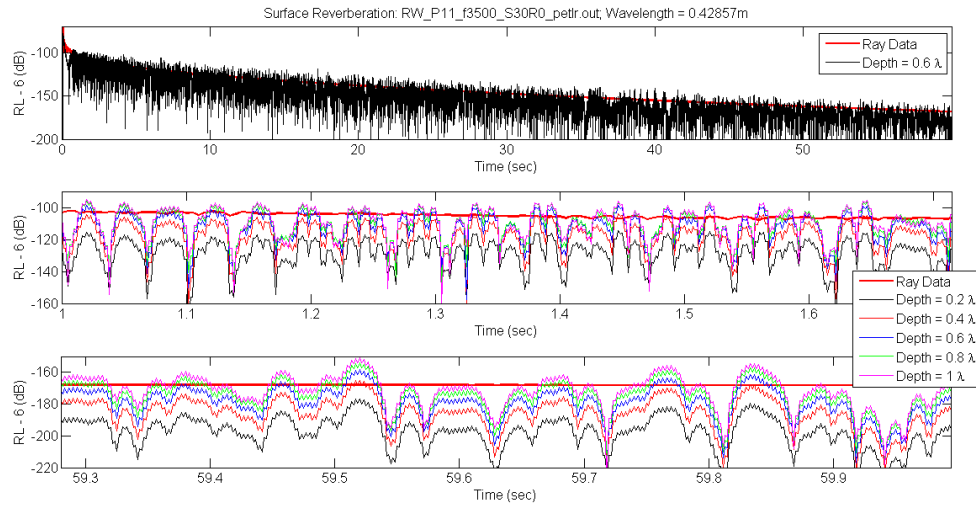


Figure 49. RW Problem 11 at 3500 Hz (isovelocity). Reverberation time series based on near surface transmission loss. Top plot shows full time series for using TL result at depth 0.6λ ; middle plot shows near range reverberation time series detail for all near surface depths; bottom plot shows long range reverberation time series detail for all near surface depths.

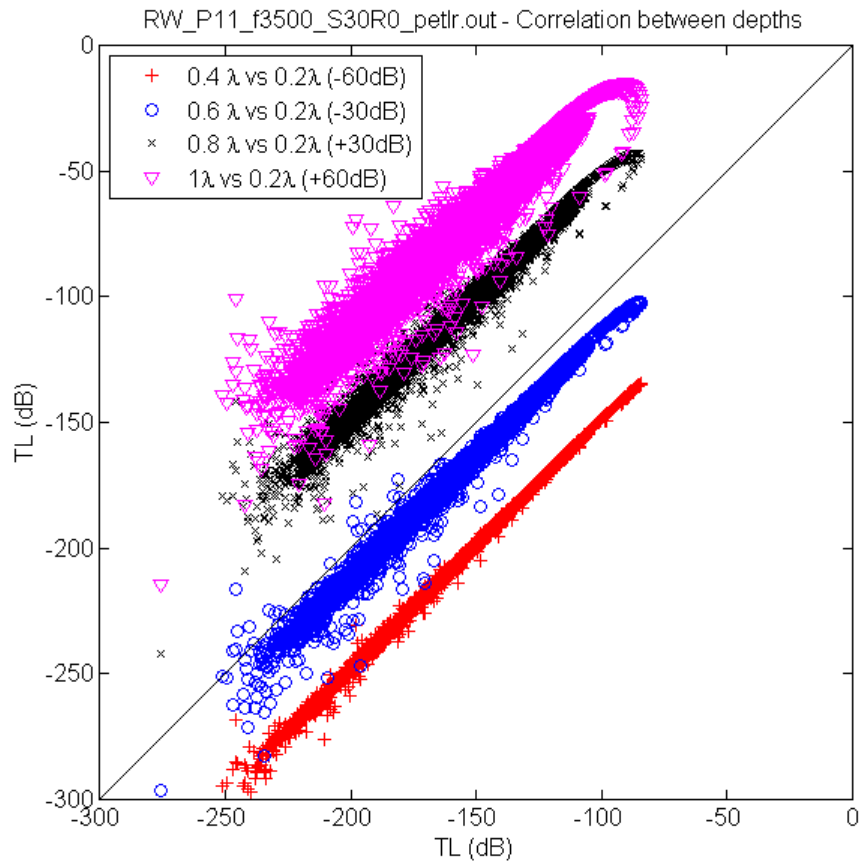


Figure 50. Correlation of transmission loss at depths of $0.4 - 1\lambda$ to the transmission loss computed at a depth of 0.2λ . Frequency = 3500 Hz, $\lambda = 0.4286m$.

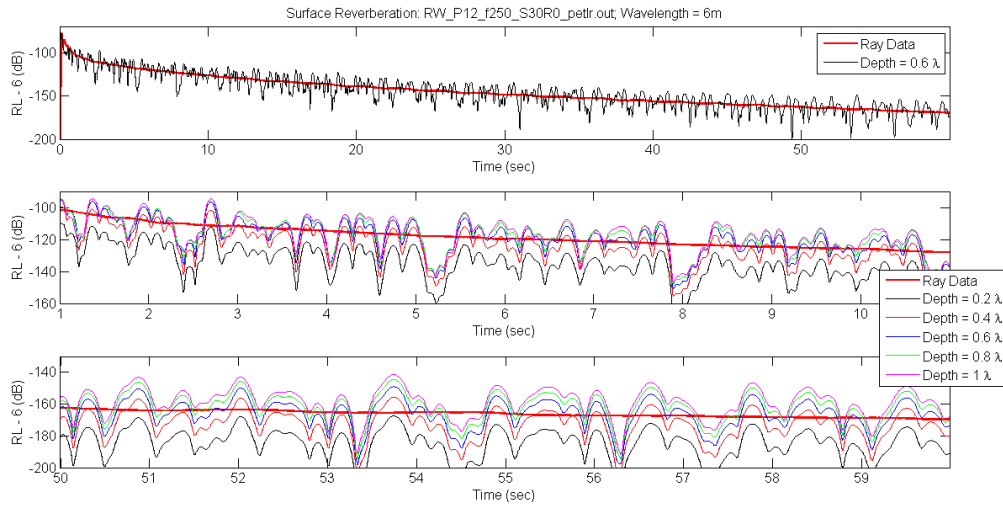


Figure 51. RW Problem 12 at 250 Hz (summer profile). Reverberation time series based on near surface transmission loss. Top plot shows full time series for using TL result at depth 0.6λ ; middle plot shows near range reverberation time series detail for all near surface depths; bottom plot shows long range reverberation time series detail for all near surface depths.

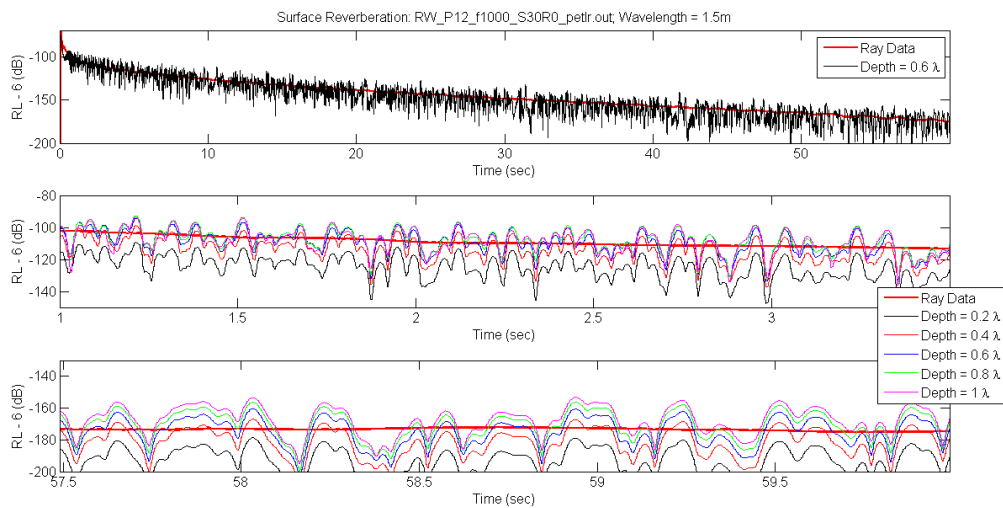


Figure 52. RW Problem 12 at 1000 Hz (summer profile). Reverberation time series based on near surface transmission loss. Top plot shows full time series for using TL result at depth 0.6λ ; middle plot shows near range reverberation time series detail for all near surface depths; bottom plot shows long range reverberation time series detail for all near surface depths.

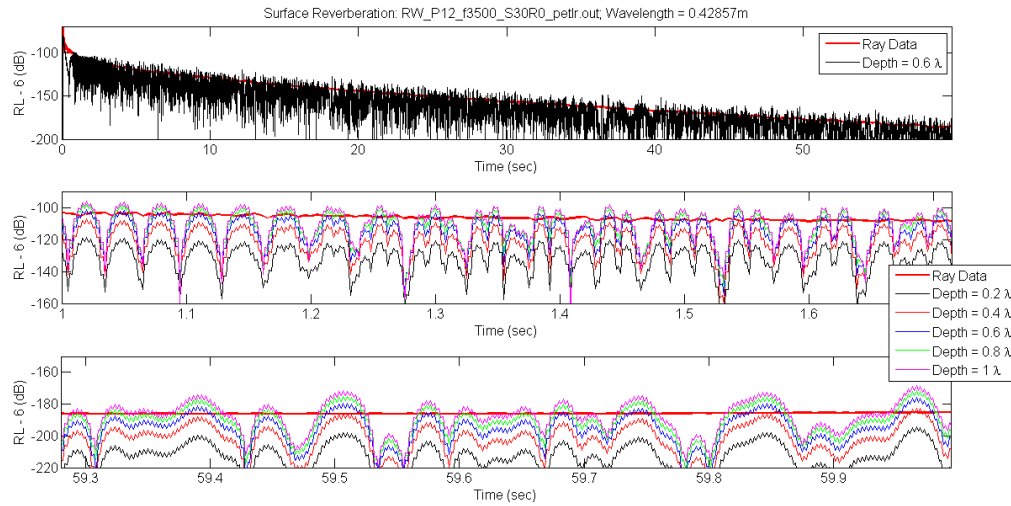


Figure 53. RW Problem 12 at 3500 Hz (summer profile). Reverberation time series based on near surface transmission loss. Top plot shows full time series for using TL result at depth 0.6λ; middle plot shows near range reverberation time series detail for all near surface depths; bottom plot shows long range reverberation time series detail for all near surface depths.

Annex B Vertical Field

B.1 Fourier Transform Analysis

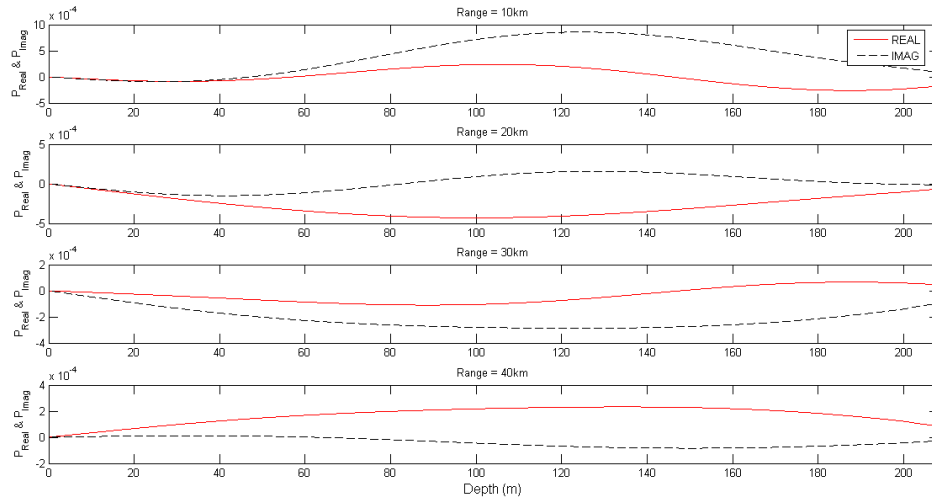


Figure 54. ASA Wedge (25 Hz) showing real and imaginary vertical field components at 4 ranges (10, 20, 30 and 40 km). File *peAllModes.tlz*. Script: *vert_field.m*.

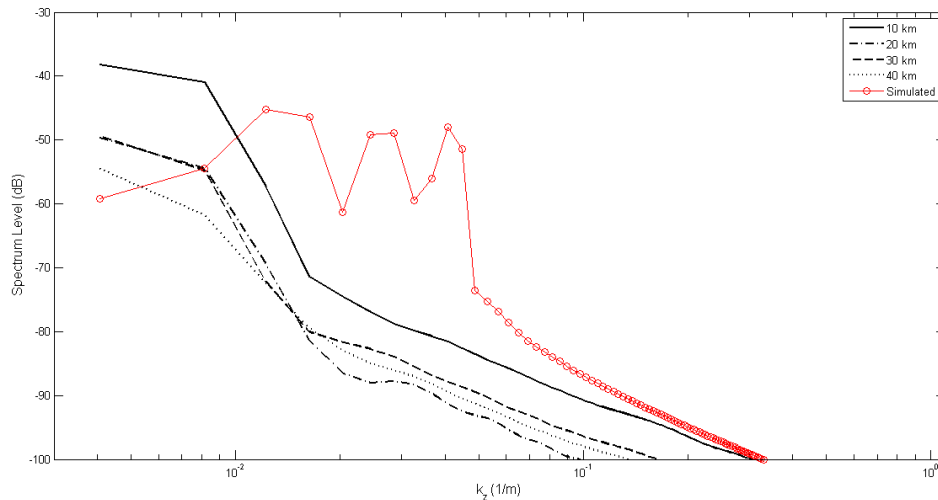


Figure 55. Spectra for the ASA Wedge (25 Hz) case containing three modes, and simulated data. Components simulated are at $k_z = 0.014, 0.027, 0.041 \text{ m}^{-1}$. File *peAllModes.tlz*; Scripts: *vert_field.m* and *determine_spectrum_params.m*.

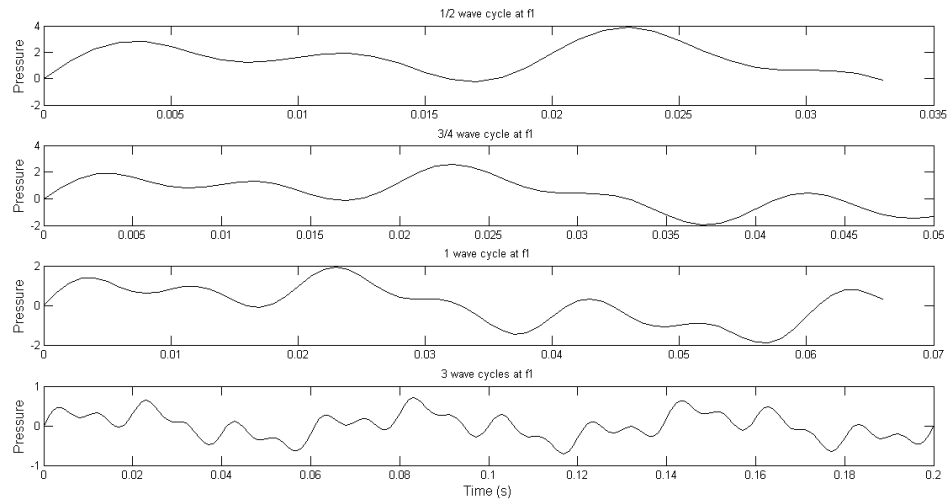


Figure 56. Synthetic time series with frequency components at 15, 50 and 100 Hz. From top to bottom the time series contain 1/2, $\frac{3}{4}$, 1, and 3 wave cycles of the lowest frequency component (15Hz).

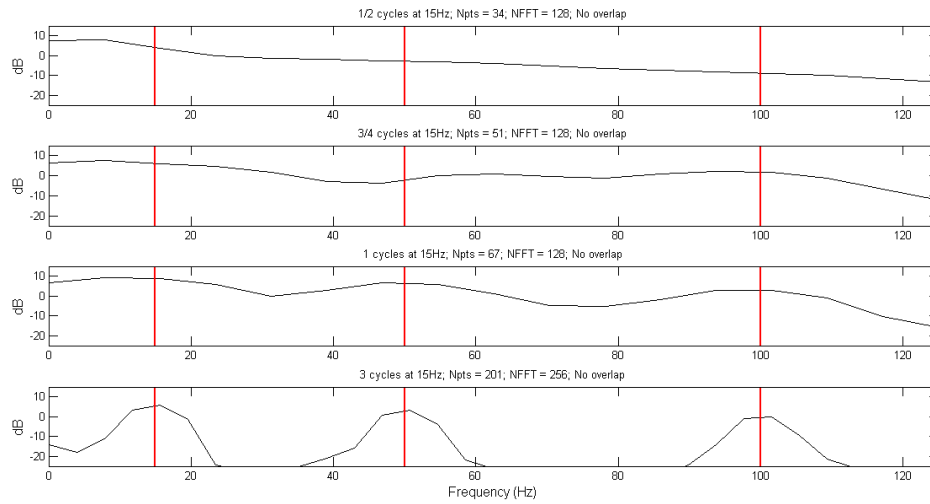


Figure 57. Spectra of the time series shown in Figure 12. Vertical red lines indicate the frequency component locations. Only when there is one full cycle of the lowest frequency to resolve does the spectrum reflect the true frequency content. Frequency components at 15, 50 and 100 Hz.

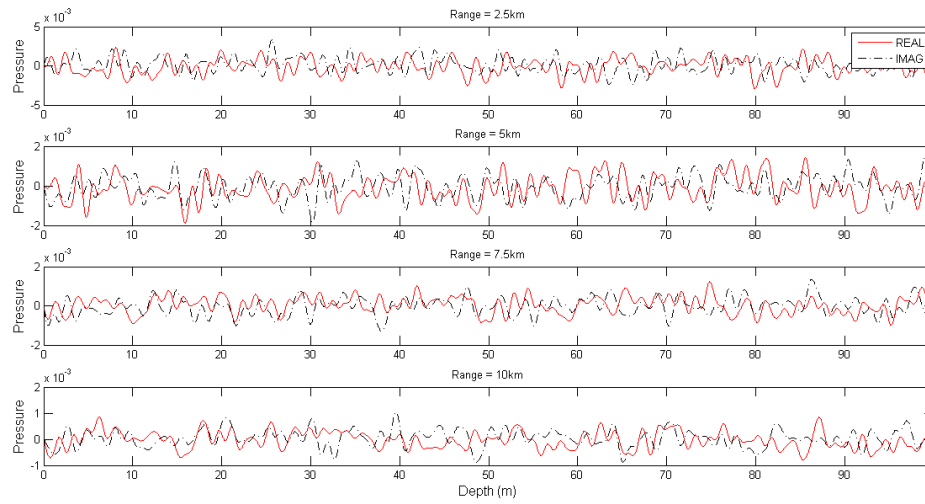


Figure 58. Vertical pressure field for the first four output ranges in the *P11_f3500_S30R50_pe.tlz* file.

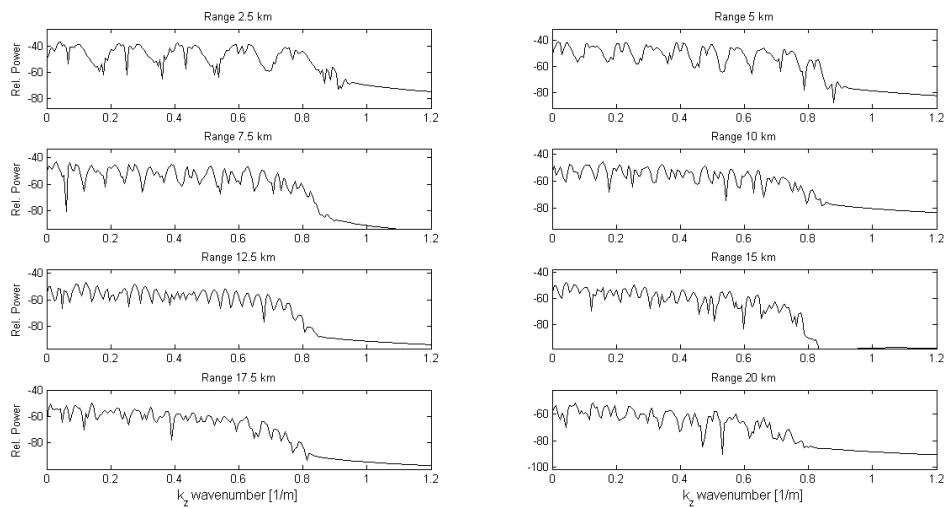


Figure 59. Vertical field spectra for the first eight ranges output in the *P11_f3500_S30R50_pe.tlz* file. Source depth = 30m.

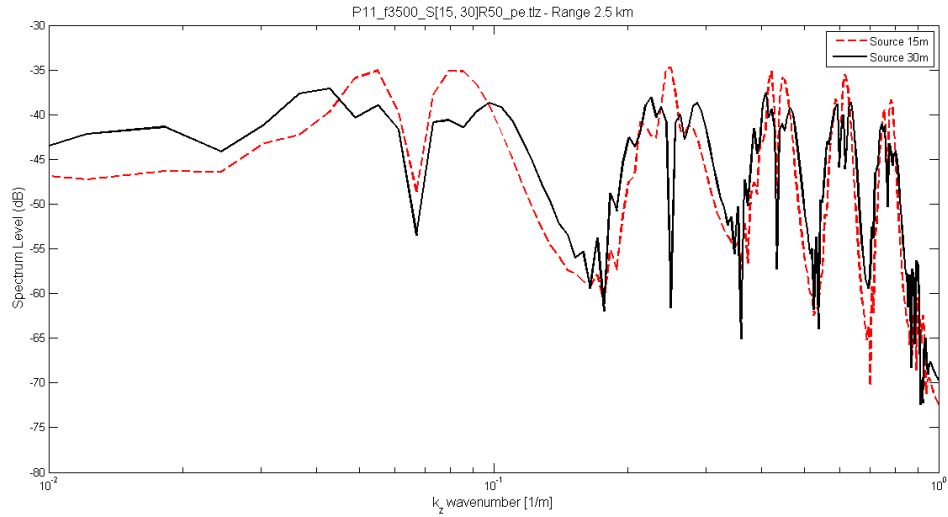


Figure 60. Comparison between two wavenumber spectra at 2.5 km range when the source depth is changed from 30m to 15m. Files: *RW_P11_f3500_S15R50_pe.tlz* and *RW_P11_f3500_S30R50_pe.tlz*.

B.2 Reducing θ_{\max} as a Function of Range

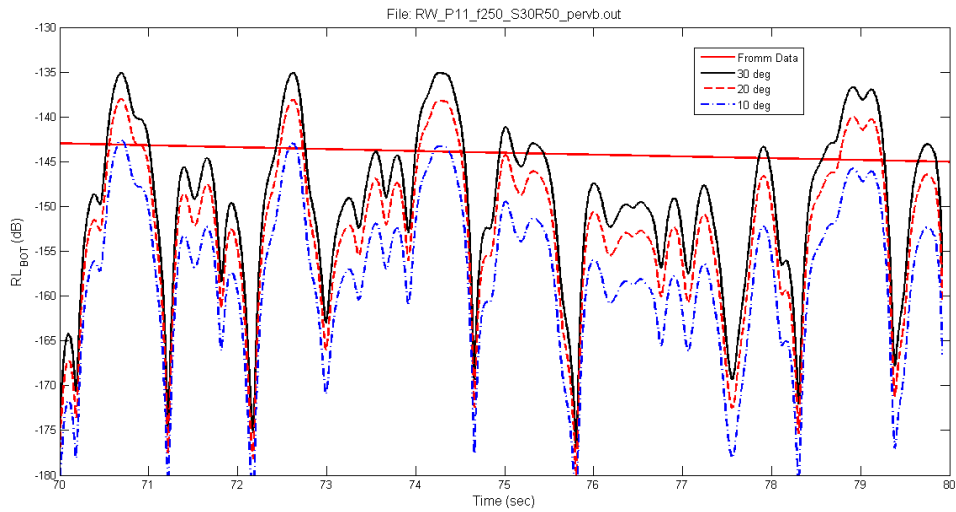


Figure 61. Bottom reverberation plotted as a function of time, computed for a reduction of θ_{\max} with range, shown for the maximum ranges where the effect is greatest. The solid red line is the reference data of Fromm [19].

Annex C 'Goodness of Fit' Results

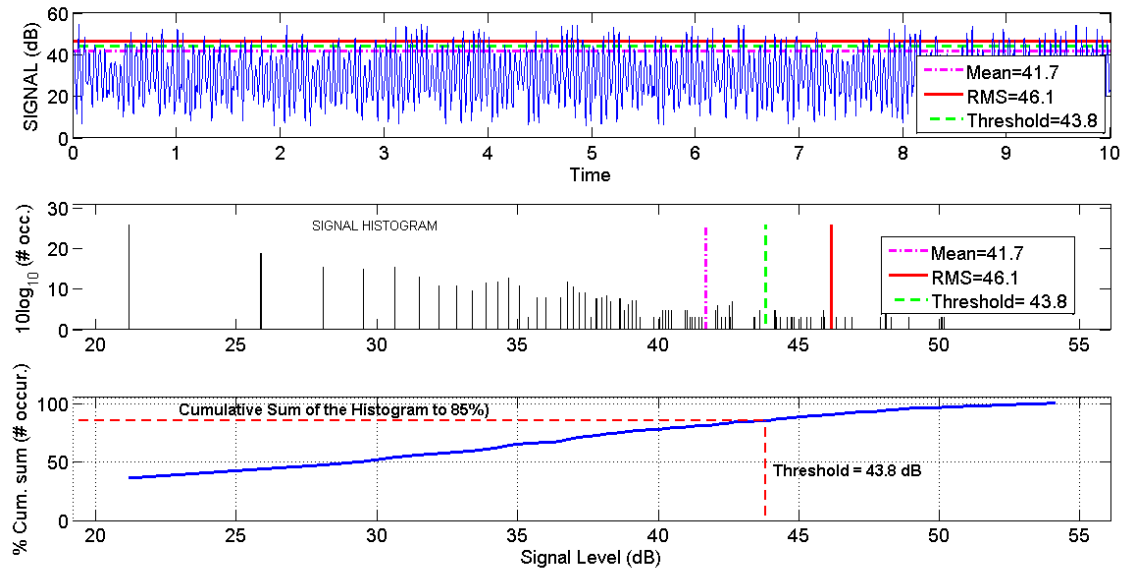


Figure 62. Output from modelled_histogram.m, simulated signal. Three different levels are shown, the mean, the RMS, and the threshold (85% of total energy) based on the histogram. Note: the histogram is computed in linear space, but has been shown in log-log for visual purposes only.

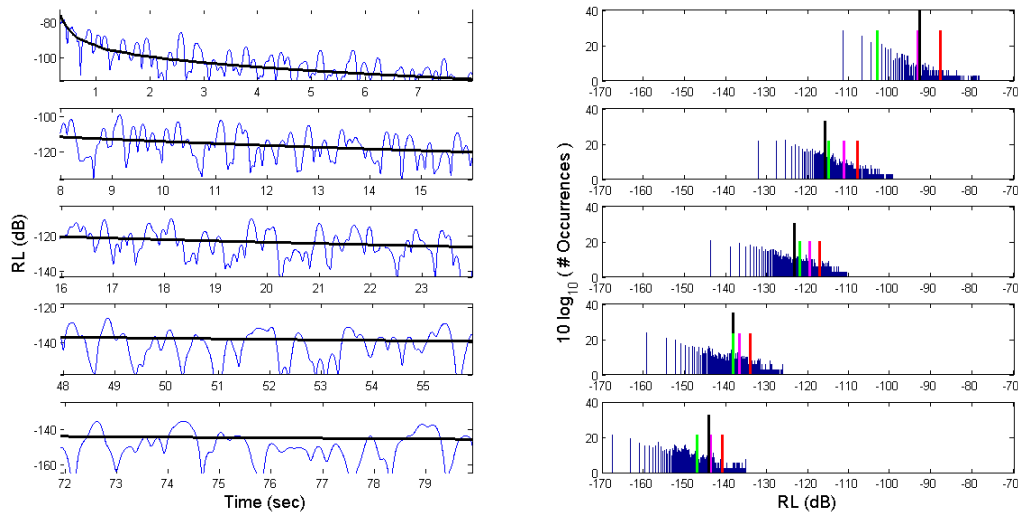


Figure 63. Mean, RMS, and histogram method applied to reverberation data and compared to Fromm (250 Hz, Problem 11). Black lines: Fromm; Red lines: RMS, Magenta: Mean; Green: Histogram-sum with threshold at 60%.

This page intentionally left blank.

Annex D Software: PECan modifications and Matlab™ Scripts

D.1 PECan modifications

The following two PECan source code files were modified to enable the output of the files described in sections D.1.1 and D.1.2.:

- PECan.f
- PECan_Prop.f

These files are included on the data DVD deliverable.

D.1.1 Output File: Petlr.out

A new PECan output file, petlr.out, based on the PECan file pe.tlr was created. This file contains decibel value Transmission Loss for each range, receiver depth, and azimuth. Compared to pe.tlr the new file has a much shorter header section. Transmission Loss values are greater than zero. During the study only one azimuth was ever used. A sample of the petlr.out format with description is provided:

```
20000          3          1      – description: nRanges, nRx, nAzimuths
30.000000                                – description: Source Depth (m)
5.00000000    10.00000000    15.00000000 – description: RxDepths (m), up to 5 Rx
0.0      1.000000 – description: Az_start, Az_increment; when only one Azimuth, Inc. = 1.0
```

The data then follows, shown here for the case of two azimuths:

```
Range1 for Rx Depth 1 spaces TL(1, 1, AZ#1) spaces TL(1, 1, AZ#2)
Range1 for Rx Depth 2 spaces TL(1, 2, AZ#1) spaces TL(1, 2, AZ#2)
...
Range1 for Rx Depth M spaces TL(1, M, AZ#1) spaces TL(1, M, AZ#2)
Range2 for Rx Depth 1 spaces TL(2, 1, AZ#1) spaces TL(2, 1, AZ#2)
Range2 for Rx Depth 2 spaces TL(2, 2, AZ#1) spaces TL(2, 2, AZ#2)
...
Range2 for Rx Depth M spaces TL(2, M, AZ#1) spaces TL(2, M, AZ#2)
RangeN for Rx Depth 1 spaces TL(N, 1, AZ#1) spaces TL(N, 1, AZ#2)
RangeN for Rx Depth 2 spaces TL(N, 2, AZ#1) spaces TL(N, 2, AZ#2)
...
RangeN for Rx Depth 5 spaces TL(N, M, AZ#1) spaces TL(N, M, AZ#2)
```

D.1.2 Output File: Pervb.out

A new PECan output file, pervb.out, was created which facilitates easier extraction of the Transmission Loss values required for estimating reverberation. This is achieved since pervb.out

contains Transmission Loss values along the waveguide boundaries and within the water column. Specifically, pervb.out contains the Range (km) in the first column, the Depth of the bathymetry (m) at that range in the second column, and then three columns present decibel values of Transmission Loss for that range. The three Transmission Loss columns, from left to right, represent TL values at the water surface, within the water volume (at the source depth) and, at the bottom of the water. It is important to note that for range dependent environments the Transmission Loss along the bottom follows the bathymetry. Note that the Transmission Loss values are greater than zero. During the study only one azimuth was ever used. A sample of the pervb.out format with description is provided:

The header is the same header as pe.tlr. The header is followed by columnar data, such as:

4.9999999E-03	199.8125	76.85912	15.53018	40.19022
9.9999998E-03	199.5625	78.35818	19.99552	39.58620
1.5000000E-02	199.4375	78.71693	23.04197	39.95741

e.g. The column order is:

R(km)	Depth@R(m)	TLSurf(dB)	TLVol(dB)	TLBot(dB)
-------	------------	------------	-----------	-----------

Note: Currently, pervb.out only produces output for the last azimuth if more than one azimuth is requested.

D.2 Matlab™ Environment Setup

This section describes the setup of the Matlab™ environment which was used. The Matlab™ release used during this study was R2011b, and it was installed on an IBM PC laptop.

The setup of Matlab™ in this study is quite standard. However, in a study where potentially dozens of different input files, and approximately ten-times the number of output files are created, a method of managing this was required. Moreover, there was a need to accommodate the need of the PECan executable for fixed filenames. To this end a specific directory structure was adopted. This directory structure enabled Matlab™ scripts to perform all the management of copying, renaming, deleting, and moving files into and out of PECan.exe while inputs remained in an input directory and outputs were placed in an outputs directory.

As mentioned the normal operation of PECan.exe utilizes file names that are fixed. That is, when running PECan, it will automatically attempt to load the file pe.dat, and only that file, without any user intervention. This was accomplished by using Matlab™ scripts. These scripts, PECan_run.m (single run) and PECan_batch_run.m (multiple runs) manage these files and their locations. The overall operation is captured in Figure 64. One can see the central role that the Matlab™ scripts play in orchestrating the file management.

Finally, if the directory structure below is adopted, the user must ensure that: a) all folders are listed in the Matlab™ path, via File → SetPath... from the command window; and b) as required, that within the scripts the location of the executable and output directories is provided (exepath and outputpath).

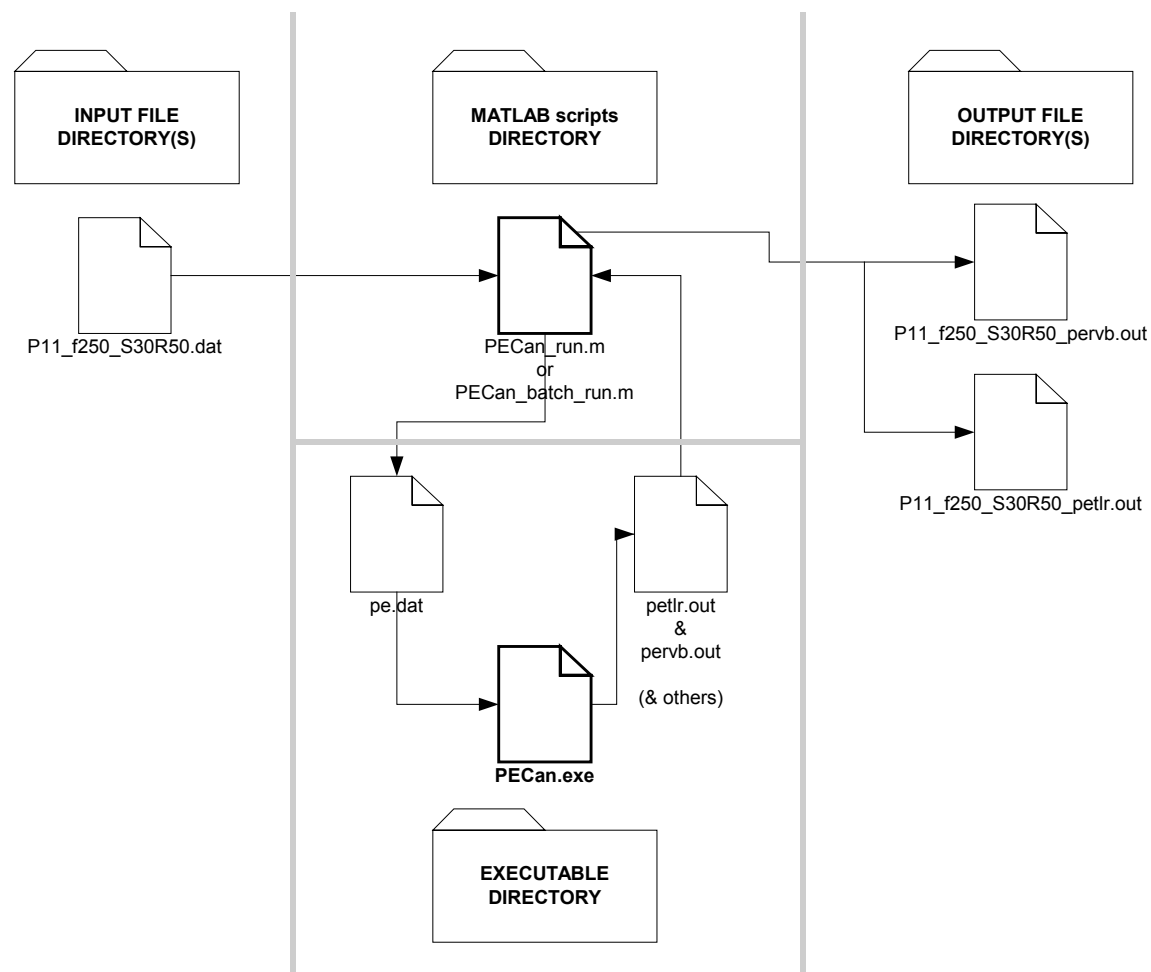


Figure 64. Directory structure and orchestration via MatlabTM scripts.

For general MatlabTM technical assistance, the following web URL is provided:
<http://www.mathworks.com/help/techdoc/>

D.3 MatlabTM Script Listings

D.3.1 Reverb_pervb4.m

The MatlabTM script reverb_pervb4.m was used to generate all the graphs provided in Annex A.

```
% reverb_pervb4.m
% Based on: reverb_pervb3.m as of March 25
% BI-STATIC
```

```

% Script to estimate Reverberation from PECan proploss (pervb.out files)
%   and Target Echo from PECan proploss (petlr.out file - contains Rx
depth TL)
% Includes: Chapman-Harris surface scattering (March 1)
% Added target strength.
% PLOTS ALL reverberation components for RW Problems XI, XII, XIII, XVII
% 15 March 2012

clear all;
close all;

global tit fHz sdep rz1 rz2 nrz rz
global nAz Num_Rx

% High level parameters
c0 = 1500; % m/s
SL = -6.29; % source level
sl = 10.^(SL/10);

TS = 8; % target strength
ts = 10.^(TS/10);
%TxDepth = input('Sonar Tx depth (m): ');
TxDepth = 30; % always 30m for Reverb Workshop problems
%RxDepth = input('Sonar Rx depth (m): ');
RxDepth = 50 % metres = target depth - could be user keyboard input
%TgtDepth = input('Target depth (m): ');
TgtDepth = 10 % Problem 17, Wedge

dB_min = -200; % min value on proploss axis
dB_max = -60;
SB_correction = -6; % Correction applied to sfc and bottom, unless
overriden below
sfcbias = 55; % this biases the free-surface surface reverb arbitrarily
by x dB

%=====
% Open the PECan data _pervb.out file - gives reverberation components

pr_input = menu('RW Problem #', '11', '12', '13', '17', 'E X I T');
if pr_input == 1, prstr='P11_'; end;
if pr_input == 2, prstr='P12_'; end;
if pr_input == 3, prstr='P13_'; end;
if pr_input == 4, prstr='P17_'; end;
if pr_input == 5, return; end;
fr_input = menu('Frequency (Hz)', '250', '1000', '3500', 'E X I T');
if fr_input == 1, frstr='f250_'; tau = 0.08; end;
if fr_input == 2, frstr='f1000_'; tau = 0.02; end;
if fr_input == 3, frstr='f3500_'; tau = 0.005714; end;
if fr_input == 4, return; end;

```

```

% UNCOMMENT THE FILE SET YOU WANT TO READ
%qualifier = 'alt_'; % dr = 1 m
qualifier = ''; % dr = 2.5 m

fname_out = ['RW_' prstr frstr 'S30R' num2str(TgtDepth) '_' qualifier];
fname_rtn = ['RW_' prstr frstr 'S' num2str(RxDepth) 'R'
num2str(TgtDepth) '_' qualifier];
outputpath = 'C:\modelling\PEreverb\outputs\';

tlfile_SVBout = [outputpath fname_out 'pervb.out']; % Suf, Bot., Vol,
outgoing path
tlfile_SVBrtn = [outputpath fname_rtn 'pervb.out']; % Return path
(different 'source' depth)

[fid_SVBout, message] = fopen(tlfile_SVBout, 'r');
disp(['Opening file: ' tlfile_SVBout]);
[fid_SVBrtn, message] = fopen(tlfile_SVBrtn, 'r');
disp(['Opening file: ' tlfile_SVBrtn]);

%-----
% Open the PEGCan petlr.out files - for target echo only
% Convention: RW_P##_f####_S[notel]R[notel2]_petlr.out (or _pervb.out)
% notel: source depth in PEGCan input
% notel2: target depth=Rx depth in PEGCan input file
fname_echo_out = ['RW_' prstr frstr 'S30R' num2str(TgtDepth) '_'
qualifier 'petlr.out'];
fname_echo_rtn = ['RW_' prstr frstr 'S' num2str(RxDepth) 'R'
num2str(TgtDepth) '_' qualifier 'petlr.out'];

disp(['Opening file: ' fname_echo_out]);
fid_echo_out = fopen(fname_echo_out, 'r'); % open fname, read only
disp(['Opening file: ' fname_echo_rtn]);
fid_echo_rtn = fopen(fname_echo_rtn, 'r'); % open fname, read only
%-----
---

% Read All Headers
fn_read_pervb_header(fid_SVBout);
fn_read_pervb_header(fid_SVBrtn);
fn_read_petlr_header(fid_echo_out);
fn_read_petlr_header(fid_echo_rtn);
%-----
% Read pervb.out files contents:
% REVERBERATION
% pervb.out header is followed by 5 columns:
% R(km) Depth@R TLSurf TLVol TLBot
% OUTGOING PATHS: Sonar Tx to scatterer (ss,sv,sb)
SVBo = fscanf(fid_SVBout, '%g %g %g %g %g', [5 Inf])'; % read 5 cols,
to eof
fclose(fid_SVBout); % Close the file
range_km = SVBo(:,1);
water_depth_m = SVBo(:,2); % water depth at range_km

```

```

TLss = SVBo(:,3); % TL @ Tx -> surface
tlss = 10.^(-SVBo(:,3)/10);
TLsv = SVBo(:,4); % TL @ Tx -> water column
tlsv = 10.^(-SVBo(:,4)/10);
TLsb = SVBo(:,5); % TL @ Tx -> bottom
tlsb = 10.^(-SVBo(:,5)/10);
range_m = range_km*1000;
Rmax = max(range_km);
nRanges = length(range_m);
clear SVBo % clean up

% RETURN PATHS: Sonar Rx to scatterer (rs,rv,rb)
SVBr = fscanf(fid_SVBrtn,'%g %g %g %g %g',[5 Inf]); % read 5 cols,
to eof
fclose(fid_SVBrtn); % Close the file
Ntemp = length(SVBr(:,1));
if Ntemp ~= nRanges, % sanity check the two files
    fclose('all');
    display('File length MISMATCH in pervb.out files - ABORTED');
    display([fname_out ': ' num2str(nRanges) ' ranges; ' fname_rtn ': '
num2str(Ntemp) ' ranges']);
end
% water_depth_m = SVBr(:,2); % should be identical to OUTGOING path data
TLrs = SVBr(:,3); % TL @ Rx -> surface
tlrs = 10.^(-SVBr(:,3)/10);
TLrv = SVBr(:,4); % TL @ Rx -> water column
tlrv = 10.^(-SVBr(:,4)/10);
TLrb = SVBr(:,5); % TL @ Rx -> bottom
tlrb = 10.^(-SVBr(:,5)/10);
clear SVBo % clean up

% - - - - -
% Read petlr.out files contents:
% TARGET ECHO
% OUTGOING PATH: Sonar Tx to target (st)
%If more than one RxDepth, this is multiplexed:
Eout = fscanf(fid_echo_out,'%g %g %g %g %g %g %g %g %g %g',[nAz+1
Inf]); % read up to 10 cols: Range + (up to 10 Az) to bottom
% Ranges - already obtained above from pervb.out files
ii = 1; % One azimuth only
for jj = 1:Num_Rx, % for each Rx depth
    TL.AzRx{ii,jj} = Eout(jj:Num_Rx:Num_Rx*nRanges+jj-1,ii+1); % dB
    if jj == 1, mkr = '-';end
    if jj == 2, mkr = '--';end
    if jj == 3, mkr = '-.';end
end
clear Eout % clean up
fclose(fid_echo_out); % Close the file
TL_e_out = TL.AzRx{1,1}; % PECO can propoloss for target. These loss values
are > 0.
tle_out = 10.^(-TL_e_out/10); % LINEAR LOSS at each range step

% RETURN PATH: Sonar Rx to target (rt)

```

```

%If more than one RxDepth, this is multiplexed:
Ertn = fscanf(fid_echo_rtn,'%g %g %g %g %g %g %g %g %g %g',[nAz+1
Inf]); % read up to 10 cols: Range + (up to 10 Az) to bottom
ii = 1; % One azimuth only
for jj = 1:Num_Rx, % for each Rx depth
    TL.AzRxr{ii,jj} = Ertn(jj:Num_Rx:Num_Rx*nRanges+jj-1,ii+1); % dB
end
clear Ertn % clean up
fclose(fid_echo_rtn); % Close the file
TLe_rtn = TL.AzRxr{1,1}; % PECAN propoloss for target. These loss
values are > 0.
tle_rtn = 10.^(-TLe_rtn/10); % LINEAR LOSS at each range step

figure(5) % Proploss from the petlr.out files
plot(range_m,TLe_rtn,'r');hold on;plot(range_m,TLe_out,'k');axis ij;
xlabel('Range (m)');ylabel('dB');title('proploss')
%-----
% Plot PECAN PROPLOSS
figure(1)
minx = 0.02;maxx=10*ceil(max(range_km+.01)/10);
miny=20;maxy=100; % plot limits
% Note: Use rigidtop pervb.out for surface
subplot(311);semilogx(range_km, TLss,'k-');hold on;semilogx(range_km,
TLrs,'r-');
axis ij;axis([minx maxx 60 140]);ylabel('TL_{ SFC} (dB)')
legend('Out path','Return path')
title(['PECAN Propoloss: ' fname_out 'pervb.out'],'interpret','none');

subplot(312);semilogx(range_km, TLsv,'k-');
axis ij;hold on;semilogx(range_km, TLrv,'r-');
ylabel('TL_{ VOL} (dB)');
axis([minx maxx miny maxy]);
legend('Out path','Return path')

subplot(313);semilogx(range_km, TLsb,'k-');hold on;semilogx(range_km,
TLrb,'r-');
axis ij;ylabel('TL_{ BOT} (dB)');
xlabel('Range(km)');axis([minx maxx miny maxy]);
legend('Out path','Return path')

%=====
% Load and plot the reference reverberation data:

% For figure 2, order is:
% subplot(311) = SURFACE
% subplot(312) = VOLUME
% subplot(313) = BOTTOM

figure(2)
if pr_input == 1, % Reverb Workshop PROBLEM 11
    if fr_input == 1,
        % 250 Hz

```

```

        subplot(311);plot_ray_P11_f250_sfcrvb;hold on;
        subplot(312);plot_ray_P11_f250_volrvb;hold on;
        subplot(313);
        plot_Fromm_P11_f250_botrvb;hold on;
    end
    if fr_input == 2,
        % 1000 Hz
        subplot(311);plot_ray_P11_f1000_sfcrvb;hold on;
        subplot(312);plot_ray_P11_f1000_volrvb;hold on;
        subplot(313);plot_Fromm_P11_f1000_botrvb;hold on;
    end
    if fr_input == 3,
        % 3500 Hz
        subplot(311);plot_ray_P11_f3500_sfcrvb;hold on;
        subplot(312);plot_ray_P11_f3500_volrvb;hold on;
        subplot(313);plot_Fromm_P11_f3500_botrvb;hold on;
    end
end

if pr_input == 2, % Reverb Workshop PROBLEM 12 - SUMMER
    if fr_input == 1,
        % 250 Hz
        subplot(311);plot_ray_P12_f250_sfcrvb;hold on; % surf
        subplot(312);plot_ray_P12_f250_volrvb;hold on;
        subplot(313);plot_Fromm_P12_f250_botrvb;hold on;
    end
    if fr_input == 2,
        % 1000 Hz
        subplot(311);plot_ray_P12_f1000_sfcrvb;hold on;
        subplot(312);plot_ray_P12_f1000_volrvb;hold on; % vol
        subplot(313);plot_Fromm_P12_f1000_botrvb;hold on;
    end
    if fr_input == 3,
        % 3500 Hz
        subplot(311);plot_ray_P12_f3500_sfcrvb;hold on; %
        subplot(312);plot_ray_P12_f3500_volrvb;hold on; % vol
        subplot(313);plot_Fromm_P12_f3500_botrvb;hold on;
    end
end

if pr_input == 3, % Reverb Workshop PROBLEM 13 - WINTER
    if fr_input == 1,
        % 250 Hz
        subplot(311);plot_ray_P13_f250_sfcrvb;hold on; % surf
        subplot(312);plot_ray_P13_f250_volrvb;hold on;
        subplot(313);plot_Fromm_P13_f250_botrvb;hold on;
    end
    if fr_input == 2,
        % 1000 Hz
        subplot(311);plot_ray_P13_f1000_sfcrvb;hold on; % surf
        subplot(312);plot_ray_P13_f1000_volrvb;hold on;
        subplot(313);plot_Fromm_P13_f1000_botrvb;hold on;
    end
end

```



```

    if fr_input == 3,
        % 3500 Hz
        subplot(311);plot_ray_P13_f3500_sfcrvb;hold on;
        subplot(312);plot_ray_P13_f3500_volrvb;hold on;
        subplot(313);plot_Fromm_P13_f3500_botrvb;hold on;
    end
end

if pr_input == 4, % Reverb Workshop PROBLEM 17 - RD
    if fr_input == 1,
        % 250 Hz
        subplot(311);plot_ray_P17_f250_sfcrvb;hold on; % surf, vol, bot
    % NO DATA
        subplot(312);plot_ray_P17_f250_volrvb; hold on;
        subplot(313);plot_ellis_P17_botrvb;hold on; % Ellis data
        subplot(313);plot_ray_P17_f250_botrvb; % Brooke, ray data
        % draw the legend at bottom of the script
    end
    if fr_input == 2,
        % 1000 Hz
        subplot(311);plot_ray_P17_f1000_sfcrvb;hold on; % surf, vol, bot
    % NO DATA
        subplot(312);plot_ray_P17_f1000_volrvb; hold on;
        subplot(313);plot_ray_P17_f1000_botrvb;hold on; % Brooke, ray
    data
        % draw the legend at bottom of the script
    end
    if fr_input == 3,
        % 3500 Hz
        subplot(311);plot_ray_P17_f3500_sfcrvb;hold on; % surf, vol, bot
    % NO DATA
        subplot(312);plot_ray_P17_f3500_volrvb; hold on;
        subplot(313);plot_ray_P17_f3500_botrvb;hold on; % Brooke, ray
    data
        % draw the legend at bottom of the script
    end
end

%=====
%=====
% Reverberation Calculations
Scatt_avg_v_dB = -73; % Volume scattering strength (could use
Tuovila/similar, here)
%-----
% For MacKenzie-Lambert Scattering (Bottom):
mu_dB = -27;
%mu = 10^(mu_dB/10);

%-----
% Chapman-Harris scattering (Surface):
% Caveat, Validity: wind speed 0-30 kt; 400 < f < 6400 Hz
% fHz - global value from header
% Wkts=input('Wind speed (kt): ');

```

```

Wind_kts = 19.44 % 10 m/s

%-----
% Scattering patch width

% Get number of PECO range steps; determine PECO range step; determine
nbins
% per pulse
dr_m = range_m(3)-range_m(2); % PECO output range step
dt = dr_m/c0; % time between range samples

nbins = round(tau/dt); % number of range (or time) bins over the pulse
length
nbins_max = 2*nRanges; % # time bins to hold reverb

jj_max = nRanges-nbins;

rls = zeros(1,nbins_max-nbins); % initialize this reverb level to ZERO
before summing, elements are in time bins
rlb = zeros(1,nbins_max-nbins);
rlv = zeros(1,nbins_max-nbins);
te = zeros(1,nbins_max-nbins);

ending_Scatt_angle = 27; % degrees
beginning_Scatt_angle = 27;
a = (ending_Scatt_angle - beginning_Scatt_angle); % a < 0

% Compute total energy back at the Tx for each range step (jj) in the
PECO output:
for jj = 1:jj_max,

    Tmax_degrees = a*range_km(jj)/Rmax + beginning_Scatt_angle; %
Theta_max versus range. Linear reduction with range.

    % BOTTOM REVERBERATION
    % This block to use a linear reduction in Theta_max with range for
Lambert Law,
    % see also: weighting_fn.m
    [Scatt_avg_b Scatt_avg_b_dB] =
fn_integrate_maclambert(mu_dB,Tmax_degrees);

    % SURFACE REVERB
    [Scatt_avg_s Scatt_avg_s_dB] =
fn_integrate_chapmanharris(fHz,Wind_kts,Tmax_degrees);

    % VOLUME REVERB-----
    Scatt_avg_v = 10^(Scatt_avg_v_dB/10); % linear average scattering
strength

    % Determine a received level at the transducer from tiny patch,
width dr, at range r(jj).

```

```

    % dA and dV: Assuming omnidirectional source, 2*pi radians
    dA = 2*pi*range_m(jj)*dr_m; % '2 pi r dr ' = scattering_patch_area
of ONE range bin, omni source in horiz.
    % beamwidth_vertical_deg = 85; % Source aperature in the PE,
or an actual beamwidth
    % dz = pi*beamwidth_vertical_deg*range_m(jj)/180; %
approximate cell height
    % if dz > water_depth_m(jj), dz = water_depth_m(jj); end
    % %disp(['H limited at ' num2str(water_depth_m(jj))
'm']); end % the volume cell height now occupies all the water column
    dz = water_depth_m(jj); % As computed in the ray model
    dV = dA*dz; % approximate volume cell volume

    Recd_scattered_energy_s = sl * tlss(jj)*tlrs(jj) * Scatt_avg_s * dA;
% NOTE: these are ONE range bin, not nbins.
    Recd_scattered_energy_v = sl * tlsv(jj)*tlrv(jj) * Scatt_avg_v * dV;
    Recd_scattered_energy_b = sl * tlsb(jj)*tlrb(jj) * Scatt_avg_b * dA;
    target_echo = sl * tle_out(jj) * tle_rtn(jj) * ts;

    % Binning the energy into the pulse width (nbins)
    % Each loop is one pulse integration
    arrival_time = 2*range_m(jj)/c0; % Front-edge arrival time pulse
from range_m
    nB0 = round(arrival_time/dt); % Best time bin in which the arrival
starts

    % for each rec'd pulse in the individual 'rays':
    for k = 0:nbins-1, % step is over each time bin, in total ONE pulse
length
        idx = nB0+k; % time bin index
        rls(idx) = rls(idx) + Recd_scattered_energy_s; % Write the
scattered level in the bins spanning the pulse duration
        rlb(idx) = rlb(idx) + Recd_scattered_energy_b;
        rlv(idx) = rlv(idx) + Recd_scattered_energy_v;
        te(idx) = te(idx) + target_echo;
    end
    % [sum(rl(nB0:nB0+nbins-1))/(nbins*Recd_scattered_energy)] = 1.0 on
first pass ('Pink Pulse' - Fig 2 of proposal)
end

% Reverb in dB
RL_dB.s = 10*log10(rls); % Convert to dB
RL_dB.b = 10*log10(rlb);
RL_dB.v = 10*log10(rlv);

% Target Echo in dB
% The sum above over counts the contributions from the pulse nbins
times.
TE = 10*log10(te/nbins);

RL_time = dt*[1:1:length(RL_dB.s)];

```

```

%-----
---
% Plotting all Sfc, Vol, Bot. reverberation:

figure(2);

minx = 0;
maxx=ceil(max(2*range_m/c0)); % ranges < 10 sec
%maxx=10*ceil(max(2*range_m/c0)/10); % ranges > 10 sec
miny=-200;maxy=-70; % plot limits
subplot(311);axis([minx maxx miny maxy]);
subplot(312);axis([minx maxx miny maxy]);
subplot(313);axis([minx maxx miny maxy]);

subplot(311);set(gca,'FontSize',12);
plot(RL_time,RL_dB.s + SB_correction + sfcbias , 'k');hold
on;ylabel('RL_{ SFC} (dB)');
title(['Files: ' fname_out 'pervb.out & ' fname_rtn
'pervb.out'], 'interpret','none');
%text(0.8*maxx,maxy-10,['NOTE: PE output + ' num2str(sfcbias) ' dB']);
text(.8*max(2*range_m/c0),-85,['NOTE: PE output - 6 + ' num2str(sfcbias)
' dB']);

subplot(312);set(gca,'FontSize',12);
plot(RL_time,RL_dB.v, 'k');hold on;ylabel('RL_{ VOL} (dB)');

subplot(313);set(gca,'FontSize',12);
plot(RL_time,RL_dB.b+SB_correction, 'k');hold on;xlabel('Time
(sec)');ylabel('RL_{ BOT} (dB)');
text(.8*max(2*range_m/c0),-85,['NOTE: PE output - 6 dB']);

%-----
---
% Plot PE method Target Echo
figure(3)
set(gca,'FontSize',12);
plot(RL_time,TE, 'k');hold on;
xlabel('Time (sec)');ylabel('Target Echo (dB)')
title(['Files: ' fname_echo_out ' & '
fname_echo_rtn], 'interpret','none');
axis([0 max(RL_time) dB_min dB_max]);

%-----
---
% Plot ray model / Reference data for Target Echo

figure(3)

if pr_input == 1, % Reverb Workshop PROBLEM 11
    if fr_input == 1,
        % 250 Hz
        plot_ray_P11_f250_echo;hold on;

```

```

end
if fr_input == 2,
    % 1000 Hz
    plot_ray_P11_f1000_echo;hold on;
end
if fr_input == 3,
    % 3500 Hz
    plot_ray_P11_f3500_echo;hold on;
end
end

if pr_input == 2, % Reverb Workshop PROBLEM 12 - SUMMER
    if fr_input == 1,
        % 250 Hz
        plot_ray_P12_f250_echo;hold on;
    end
    if fr_input == 2,
        % 1000 Hz
        plot_ray_P12_f1000_echo; hold on;
    end
    if fr_input == 3,
        % 3500 Hz
        plot_ray_P12_f3500_echo;hold on;
    end
end

if pr_input == 3, % Reverb Workshop PROBLEM 13 - WINTER
    if fr_input == 1,
        % 250 Hz
        plot_ray_P13_f250_echo;hold on;
    end
    if fr_input == 2,
        % 1000 Hz
        plot_ray_P13_f1000_echo; hold on;
    end
    if fr_input == 3,
        % 3500 Hz
        plot_ray_P13_f3500_echo;hold on;
    end
end

if pr_input == 4, % Reverb Workshop PROBLEM 17 - RD
    if fr_input == 1,
        % 250 Hz
        plot_ellis_P17_echo; % Ellis data - 250 Hz
        plot_ray_P17_f250_echo; % Brooke, ray data - no data
        legend('PE','Normal Mode','Ray')
        title(['Problem 17 (RD). TS = ' num2str(TS) ' ; SL = '
num2str(SL) ' dB; f = 250 Hz'])
        % grid on
        % Use this chance to adjust axes on Figure 2 for this case:
        minx = 0;maxx=11;miny=-140;maxy=-70; % plot limits
        legend('Normal Mode','RAY','PE');

```

```

elseif fr_input == 2,
    plot_ray_P17_f1000_echo; % Brooke ray data
    title(['Problem 17 (RD). TS = ' num2str(TS) '; SL = '
num2str(SL) ' dB; f = 1000 Hz'])
elseif fr_input == 3,
    plot_ray_P17_f3500_echo; % Brooke ray data
    title(['Problem 17 (RD). TS = ' num2str(TS) '; SL = '
num2str(SL) ' dB; f = 3500 Hz'])
end

figure(2)
subplot(311);axis([minx maxx miny maxy]);
subplot(312);axis([minx maxx miny maxy]);
subplot(313);axis([minx maxx miny maxy]);

figure(4); % environment profile
x = [-1 0 7.4 8.0];
y = [-200 200 10 10];
plot(2*x/1.5,y,'k','LineWidth',3);hold on;
plot(2*[0 0]/1.5,-[30 30],'ro','LineWidth',4) % Tx
plot(2*[0 4 8]/1.5,-[10 10 10],'k--','LineWidth',2) % Target
plot(2*[0 4 8]/1.5,-[50 50 50],'k--','LineWidth',2) % Rx
t = -1:.01:10.6;s=1*sin(2*pi*.75*t);
plot(t,s,'b','LineWidth',3)
xlabel('Time (s)');ylabel('Depth (m)');
grid on;title('PROBLEM XVII ENVIRONMENT');
%axis([-3 8 -220 20]);
end

```

D.3.2 Header Reads for pervb.out and petlr.out

The Matlab™ scripts provide in this Annex are functions called from, among others, the reverb_pervb4.m script listed in the previous section (D.3.1). These functions read the header portion of the pervb.out and petlr.out output files from PECan.exe.

For reading the Pervb.out header:

```

function fn_read_pervb_header(fid)
global tit fHz sdep rz1 rz2 nrz rz

% Read Header
tit=fgetl(fid); tit=deblank(tit);

while ~feof(fid)
    txt=fgetl(fid);
    idx=strfind(txt,'F =');
    if (isempty(idx)==0)
        break
    end
end
[s1,s2,fHz,s3]=strread(txt,'%s %s %f %s'); % frequency (Hz)

```

```

while ~feof(fid)
    txt=fgetl(fid);
    idx=strfind(txt,'Sz =');
    if (isempty(idx)==0)
        break
    end
end
[s1,s2,sdep,s3]=strread(txt,'%s %s %f %s'); % source depth
while ~feof(fid)
    txt=fgetl(fid);
    idx=strfind(txt,'Rz1 =');
    if (isempty(idx)==0)
        break
    end
end
[s1,s2,rz1,s3]=strread(txt,'%s %s %f %s'); % Top Rx depth
txt=fgetl(fid);
[s1,s2,rz2,s3]=strread(txt,'%s %s %f %s'); % Bottom Rx depth
txt=fgetl(fid);
[s1,s2,nrz,s3]=strread(txt,'%s %s %d %s'); % # Rx
rz=linspace(rz1,rz2,nrz);
while ~feof(fid)
    txt=fgetl(fid);
    idx=strfind(txt,'Block9');
    if (isempty(idx)==0)
        break
    end
end
for j=1:5
    txt=fgetl(fid);
end

```

For reading the petlr.out file header:

```

function fn_read_petlr_header(fid)
global nRanges Num_Rx nAz SourceDepth RxDepth Az_start Az_increment

% Note: Frequency is not contained in this header.

% Read header
A = fscanf(fid,'%u %u %u',[3 1]); % read 3 cols, first row
nRanges = A(1); % max = 20000
Num_Rx = A(2); % max = 5
nAz = A(3); % max = 64
A = fscanf(fid,'%g',[1,1]); % read single value, metres
SourceDepth = A;
[A,count] = fscanf(fid,'%g %g %g %g %g',[Num_Rx 1]); % read <=5 cols,
% read up to 5 Rx depth values
RxDepth(1:Num_Rx) = A;
% read 2 cols: Theta_start, Theta_increment. When only one Az, Incr =
1.0
[A,count] = fscanf(fid,'%g %g',[2,1]);
Az_start = A(1);

```

```
Az_increment = A(2);
```


Annex E PECan Input and Output Files

This Annex contains a description of the input file naming convention and a subset of input files used during the study.

E.1 PECan Input Files

E.1.1 Naming Convention for this study

The file naming convention for the Reverberation Workshop runs adhere to the following convention:

RW_P##_f####_S##R##_*[optional qualifiers]*.dat

Where:

RW signifies Reverberation Workshop

P## signifies the Problem, or Case, number

f#### signifies the frequency

S### indicates the PECan input file Source depth

R### indicates the PECan input file Receiver depth

For example, RW_P12_f3500_S30R50.dat indicates the input file models Reverberation Workshop Problem 12, at 3500 Hz, with a source depth of 50m and a receiver depth of 50m.

Using the optional qualifier, RW_P12_f3500_S30R50_rigidtop.dat, would indicate the same as the first example, except that the top boundary condition has been set to a rigid top, as opposed to normal condition of a free surface.

In cases where the receiver depth is listed as zero, it means the receiver depth is set to zero or, possibly, a series of depths near the surface.

E.1.2 PECan Input File description

Sample input:

```
Norda 3a (PML)
250 50 0 0 80 1500 2
0.125 2.5 960 4000 0 0 1
50 50 1 1
2 -1 -1 0 0 0 4 1
T F F T
4 1 1
```

```

0 0
0.00 1.0 1500.0 0.0 0.0 0.0
100.00 1.0 1500.0 0.0 0.0 0.0
100.00 1.2 1590.0 0.5 0.0 0.0
120.00 1.2 1590.0 0.5 0.0 0.0
1.2 1590. 0.5 0.0 0.0
0.0 0.0

```

Explanation:

BLOCK 0 (first row)
Title

BLOCK 1 (1st row below title)
Frequency (Hz)
Sd - source depth (m)
Sr - source range (km) (always set to 0)
St - source bearing (deg) (always set to 0)
Sa - source aperture (deg) (vertical angle content of SinX/X
source with SType = 0)
c0 - reference value of sound speed (1500 m/s...wide angle PE not
sensitive to this parameter)
SType :
 0 - SinX/X starter
 1 - Tappert starter
 2 - Greene starter (safe bet)
 3 - self-starter
 >10 - mode starter (special starting field)

BLOCK 2 (2nd row below title)
Dz - grid size in depth (m)
Dr - grid size in range (m)
Nz - No. of grid points in depth (Nz*Dz = deepest depth in
environment block below)
Nr - No. of grid points in range (Nr*Dr should cover maximum
range of interest)
Th0 - starting angle for Nx2D or 3D calculations (deg)
Th1 - final angle for Nx2D or 3D calculations (deg)
nTh - No. of azimuths in the range Th0 to Th1

BLOCK 3
Rz1 - upper Rx depth (m)
Rz2 - lower Rx depth (m)
nRz - No. of Rx's between Rz1 and Rz2 inclusive
nRth - the subsampling interval for the nTh azimuths

BLOCK 4
IEqn - 2 (For Split-Step Pade)

ITop : -1 free surface; 1 rigid surface (this is the top of the depth grid, nominally the ocean surface) use -1
iBot : -1 free surface; 1 rigid surface (this is the bottom of the depth grid - usually not the ocean bottom) use -1
iRDep : 0 range independent; 1 range dependent
iFld : 0 no full field output; 1 full field output (use 0)
i3d : 0 nx2d ; 1 full 3d calculations (use 0)
mP : No. of Pade terms (I usually use 4 terms)
iStability : 1 and leave it.

BLOCK 4.5

lgEnercon : T energy conservation (use this) ; F no energy conservation
lgTopNLBC : F no top nonlocal boundary condition (use this)
lgBotNLBC : F no bottom nonlocal boundary condition (for our stuff use this)
lgPML : F no Perfectly Matched Layer; **T use Perfectly Matched Layer termination at bottom of grid** (we will try to use this always).

BLOCK 5

nI - number of coarse layers (in depth) of the environment
nRj - number of coarse Range pts at which environment is specified
nTj - number of coarse Cross-Range pts at which Environment is specified

BLOCK 6

Loop over Rj

Loop over Tk

Rj - Range coordinate of jth range point (km)

Tj - Cross-range coordinate of the kth cross-range point (km)

Loop over nI

Zi - depth of ith layer (m)

di - density of ith layer (g/cc)

ci - sound speed in the ith layer (m/s)

ai - attenuation in the ith layer (db/lam)

csi - shear speed in ith layer (m/s)

asi - shear attenuation in the ith layer (dB/lam)

end i

end k

end j

BLOCK 7 - these parameters apply only if we are using the non-local bc.

DBot - density of the basement (m)
 CBot - sound speed of the basement (m/s)
 ABot - attenuation of the basement (dB/Lam)
 CsBot - shear sound speed of the basement (m/s)
 AsBot - shear attenuation of the basement (dB/Lam)

BLOCK 8

RsigTop - rms roughness (m) of the top surface (use decimal)
 RsigBot - rms roughness (m) of the ocean bottom surface (use decimal)

NOTES

1. Should allow for at least 3 wavelengths of bottom material before we apply the PML. For example, if the water depth is 100 m and we have allowed for 20 m of material before we set the depth of the PML. $\text{Freq} = 250 \text{ Hz}$ the wavelength is 6.36 m in the bottom and we have allowed for 20 m which is $> 3 \times 6.36 = 19.08$
2. PML is preferred because it limits depths that need be considered and it is efficient. The nonlocal BC limits depths more but it is not quite as efficient.
3. Typically 3D calculations are not performed because they are very time consuming. It requires a 1024 or 2048 FFT for every grid point in the waveguide.
4. Coarse environmental information is input on a grid in (R,T) coordinates. The same number of layers must be used at every grid point.

E.1.3 PECan Input File examples

P12_f250_S30R50.dat

```

Prob XII: Reverb Workshop, Source 30m Rx 50m, summer
250 30 0 0 80 1500 2
.25 5 480 12000 0 0 1
50.0 50.0 1 1
2 -1 -1 0 0 0 4 1
T F F T
4 1 1
      0.000000 0.0
      0.000000 1.0      1530.00 0.00006276 0 0
      100.0000 1.0      1500.00 0.00006276 0 0
      100.0000 2.0      1700 0.5 0 0
      120 2.0      1700 0.5 0 0
2 1700. 0.5 0 0
0.0 0.0

```

P13_f1000_S30R50.dat

Prob XIII: Reverb Workshop, Source 30m Rx 50m, WINTER

```
1000 30 0 0 80 1500 2
0.05 2.5 2400 20000 0 0 1
50.0 50.0 1 1
2 -1 -1 0 0 0 4 1
T F F T
4 1 1
      0.000000 0.0
      0.000000 1.0      1490.00 0.000104 0 0
      100.0000 1.0      1500.00 0.000104 0 0
      100.0000 2.0      1700 0.5 0 0
      120 2.0      1700 0.5 0 0
2 1700. 0.5 0 0
0.0 0.0
```

P11_f3500_S30R50.dat

Prob XI: Reverb Workshop, Source 30m Rx 50m

```
3500 30 0 0 80 1500 2
0.02 2.5 6000 20000 0 0 1
50.0 50.0 1 1
2 -1 -1 0 0 0 4 1
T F F T
4 1 1
      0.000000 0.0
      0.000000 1.0      1500.00 0.00010275 0 0
      100.0000 1.0      1500.00 0.00010275 0 0
      100.0000 2.0      1700 0.5 0 0
      120 2.0      1700 0.5 0 0
2 1700. 0.5 0 0
0.0 0.0
```

RW_P11_f250_S30R0.dat (near surface study)

Prob XI: Reverb Workshop, Source 30m Rx 1.2-6m, lambda=6m

```
250 30 0 0 80 1500 2
.25 5 480 12000 0 0 1
1.2 6 5 1
2 -1 -1 0 0 0 4 1
T F F T
4 1 1
      0.000000 0.0
      0.000000 1.0      1500.00 0.00006276 0 0
      100.0000 1.0      1500.00 0.00006276 0 0
      100.0000 2.0      1700 0.5 0 0
      120 2.0      1700 0.5 0 0
2 1700. 0.5 0 0
```

0.0 0.0

RW_P11_f250_S30R0_air.dat

Prob XI: Reverb Workshop, Source 30m Rx 0m in H2O, 5m air top

```
250 35 0 0 80 1500 2
.25 5 500 12000 0 0 1
5.0 5.0 1 1
2 -1 -1 0 0 0 4 1
T F F T
6 1 1
0.000000 0.0
0.000000 0.001 330.000 0.001 0 0
5.000000 0.001 330.000 0.001 0 0
5.000000 1.0 1500.00 0.00006276 0 0
105.0000 1.0 1500.00 0.00006276 0 0
105.0000 2.0 1700 0.5 0 0
125.0000 2.0 1700 0.5 0 0
2 1700.0 0.5 0 0
0.0 0.0
```

ASAWedge.dat

ASA Wedge Parameters - 3 modes

```
25 100 0 0 85 1500 13
.125 10 4800 4000 0 0 1
30 30 1 1
2 -1 -1 1 0 0 2 1
T F F F
5 1 1
0 0
0.0 1.0 1500 0.0 0 0
200 1.0 1500 0.0 0 0
200 1.5 1700 0.50 0 0
400 1.5 1700 0.50 0 0
600 1.5 1700 2.0 0 0
1.5 1700 0 0 0
0 0
```

E.2 Output Files

Through the scripts `PECan_run.m` and `PECan_batch_run.m` the standard output file names are renamed such that they are prefixed by the naming convention above in Annex E.1. Based up the example in E.1 the following would occur as a result of running the MatlabTM run scripts:

Input file:

- `RW_P12_f3500_S30R50.dat`

Results in the output files (as used in this study):

- RW_P12_f3500_S30R50_petlr.out
- RW_P12_f3500_S30R50_pervb.out

No output files are included in this report, but are available on the data DVD supplied as a deliverable.

List of symbols/abbreviations/acronyms/initialisms

2D	Two dimensional
3D	Three dimensional
APL/UW	Applied Physics Laboratory, University of Washington
BNS	Brooke Numerical Services
CASS	Comprehensive Acoustic System Simulation (USN model)
dB	Decibel. One tenth of a bel.
DND	Department of National Defence
DRDC	Defence Research & Development Canada
FFT	Fast Fourier Transform
FORTTRAN	Programming language
GRAB	Gaussian Ray Bundle, modelling technique
Matlab TM	Programming language by MathWorks
MWS	Maritime Way Scientific Ltd.
PC	Personal Computer
PE	Parabolic Equation
RD	Range Dependent
RI	Range Independent
RW	Reverberation Workshop
Rx	Receiver (shorthand)
SA	Scientific Authority
TL	Transmission Loss
Tx	Transmitter (shorthand)
URL	Universal Resource Locator (a world wide web 'link')

Distribution list

Document No.: DRDC Atlantic CR 2012-077

LIST PART 1: Internal Distribution by Centre

- 3 DRDC Atlantic Library
- 1 Dale Ellis
- 1 Sean Pecknold
- 1 Garry Heard
- 1 Paul Hines

7 TOTAL LIST PART 1

LIST PART 2: External Distribution by DRDKIM

- 1 Library and Archives Canada
Attn: Military Archivist, Government Records Branch
- 1 DRDKIM
- 1 Maritime Way Scientific Limited
2110 Blue Willow Crescent
Ottawa, ON Canada K1W 1K3
- 1 Brooke Numerical Services
3440 Seaton Street
Victoria, BC Canada V8Z 3V9

4 TOTAL LIST PART 2

11 TOTAL COPIES REQUIRED

This page intentionally left blank.

DOCUMENT CONTROL DATA		
(Security classification of title, body of abstract and indexing annotation must be entered when the overall document is classified)		
1. ORIGINATOR (The name and address of the organization preparing the document. Organizations for whom the document was prepared, e.g. Centre sponsoring a contractor's report, or tasking agency, are entered in section 8.) Defence R&D Canada – Atlantic PO Box 1012, 9 Grove Street Dartmouth, Nova Scotia B3A 3C5	2. SECURITY CLASSIFICATION (Overall security classification of the document including special warning terms if applicable.) UNCLASSIFIED (NON-CONTROLLED GOODS) DMC A REVIEW: GCEC JUNE 2010	
3. TITLE (The complete document title as indicated on the title page. Its classification should be indicated by the appropriate abbreviation (S, C or U) in parentheses after the title.) Reverberation Modelling using a Parabolic Equation Method		
4. AUTHORS (last name, followed by initials – ranks, titles, etc. not to be used) Hamm, C.A., Brooke, G.H., Thomson, D.J., Taillefer, M.L.		
5. DATE OF PUBLICATION (Month and year of publication of document.) October 2012	6a. NO. OF PAGES (Total containing information, including Annexes, Appendices, etc.) 114	6b. NO. OF REFS (Total cited in document.) 26
7. DESCRIPTIVE NOTES (The category of the document, e.g. technical report, technical note or memorandum. If appropriate, enter the type of report, e.g. interim, progress, summary, annual or final. Give the inclusive dates when a specific reporting period is covered.) Contract Report		
8. SPONSORING ACTIVITY (The name of the department project office or laboratory sponsoring the research and development – include address.) Defence R&D Canada – Atlantic PO Box 1012, 9 Grove Street Dartmouth, Nova Scotia B3A 3C5		
9a. PROJECT OR GRANT NO. (If appropriate, the applicable research and development project or grant number under which the document was written. Please specify whether project or grant.)	9b. CONTRACT NO. (If appropriate, the applicable number under which the document was written.) W7707-125517/001/HAL	
10a. ORIGINATOR'S DOCUMENT NUMBER (The official document number by which the document is identified by the originating activity. This number must be unique to this document.) DRDC Atlantic CR 2012-077	10b. OTHER DOCUMENT NO(s). (Any other numbers which may be assigned this document either by the originator or by the sponsor.)	
11. DOCUMENT AVAILABILITY (Any limitations on further dissemination of the document, other than those imposed by security classification.)		
12. DOCUMENT ANNOUNCEMENT (Any limitation to the bibliographic announcement of this document. This will normally correspond to the Document Availability (11). However, where further distribution (beyond the audience specified in (11) is possible, a wider announcement audience may be selected.)		

13. **ABSTRACT** (A brief and factual summary of the document. It may also appear elsewhere in the body of the document itself. It is highly desirable that the abstract of classified documents be unclassified. Each paragraph of the abstract shall begin with an indication of the security classification of the information in the paragraph (unless the document itself is unclassified) represented as (S), (C), (R), or (U). It is not necessary to include here abstracts in both official languages unless the text is bilingual.)

DRDC Atlantic has developed a Clutter Model for range-dependent environments based on adiabatic normal modes; however, this approach is expected to fail for strongly range-dependent environments. Alternatively, parabolic equation (PE) models are robust in strongly range-dependent environments. In this study the use of the DRDC PE model 'PECan' was used to determine the feasibility of computing the reverberation and target echo fields in a variety of ocean waveguides. Calculations are compared to some problems from the US Reverberation Modelling Workshops. The PE method reverberation estimates compare favourably to previously published results obtained by other authors and methods.

14. **KEYWORDS, DESCRIPTORS or IDENTIFIERS** (Technically meaningful terms or short phrases that characterize a document and could be helpful in cataloguing the document. They should be selected so that no security classification is required. Identifiers, such as equipment model designation, trade name, military project code name, geographic location may also be included. If possible keywords should be selected from a published thesaurus, e.g. Thesaurus of Engineering and Scientific Terms (TEST) and that thesaurus identified. If it is not possible to select indexing terms which are Unclassified, the classification of each should be indicated as with the title.)

Reverberation, parabolic equation, modelling

This page intentionally left blank.

Defence R&D Canada

Canada's leader in defence
and National Security
Science and Technology

R & D pour la défense Canada

Chef de file au Canada en matière
de science et de technologie pour
la défense et la sécurité nationale



www.drdc-rddc.gc.ca